

## A review on carbon dioxide sequestration potentiality in basaltic rocks: Experiments, simulations, and pilot tests applications

Grant Charles Mwakipunda<sup>a</sup>, Ping Yu<sup>b</sup>, Norga Alloyce Komba<sup>c</sup>, Edwin Twum Ayimadu<sup>d</sup>, Jennifer Sanford Moshi<sup>a</sup>, Fravian Mwizarubi<sup>a</sup>, Irene Martin Ndunguru<sup>a</sup>, Long Yu<sup>a,\*</sup>

<sup>a</sup> Key Laboratory of Theory and Technology of Petroleum Exploration and Development in Hubei Province, China University of Geosciences, Wuhan, 430074, China

<sup>b</sup> Science and Technology Administrative Department, Liaohe Oilfield, CNPC, Panjin City, Liaoning Province, 124010, China

<sup>c</sup> Research Institute of Environmental Law, Wuhan University, No. 299, Luoyu Road, 10 Wuchang District, Wuhan City, Hubei Province, China

<sup>d</sup> School of Resource and Environmental Science, Wuhan University, No. 299, Luoyu Road, 10 Wuchang District, Wuhan City, Hubei Province, China

### ARTICLE INFO

#### Keywords:

CO<sub>2</sub> sequestration  
Basaltic rocks  
Rapid formation  
Mineral carbonation  
Carbonate rocks

### ABSTRACT

Carbon dioxide (CO<sub>2</sub>) sequestration in basaltic rocks is stored mainly through mineral carbonation. It has the potential to store 100,000 to 250,000 gigatons. This review aims to investigate the potentiality of storing CO<sub>2</sub> in subsurface basaltic rocks from experiments, modeling and simulations, and pilot test findings. Further, it discusses well integrity issues in CO<sub>2</sub> storage in basaltic rocks, geomechanical effects for CO<sub>2</sub> sequestration on basalts, nanoparticles potential applications for CO<sub>2</sub> storage in basaltic rocks, economic aspects comparison between CO<sub>2</sub> storage in basaltic rocks and sedimentary basins, etc, which were overlooked on previous review papers. It was revealed that CO<sub>2</sub> can be sequestered in basaltic rocks, especially after two successful pilot test studies in Hellisheidi, Iceland and Wallula, USA. In addition, it was found that nanoparticles and surfactant applications have great potential to enhance CO<sub>2</sub> sequestration in basaltic rocks. Still, the potential environmental impact of using nanoparticles and surfactants for CO<sub>2</sub> sequestration needs to be assessed. However, some challenges need to be solved for CO<sub>2</sub> sequestration implementation in basalts to be scaled to full field operations, such as site selection problems, storage capacity estimation difficultness, permeability reduction during injection due to precipitations, cost estimation difficultness, well integrity problems, variations of geochemical reactions and mineralization rate which depends on the properties of the formations etc. This review aims to stimulate further investigation and development on CO<sub>2</sub> sequestration in basaltic rocks by highlighting areas where research is inconclusive. Bridging these knowledge gaps is essential for optimizing the efficiency, safety, and cost-effectiveness of CO<sub>2</sub> storage in basaltic formations. Ultimately, such advancements can pave the way for the widespread adoption of basalt sequestration as a key technology for mitigating global climate change.

### 1. Introduction

Over the past few years, a rapid rise in global energy consumption has been fueled by population growth and economic booms in developing countries, particularly Asian nations (Balani, 2023; Bigdeli and Delshad, 2024; Dong et al., 2024; Mkono et al., 2023; Nadege et al., 2024). Around 85% of global energy consumption currently comes from non-renewable sources, specifically fossil fuels, including oil, natural gas, and coal (Bergougui, 2024; Hohendorff Filho et al., 2024; Kumar et al., 2024; Sambo et al., 2022). Carbon dioxide (CO<sub>2</sub>) is the main greenhouse gas (GHG), contributing 76% of total emitted gas in the atmosphere (Mwakipunda et al., 2024). According to a report published

on Our World in Data website in 2020, the top seven countries with the most annual CO<sub>2</sub> emissions are China with 30.9%, followed by the USA with 13.49%, India with 7.3%, Russia with 4.73%, Iran with 2.02%, Germany with 1.82%, and Brazil with 1.32%. Continentally, Asia is the most emitter, contributing 53%, followed by North America with 18% and Europe with 17%, with the remaining percent contributed by each continent having less than 10% of global CO<sub>2</sub> emissions (Ritchie et al., 2020). Atmospheric CO<sub>2</sub> concentration is rising primarily due to human activity, particularly the burning of fossil fuels for energy. Since the industrial revolution, human CO<sub>2</sub> emissions have increased significantly, from ~280 ppm before industrial evolution to ~425 ppm in March 2024, continuing to affect global climatic change (Statista, 2024).

\* Corresponding author.

E-mail address: [yulong36@cug.edu.cn](mailto:yulong36@cug.edu.cn) (L. Yu).

<https://doi.org/10.1016/j.geoen.2024.213253>

Received 19 July 2024; Received in revised form 10 August 2024; Accepted 24 August 2024

Available online 28 August 2024

2949-8910/© 2024 Elsevier B.V. All rights are reserved, including those for text and data mining, AI training, and similar technologies.

To meet the Paris Climate Summit agreement of global warming to well below 2 °C above pre-industrial levels and pursue efforts to limit it even further to 1.5 °C by 2050 (Mao and Jahanbani Ghahfarokhi, 2024; Mwakipunda et al., 2023a), transitioning to renewable energy sources is crucial for long-term decarbonization while effective strategies for carbon capture and storage (CCS) become a key technology for mitigating climate change and achieving net-zero emissions targets.

CCS involves capturing CO<sub>2</sub> emissions from anthropogenic sources, such as power plants and industrial facilities, transporting it to suitable geological formations, and permanently storing it underground (Boot-Handford et al., 2014; Hosseinzadeh et al., 2024; Mwakipunda et al., 2023c). However, it is still a developing technology with some challenges, including the high cost of capture, transportation, and storage (Bowen, 2011; Ngata et al., 2023; Wilberforce et al., 2019). Several methods exist for storing captured CO<sub>2</sub>. These methods can be broadly categorized into geological, biological, and oceanic storage approaches, as discussed by Zheng et al. (2020). Geological formations offer various options for CO<sub>2</sub> storage, each with its advantages and limitations. Unmineable coal seams and methane hydrate reservoirs represent potential storage sites, but technical challenges and uncertainties regarding long-term stability require further research. Saline aquifers and depleted oil and gas reservoirs with residual oil saturation targeted for enhanced oil recovery (EOR) are more developed options. Saline aquifers offer vast storage capacity (Mwakipunda et al., 2023b), while depleted oil and gas reservoirs often possess existing infrastructure for CO<sub>2</sub> injection (Li et al., 2006). EOR techniques can utilize CO<sub>2</sub> for improved oil extraction while storing it underground. Basalt formations present a unique opportunity for CO<sub>2</sub> sequestration through mineral carbonation, where CO<sub>2</sub> reacts with rock minerals to form stable carbonate minerals over time. The most favorite storage option implemented in large-scale fields is deep saline aquifers due to their large storage capacity (10–10,000 gigatonnes) and low-risk leakage (Bruant et al., 2002).

One of the CO<sub>2</sub> storage options given little attention is carbon mineralization, which occurs in basaltic, mafic and ultramafic rocks. It has been found that carbon mineralization happens naturally when basaltic rocks are exposed to CO<sub>2</sub> and can store approximately one giga tones permanently from the atmosphere each year through enhanced rock weathering (Paulo et al., 2023). If carbon mineralization gets much attention from government support globally, it has been found that one giga ton per year of CO<sub>2</sub> will be removed from the atmosphere by 2035 and 10 giga tons per year by 2050. There are two ways in which CO<sub>2</sub> can be stored through mineral carbonation in basalts, which are either injecting CO<sub>2</sub> directly into basaltic rocks, known as in-situ mineralization or exposing the basaltic rocks on the earth's surface to CO<sub>2</sub>, known as ex-situ mineralization or surficial mineralization (Liu et al., 2024). The differences between in-situ and ex-situ mineralization are summarized in Table 1. This review paper will focus on in-situ mineralization. The reasons behind this are in-situ CO<sub>2</sub> mineralization emerges as the more favorable option for large-scale applications due to its economical and practical advantages. Firstly, it bypasses the need for expensive capture facilities, transport pipelines, and ex-situ processing plants, significantly reducing overall costs. Secondly, the vastness of suitable geological formations allows in-situ methods to be scaled up for efficiently handling massive amounts of CO<sub>2</sub>, which is a critical aspect of tackling climate change. Additionally, the natural containment offered by the underground formations potentially lowers the risk of CO<sub>2</sub> leakage compared to ex-situ methods. Finally, in-situ processes require less energy as they eliminate the energy-intensive steps of CO<sub>2</sub> capture, transport, and processing for ex-situ methods. These combined factors make in-situ CO<sub>2</sub> mineralization a more promising approach for large-scale CO<sub>2</sub> capture and storage. In-situ CO<sub>2</sub> mineralization in basalts offers several advantages over other storage options, as summarized in Table 2. However, more research is required to identify the ideal conditions for carbon mineralization and address the existing challenges to achieve low-cost and large-scale implementation (Finstad et al., 2023;

**Table 1**  
Differences between in-situ and ex-situ mineralization.

Feature	In-situ mineralization	Ex-situ mineralization
Location of mineralization	Occurs underground in geological formations	Occurs above ground in processing facilities
CO <sub>2</sub> injection	CO <sub>2</sub> is directly injected into rock formations	Captured CO <sub>2</sub> is transported to the processing facility
Mineral reaction	CO <sub>2</sub> reacts with minerals naturally present in the rock formations	CO <sub>2</sub> reacts with crushed or mined minerals in controlled conditions
Mineralization rate	Slower due to reliance on natural processes	Potentially faster due to optimized reaction conditions
Leakage risk	Potentially lower due to CO <sub>2</sub> being trapped within the formation	Potentially higher due to reliance on containment measures
Monitoring needs	May require monitoring of injection wells in the surrounding area	Requires monitoring of processing facility and potential storage sites for mineral products
Energy use	Lower energy consumption for CO <sub>2</sub> injection	Higher energy consumption for CO <sub>2</sub> capture, transport, and processing
Scalability	Potentially more scalable due to vastness of suitable geological formations	Limited by processing capacity and availability of suitable mined minerals
Cost	Potentially lower due to less infrastructure and processing needed	Potentially higher due to additional capture, transport, and processing steps

**Table 2**  
Few advantages of basalts over other CO<sub>2</sub> storage options.

Advantages	Descriptions
Rapid mineralization	Basalt minerals react with CO <sub>2</sub> to form stable carbonate minerals, permanently trapping CO <sub>2</sub> within a few years.
Large storage capacity	Basalt formations are widespread and abundant, offering vast potential for CO <sub>2</sub> storage.
Reduced leakage risk	Mineralization and potential capillary trapping mechanisms in basalt formations can significantly reduce the risk of CO <sub>2</sub> leakage compared to relying solely on trapping mechanisms in other formations.
Lower monitoring costs	Due to rapid mineralization and lower leakage risk, basalt formations may require less intensive monitoring.
Potential for heat extraction	Basalt formations undergoing CO <sub>2</sub> mineralization can generate heat that could be harnessed as renewable energy.
Reduce induced seismicity risk	Reduced risk due to solid mineral formation, reducing pressure and stress.
Regulatory and public acceptance	Basalts may be located in remote areas, potentially reducing regulatory hurdles and public opposition.

Kebede et al., 2023; Myers and Nakagaki, 2020; Sandalow et al., 2021).

Despite the success of recently published experiments, modeling and simulations, and two pilot test results, many existing challenges and research gaps still need to be solved to pave the way toward full-field operations. Hence, this paper reviewed the potentiality of sequestering CO<sub>2</sub> in basaltic rocks, focused on experiments, modeling and simulations, and pilot test applications findings. The identified challenges, research gaps, and successes aim to motivate researchers and stakeholders to investigate CO<sub>2</sub> sequestration potentiality in basaltic rocks further. Further, this review paper has discussed the potential nanoparticle's application in enhancing CO<sub>2</sub> sequestration in basaltic rocks, which has not been addressed in previously published review papers. Furthermore, this review paper has discussed the estimation method for CO<sub>2</sub> sequestration in basaltic rocks. Additionally, well integrity in basaltic rocks and geomechanical effects for CO<sub>2</sub> sequestration on basalts have been addressed in this review paper as being overlooked in previously published review papers. Moreover, economic analysis of CO<sub>2</sub> storage between basalts and other storage options was conducted, and recommendations were made. The sections of this review include introduction, theory, experiments, potential applications of

nanoparticles application on enhancing CO<sub>2</sub> sequestration in basalts, modeling and simulations, pilot tests applications, impacts of surface facilities for CO<sub>2</sub> injection in basaltic rocks, well integrity in CO<sub>2</sub> sequestration in basalts, geomechanical effects for CO<sub>2</sub> sequestration on basalts, estimation of CO<sub>2</sub> sequestration capacity in basaltic rocks, challenges encountered during CO<sub>2</sub> sequestration in basaltic rocks, research gaps and future works, and conclusions and recommendations.

## 2. Theory

### 2.1. Basaltic formations

Basalts are fine-grained, dark igneous rocks predominantly made up of pyroxene and plagioclase, along with trace amounts of minerals like olivine formed after rapid cooling of lava at or near the earth's surface (Lu et al., 2024b). Basalt is the general term for all igneous rocks with a high magnesium and iron content and a low silica content (less than 53%). Basalts can be classified into seven groups based on the Total Alkali-Silica (TAS) diagram, as depicted in Fig. 1 and outlined in Table 3, based on geochemistry (Rasool and Ahmad, 2023). The global map distribution of basaltic rocks is shown in Fig. 2. It occupies 77% of igneous rocks (earth's surface) (Al Maqbali et al., 2023b; Ali et al., 2023a), of which 67% is on the ocean floor, with 10% being land surfaces. After CO<sub>2</sub> injection into the basaltic rocks, divalent cations are released, mainly Mg<sup>2+</sup>, Fe<sup>2+</sup>, and Ca<sup>2+</sup>, forming carbonate minerals such as magnesite, siderite, and calcite (Tutolo et al., 2021; Wells et al., 2017). A typical basalt contains 5–6 wt% Mg, 7–10 wt% Ca, and 7–10 wt % Fe (Oelkers et al., 2008). Basalt formations on land typically exhibit ropy, massive, or columnar structures. In contrast, basalt that forms beneath the surface, particularly underwater, tends to develop pillow-like structures. The porosity of basaltic rocks is from 5 to 20%, whereas permeability ranges from 10<sup>-18</sup> to 10<sup>-16</sup> m<sup>2</sup> (White et al., 2020a). The permeability in basalts is usually quite low due to the fine-grained nature of the rock and the tight interlocking of mineral crystals. The permeability of basaltic rocks depends on several factors, including the thickness of the flowing lava, the cooling rate of the lava, and the number and character of interflow zones. The basaltic cooling rate is usually high when the lava meets water and leads to the formation of pillow basalt, which has high permeability. In contrast, when lava cools slowly, basaltic rocks formed tend to have low permeability in the middle of pillow basalt bounded with top and bottom permeability zones (Roy et al., 2016). The basaltic rock hardness is approximately six per Mohs scale, whereas its compressive strength ranges from 100 to 300 MPa. Also, its tensile strength ranges from 20 to 60 MPa, while its

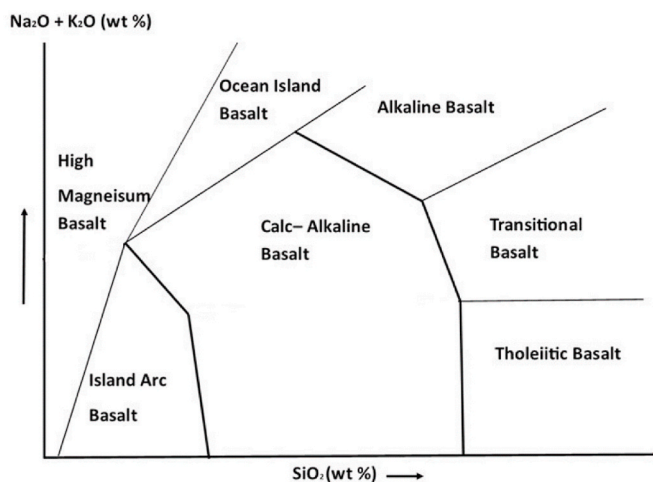


Fig. 1. TAS diagram application on basalts classification based on silica (SiO<sub>2</sub>) and alkali (NaO + K<sub>2</sub>O) content (Rasool and Ahmad, 2023).

Table 3

Basalts categories based on geochemistry (Rasool and Ahmad, 2023).

Type of basalts	Petrography	Trace elements	Major elements	Mineralogy
Alkaline basalts	Fine to coarse grained texture with small mineral crystals	Nb, Rb, Th, U, LREE, Ba, Sr, Zr, Hf	Na <sub>2</sub> O, K <sub>2</sub> O, SiO <sub>2</sub>	Plagioclase feldspar (30–45%) Amphibole (<5%) Pyroxene (20–40%) Olivine (5–30%)
Tholeiitic basalts	Porphyritic texture with phenocrysts in a fine-grained matrix	Ni, Cr, Sc, V, Ti, P, Zn, Co, Mn	FeO, MgO, SiO <sub>2</sub>	Plagioclase feldspar (40–70%) Olivine (5–25%) Pyroxene (20–40%) Magnetite (5–15%)
Transitional basalts	Variable textures (Porphyritic, intersertal, aphanitic)	REE, Ti, P, Zr, Hf, Ba, Sr, Nb, Rb, Th, U	Na <sub>2</sub> O, K <sub>2</sub> O, SiO <sub>2</sub> , FeO, MgO	Magnetite (5–15%) Pyroxene (20–40%) Plagioclase feldspar (30–50%) Alkali feldspar and clinopyroxene (<5%) Olivine (5–25%)
High magnesium basalts	Large olivine phenocrysts with a fine-grained groundmass	Ni, Cr, Co, Mn, Sc, V	MgO, SiO <sub>2</sub>	Plagioclase feldspar (<10%) Olivine (30–60%) Spinifex texture (<5%) Pyroxene (10–40%)
Calc-alkaline basalts	Porphyritic texture with visible phenocrysts	Pb, Ti, Sr, Ba, Rb, Zr, Hf, LREE, HFSEs	Al <sub>2</sub> O <sub>3</sub> , SiO <sub>2</sub> , FeO, MgO	Magnetite (5–15%) Plagioclase feldspar (10–40%) Amphibole (<5%) Pyroxene (20–30%) Olivine (5–25%)
Island arc basalts	Variable textures (Porphyritic, vesicular, aphanitic)	Pb, Ti, Ba, Sr, Rb, LREE, HFSEs, LILEs	Al <sub>2</sub> O <sub>3</sub> , SiO <sub>2</sub> , FeO, MgO	Magnetite (<5%) Plagioclase feldspar (30–60%) Amphibole (<5%) Olivine (5–25%) Pyroxene (10–40%)
Ocean island basalts	Aphanitic to porphyritic texture	Nb, Ta, K, Pb, Th, U, LREE, HFSEs	SiO <sub>2</sub> , FeO, MgO	Amphibole (<5%) Olivine (40–50%) Plagioclase feldspar (10–40%) Pyroxene (10–40%) Magnetite (5–15%)



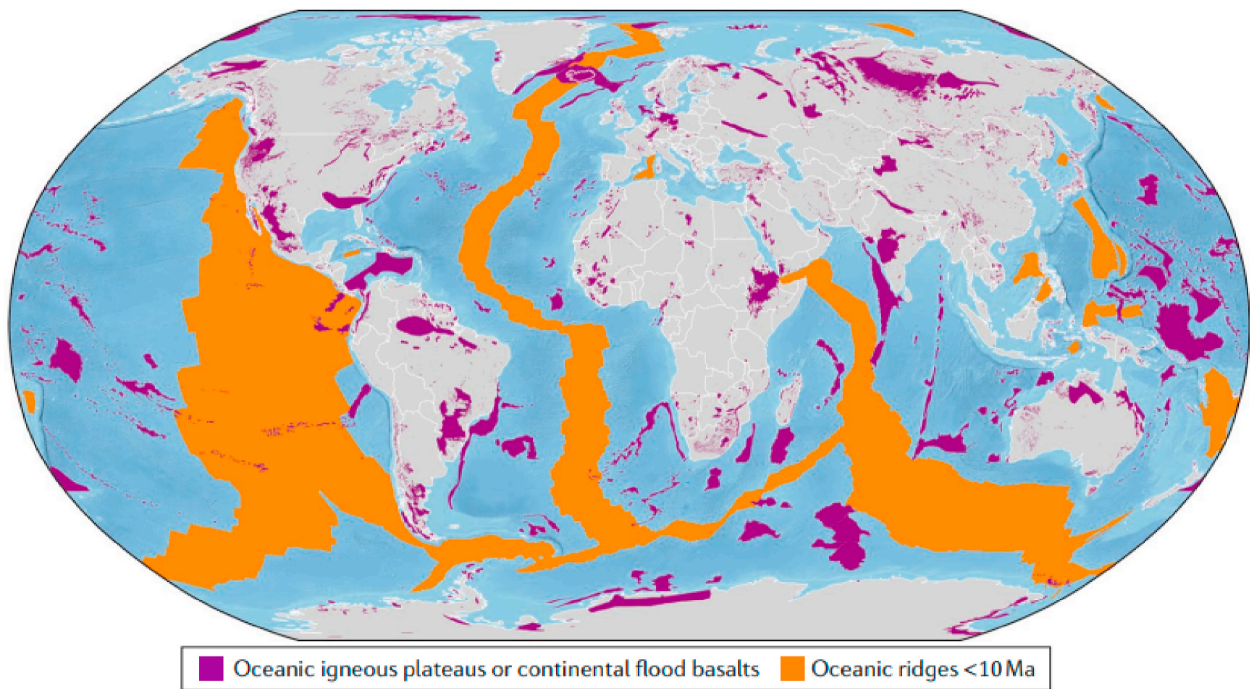


Fig. 2. Global distributions of basaltic rocks (Snæbjörnsdóttir et al., 2020).

bulk density ranges from 2.8 to 3 Mg/m<sup>3</sup> (Roy et al., 2016; Xiong et al., 2018).

## 2.2. CO<sub>2</sub> trapping mechanisms in basaltic rocks

There are mainly four trapping mechanisms after CO<sub>2</sub> injection in the basaltic formation, which are 1) Mineral trapping (mineral carbonation), 2) Solubility trapping, 3) Residual trapping, and 4) Stratigraphic or structural trapping. Basaltic rock minerals such as Mg<sup>2+</sup>, Fe<sup>2+</sup>, and Ca<sup>2+</sup> react with injected CO<sub>2</sub> to form carbonate minerals in the mineral trapping mechanism. The reaction triggers CO<sub>2</sub> to precipitate and immobilize solid carbonate minerals inside the basalt matrix, such as calcium carbonate (CaCO<sub>3</sub>) or magnesium carbonate (MgCO<sub>3</sub>). This is the CO<sub>2</sub> dominant trapping mechanism in basaltic rocks due to its long-

term stability and potential for large-scale CO<sub>2</sub> sequestration, as shown in Fig. 3. It was revealed from pilot tests that the mineral carbonation process can take up to two years (Mouallem et al., 2023). For solubility trapping, the mechanism involves the reaction of injected CO<sub>2</sub> with pore fluids, especially brine, which remains dissolved within the new aqueous solution to prevent leakage risk. Mostly, the reaction results in the formation of carbonic acids (H<sub>2</sub>CO<sub>3</sub>), which can react with basaltic minerals, enhancing the mineral carbonation process (Punnam et al., 2022). In residual trapping mechanisms, the injected CO<sub>2</sub> is retained as a residual phase in the basaltic pore spaces due to capillary forces and interfacial tension (IFT) between CO<sub>2</sub> and the pore fluids or solid surfaces (Al-Yaseri et al., 2021b; Punnam et al., 2021). For the stratigraphic trapping mechanism, the denser injected CO<sub>2</sub> is trapped by cap rocks and becomes immobile in less permeable layers. These layers differ in

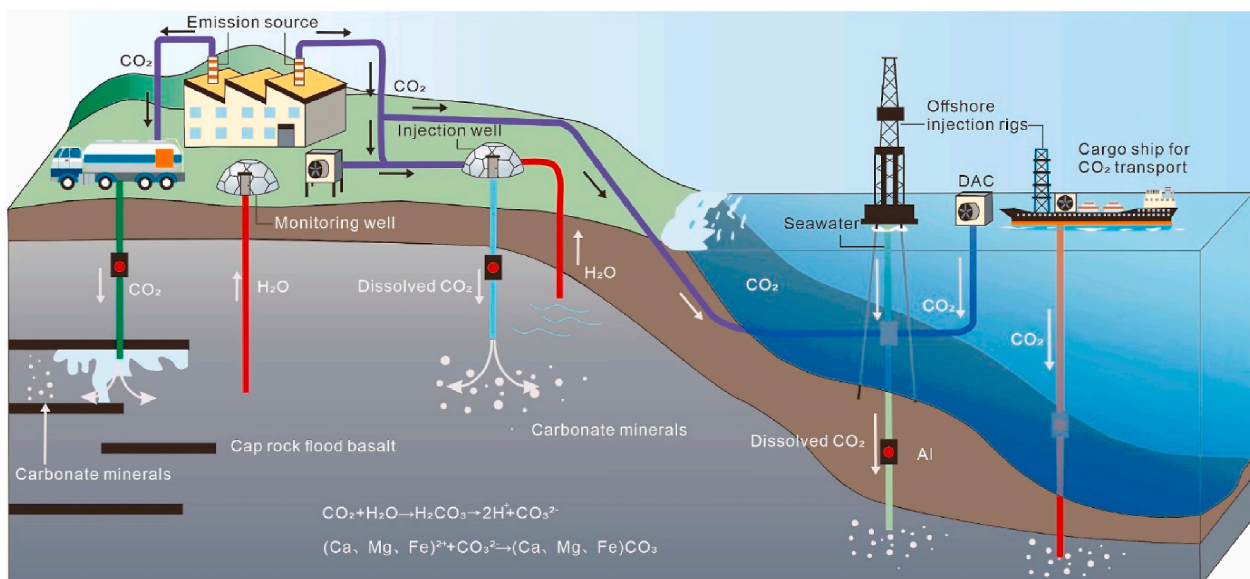


Fig. 3. Mineral carbonation in basaltic rocks (Lu et al., 2024c).



lithology and permeability, enhancing the trapping mechanisms when encountered by injected CO<sub>2</sub>. Also, the natural fractures, faults or fissures act as a barrier preventing the vertical migration and escape of injected CO<sub>2</sub> physically (Al Maqbali et al., 2023a; Kebede et al., 2023; Mouallem et al., 2023).

Combining these trapping mechanisms creates multiple barriers to CO<sub>2</sub> migration and ensures permanent storage in basaltic rocks. Mineral trapping mechanism, especially through mineral carbonation, is a significant and durable mechanism for CO<sub>2</sub> immobilization in basaltic rocks. Understanding and optimizing these trapping mechanisms is essential for evaluating the storage capacity and assuring the secure and efficient sequestration of CO<sub>2</sub> in basaltic rocks.

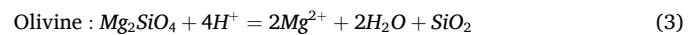
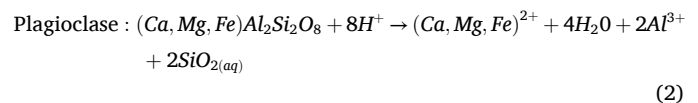
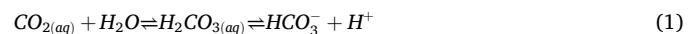
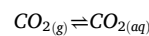
### 2.3. Key parameters for CO<sub>2</sub> sequestration in basaltic rocks

CO<sub>2</sub> sequestration in basalt requires metallic divalent cations that precipitate when they react with injected CO<sub>2</sub> to form carbonate minerals like calcite, magnetite, and siderite. When injected, CO<sub>2</sub> dissolves in the formation water, lowering the pH of the system, which causes the host rock to react by releasing divalent cations (Mg<sup>2+</sup>, Fe<sup>2+</sup>, and Ca<sup>2+</sup>) through dissolution reaction (Berrezueta et al., 2023; de Obeso et al., 2023). With regard the presence of divalent cations remains the main factor for carbon dioxide sequestration in basaltic rocks (mineral carbonation); other key factors include 1) Availability of water for injection, as it has been found that during injection, CO<sub>2</sub> was mixed with water at CarbFix to enhance dissolution of CO<sub>2</sub> by increasing its partial pressure and lowering the temperature and water enhance dissolution of host rocks. This shows that a field with a nearby water source, like seawater, can help reduce the cost of injecting water from underground. It has been proved that using seawater for the dissolution process has a positive influence (Snæbjörnsdóttir et al., 2014, 2017; Wolff-Boenisch et al., 2011).2) Temperature: it has been proved that increasing the system's temperature (0–100 °C) at a pH of 3.5 helps to enhance the dissolution of host rocks 60 times to release plenty of divalent metallic cations, which helps the mineral carbonation process. Similarly, the rising temperature of altered basaltic rocks, such as clays and zeolites, enhances the dissolution process. The temperature is raised by increasing the depth of injection wells or drilling in geothermal-prone areas (Gislason and Oelkers, 2003; Snæbjörnsdóttir et al., 2014).3) CO<sub>2</sub> partial pressure: it has been found that increasing CO<sub>2</sub> partial pressure enhances the mineral carbonation process because more divalent metallic cations are released from host rocks instead of clays and zeolites (Bullock et al., 2023; Snæbjörnsdóttir et al., 2014).4) Porosity and permeability; it has been found that younger rocks have higher porosity and permeability than older rocks and are favorable for mineral carbonation because ease injection process and are prone to underground water flows which can help on dissolution process (Singh and Nayak, 2023; Snæbjörnsdóttir et al., 2014).5)Depth; dissolution of CO<sub>2</sub> and water according need a minimum depth and CO<sub>2</sub> undergo dissolution reaction at minimum pressure of 25 bars which is below 250 m. Also, CO<sub>2</sub> bubbles need to dissolve, so the minimum depth increases to 350 m. However, injecting at high depth, like in geothermal systems with high temperatures, helps to enhance dissolution reactions. Hence, the depth range proposed for CO<sub>2</sub> injection in basaltic rocks is 500–1500 m (Li et al., 2023; Snæbjörnsdóttir et al., 2014).6) Risk of contamination of groundwater; the reaction between injected CO<sub>2</sub> and water and the basaltic rocks releases metallic divalent cations that cause mineral carbonation and other metals that cause pollution to water and biota like Al, Fe, Cr, and Mn. These elements are released early during CO<sub>2</sub> injection, so they must be handled to avoid pollution. However, during CO<sub>2</sub> injection in CarbFix, samples collected through monitoring wells revealed that the metals did not affect the groundwater (Galeczka et al., 2013; Zheng et al., 2021).

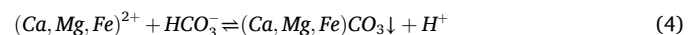
### 2.4. Basalts key characteristics for CO<sub>2</sub> sequestration

Basalts are considered suitable for CO<sub>2</sub> sequestration because they are enriched with divalent cations, have a high reaction rate, and occupy a large area of the earth's surface (Galeczka et al., 2014). Several processes are involved in mineral carbonation in basaltic rocks. First, the injected CO<sub>2</sub> in basaltic rocks reacts with water to form carbonic acid, as shown in Eq. (1). After that, the carbon-fixing minerals in basaltic rocks react with H<sup>+</sup> to release divalent cations Mg<sup>2+</sup>, Fe<sup>2+</sup>, and Ca<sup>2+</sup>. For instance, plagioclase and olivine dissolution reactions are shown in Eqs. (2) and (3), respectively. Then, divalent cations react with HCO<sub>3</sub><sup>-</sup> to form carbonate rocks through the mineral carbonation process in precipitation reaction, as shown in Eq. (4) (Gislason et al., 2010; Matter et al., 2007; Sanna et al., 2014; Zhang et al., 2023). During carbon fixation, CO<sub>2</sub> rapidly dissolves in the formation water and subsequently reacts with divalent cations to form carbonate minerals. The overall speed of CO<sub>2</sub> mineral trapping depends on the dissolution rate of carbon-fixing minerals in basalt, which is generally slow. This is due to the limited reaction surface area and the constrained volume of CO<sub>2</sub> within the pore spaces (Liu et al., 2021; Matter et al., 2009). The potential minerals for the mineral carbonation process are shown in Table 4, with forsterite being the most efficient compared to others, where 6.4 mega tons are required to sequester four megatons of CO<sub>2</sub> to produce 2.6 million m<sup>3</sup> of magnesite (Oelkers et al., 2008). The whole process is illustrated in Fig. 4.

#### Dissolution



#### Precipitation



### 2.5. CO<sub>2</sub> injection in basaltic rocks

There are two options in which CO<sub>2</sub> can be injected into basaltic rocks for storage. The first option is the injection of pure CO<sub>2</sub> into the formation, and the second option is the injection of CO<sub>2</sub> dissolved in water, known as the CarbFix method, as shown in Fig. 5 (Zhang et al., 2023). In the first option, after the pure CO<sub>2</sub> is injected into the formation, the CO<sub>2</sub> is trapped below the impermeable caprock (structural trapping or stratigraphic trapping) with others trapped in small pore

**Table 4**  
Promising minerals for the mineral carbonation process in basalts (Oelkers et al., 2008).

Mineral	Chemical formula	Tons required to sequester 1 ton of carbon
Wollastonite	CaSiO <sub>3</sub>	9.68 <sup>a</sup>
Forsterite	Mg <sub>2</sub> SiO <sub>4</sub>	5.86 <sup>b</sup>
Serpentine/ Chrysotile	Mg <sub>3</sub> Si <sub>2</sub> O <sub>5</sub> (OH) <sub>4</sub>	7.69 <sup>b</sup>
Anorthite	CaAl <sub>2</sub> Si <sub>2</sub> O <sub>8</sub> Na <sub>0.08</sub> K <sub>0.008</sub> Fe (II) <sub>0.17</sub> Mg <sub>0.28</sub> Ca <sub>0.26</sub>	23.1 <sup>a</sup>
Basaltic glass	Al <sub>0.36</sub> Fe (III) <sub>0.02</sub> SiTi <sub>0.02</sub> O <sub>3.45</sub>	8.67 <sup>c</sup>

a Stand for Calcite; b for Magnesite; c assumes that all Mg<sup>2+</sup>, Fe<sup>2+</sup>, and Ca<sup>2+</sup> are converted to Magnesite, Siderite, and Calcite.

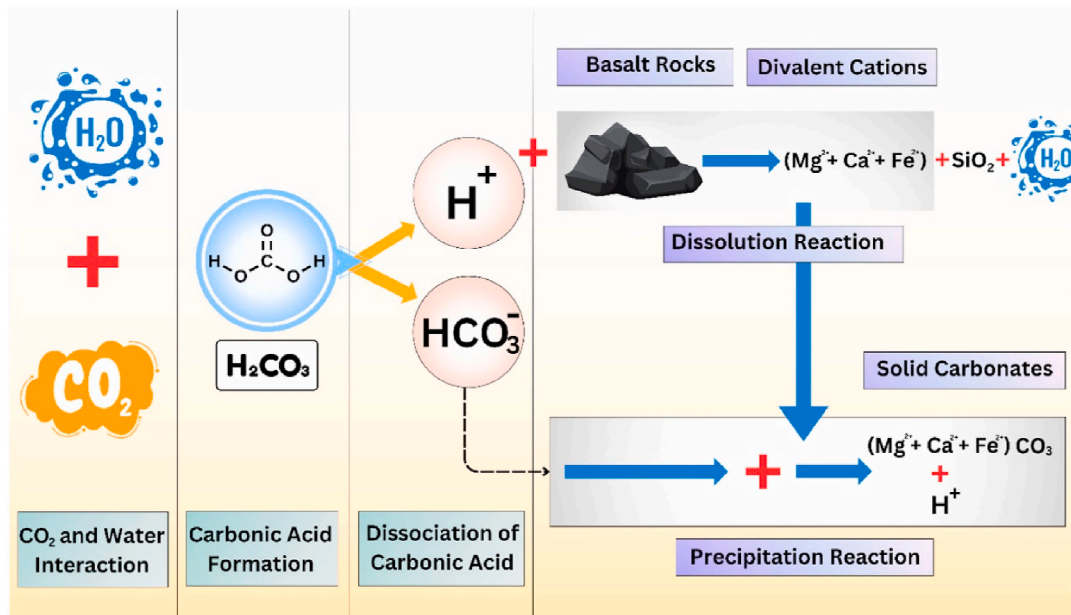


Fig. 4. Mineral carbonation process (Singh et al., 2024).

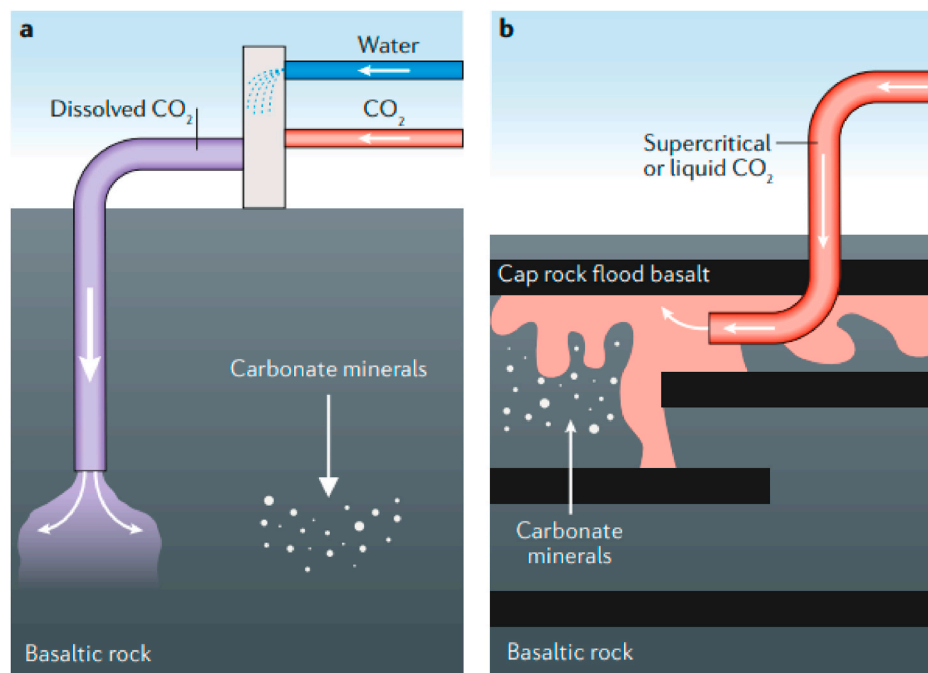


Fig. 5. CO<sub>2</sub> injection options in basaltic rocks a) CarbFix basalt b) Supercritical CO<sub>2</sub> (Wallula basalt) (Snæbjörnsdóttir et al., 2020).

spaces due to capillary forces and limits its movement (residual trapping). Progressively, other injected CO<sub>2</sub> dissolves in brine (solubility trapping), and later on, some of the dissolved CO<sub>2</sub> in brine reacts with surrounding rocks to form carbonate minerals (mineral trapping), which can take more than ten years to form minerals (Omari et al., 2022). For the CarbFix method, injected CO<sub>2</sub>, which is usually mixed with water, reacts with basaltic rocks to form carbonate minerals within two years through a process known as mineral carbonation, which consumes 95% of injected CO<sub>2</sub> (Gislason and Oelkers, 2014; Snæbjörnsdóttir et al., 2020). Usually, dissolving one tone of CO<sub>2</sub> at a partial pressure of 25 bars requires almost 27 tons of water (Oelkers et al., 2008).

### 3. Experiments

Several researchers conducted experiments to investigate the potentiality of storing CO<sub>2</sub> on basaltic rocks towards full field operations to mitigate global climate change. The experiments are conducted under different conditions to reflect the natural conditions of the basaltic formations, solve existing challenges, and discover new knowledge. Moreover, these experiments help generate data that can be used for modeling and simulations. In this section, the findings of the recently conducted experiments are discussed.

Oelkers et al. (2022) experimented to investigate the potentiality of Jizan basaltic rocks in the Southwest of Saudi Arabia to store CO<sub>2</sub>. Jizan basaltic group includes plagioclase, clinopyroxene, and magnetite, in

which some areas are altered to albite, chlorite, calcite, epidote, hematite, and pumpellyite after the metamorphism. 14 samples were collected and analyzed in which geochemical and mineralogical compositions were analyzed using optical and reflected light microscope, X-ray diffractometry (XRD) was analyzed semi-quantitative, whole rock was analyzed using X-ray fluorescence (XRF) and electron microprobe analysis (EMPA). It was found that either seawater or freshwater altered Jizan basaltic rocks to form carbonates after CO<sub>2</sub> injection at 25 and 100 °C. Also, the most dominant metallic cations from Jizan basaltic rocks were Ca<sup>2+</sup> and Mg<sup>2+</sup>, which precipitated to form carbonates. In general, it was concluded that altered Jizan basaltic rocks have great potential to store CO<sub>2</sub> in carbonate form with a capacity of 1.4–10.2 gigatons in 140–1000 years.

Also, Ali et al. (2023a) experimented to analyze the wettability change of the CO<sub>2</sub>-H<sub>2</sub>O-basaltic rocks system of Harrat Rahat near the Red Sea coast of Western Saudi Arabia (SA), which determines the mineral carbonation process. Contact angle measurement, including advancing contact angle ( $\theta_a$ ) and receding contact angle ( $\theta_r$ ), were measured to assess its wettability at a temperature and pressure of 298 and 323 K and 1–20 MPa, respectively, in the absence and presence of organic acid. It was revealed that at a temperature of 323 K and pressure of 20 MPa, the pure SA remained strongly water-wet with  $\theta_a$  and  $\theta_r$  of 46.7° and 43.2°, respectively, while organic aged SA basalt altered to CO<sub>2</sub>-wet with  $\theta_a$  and  $\theta_r$  of 106.8° and 95.2°, respectively. Also, it was shown that at a temperature of 323 K and various pressures, the pure SA remained strongly water-wet with, as shown in Fig. 6, while organic aged SA basalt altered to CO<sub>2</sub>-wet with, as shown in Fig. 6. In general, contact angles increased with the increase of pressure and temperature in which pure SA basalt contact angles were smaller than organic aged SA basalt. This indicates that organic acids may increase the mobility of CO<sub>2</sub> within the SA basalt formation, potentially reducing its capacity to permanently store CO<sub>2</sub> through residual trapping and mineral trapping mechanisms. This could lead to a higher risk of CO<sub>2</sub> leakage.

Al-Yaseri et al. (2021b) did an experiment investigating the temperature and pressure effects on wettability alteration on the CO<sub>2</sub>-brine-basaltic rocks system of Western Australian basalt (WA). Two temperatures (298 K and 323 K) and pressure of 0.1, 5, 8, 15, and 20 MPa. It was revealed that the wettability of WA kept on weakly water wet when the temperature was 298 K and pressure >8 MPa ( $\theta_a = 68^\circ$  at 8 MPa and  $81^\circ$  at 20 MPa). At a temperature of 323 K and pressure >5 MPa ( $\theta_a = 60^\circ$ ) wettability of WA remained weakly water-wet and changed to CO<sub>2</sub> wet at a pressure of 15 MPa ( $\theta_a > 90^\circ$ ). It seems that the pressure increase causes the contact angle to increase because of the rise in CO<sub>2</sub> density, which influences intermolecular interactions between CO<sub>2</sub> and

basalt, which causes a change in wettability. These contact angle observations confirm that the basalt-CO<sub>2</sub> mineralization reaction is affected by wettability alteration because CO<sub>2</sub>-basalt and H<sub>2</sub>O-basalt interfacial areas will be different in weakly and strongly water-wet systems, respectively. In addition, at higher contact angles (weakly water wet  $\theta_a > 50^\circ$ ), slower dissolution rates and precipitation reactions are anticipated due to the reduction of the interfacial surface area of basalt and water. This implies that dissolution and precipitation rates are high at lower contact angles, and wettability is favorable for CO<sub>2</sub> sequestration. Moreover, intermediate water wet ( $\theta_a < 90^\circ$ ) and CO<sub>2</sub> wet ( $\theta_a > 90^\circ$ ) cause a reduction in structural and residual trapping capacities, which results in easier vertical CO<sub>2</sub> migration, which increases the leakage risk in caprock. This agrees with other basaltic rocks in different areas, as shown in Fig. 7.

Furthermore, Iglauer and Al-Yaseri (2021) did an experiment intending to improve the wettability of basaltic rocks favorable for CO<sub>2</sub> sequestration in the CarbFix area in Scotland. Similarly,  $\theta_a$  and  $\theta_r$  contact angle changes were measured using the tilted plate method at pressures of 5, 10, and 15 and a temperature of 323 K after adding sodium dodecyl benzene sulfonate (SDBS) surfactant to the system with different concentrations. The contact angles were measured in pure and aged basalt with SDBS surfactants. It was revealed that the contact angles altered to water-wet even with a small concentration of SDBS, as shown in Fig. 8. This strong water wet favors CO<sub>2</sub> sequestration in basaltic rocks. Moreover, Iglauer et al. (2020) experimented to examine the wettability alteration of the supercritical CO<sub>2</sub>-brine-basaltic rocks system of Hellisheidi in Southwest Iceland. Both advancing  $\theta_a$  and  $\theta_r$  changes were measured using the tilted plate method at a temperature of 308.15 K and 333.15 K and a pressure range of 4.48–17.23 MPa with different brine concentrations. It was revealed that brine contact angles increase rapidly with pressure to intermediate water wet and, as pressure rises, turns to CO<sub>2</sub> wet which affects mineralization process.

Apart from that, Kikuchi et al. (2023) experimented to investigate the effects of adding NaHCO<sub>3</sub> on changing the wettability of basaltic rocks collected from Iceland's mid-oceanic ridge (MOR). The experiment was conducted in a batch reactor to accommodate the

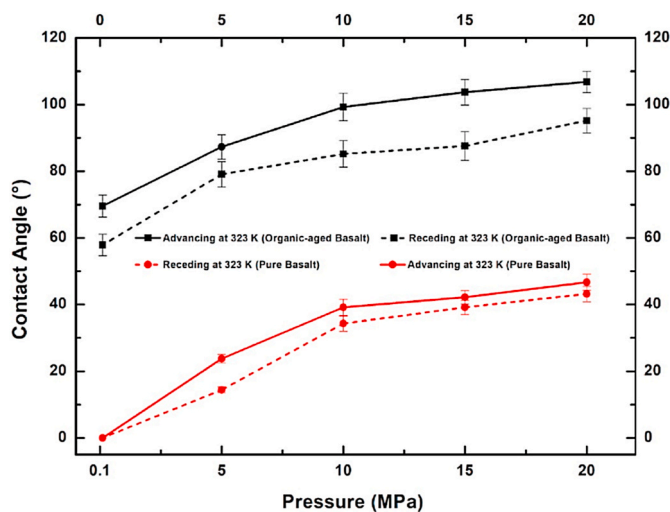


Fig. 6. Contacts angle measurements of pure and organic aged basalts at different pressures (Ali et al., 2023a).

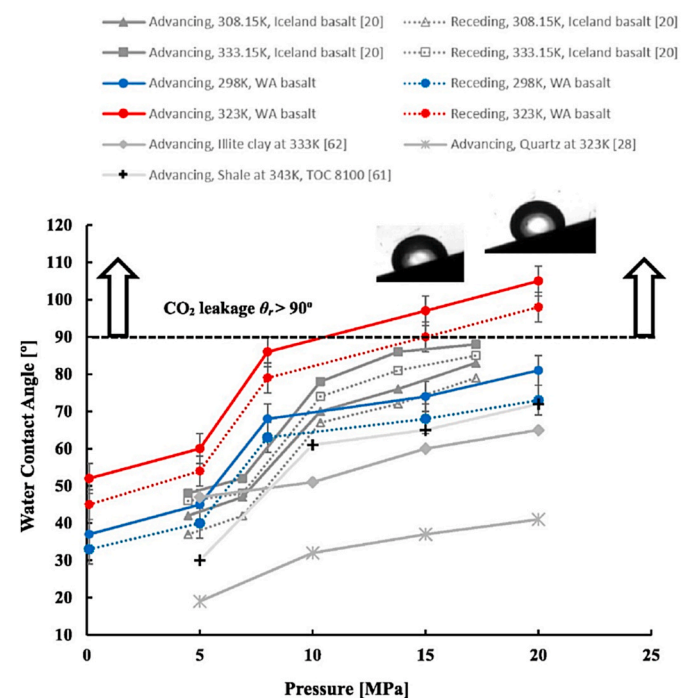


Fig. 7. Contacts angle measurements of WA basalts at different pressures and temperatures compared to other basalts in other regions (Al-Yaseri et al., 2021b).



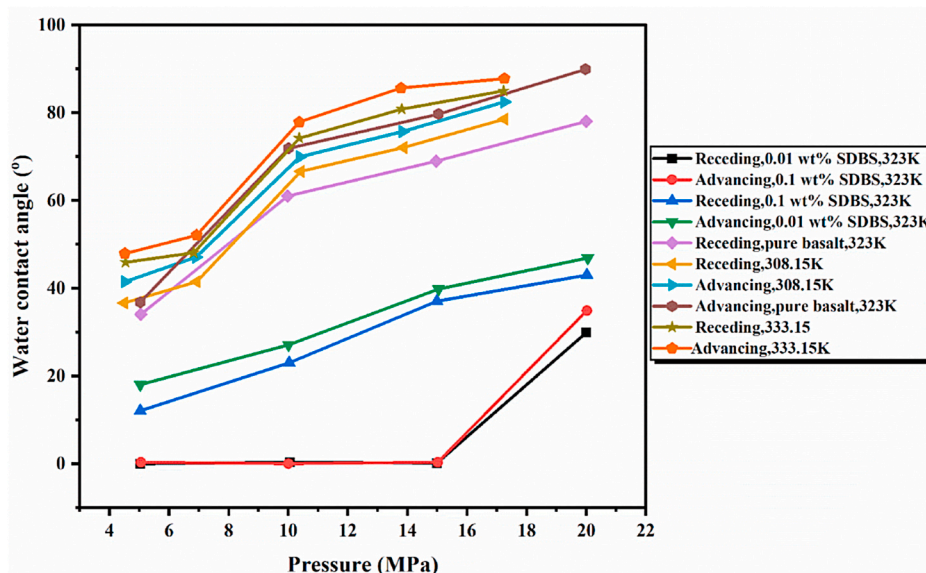


Fig. 8. Effects of SDBS on wettability changes in basaltic rocks (Iglauer and Al-Yaseri, 2021).

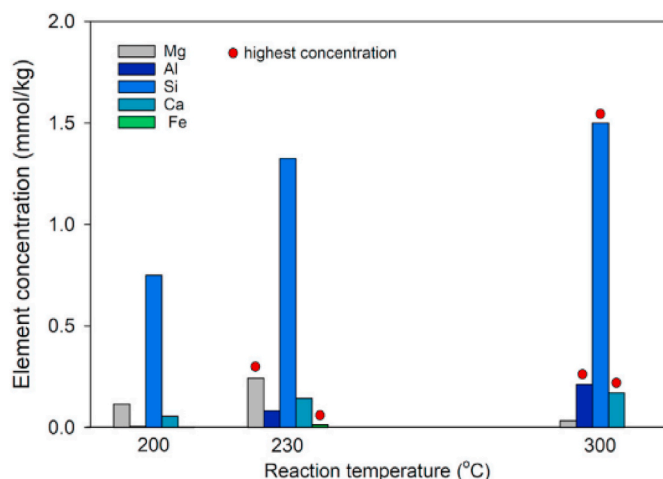


Fig. 9. Mg, Al, Si, Ca, and Fe concentration in  $\text{NaHCO}_3$  after reacting with basalt for 5 days (Kikuchi et al., 2023).

hydrothermal conditions at different temperatures (200–300 °C) to observe the mineralization reactions. It was revealed that  $\text{NaHCO}_3$  enhanced the wettability change to water wet, which influenced mineral carbonation at higher temperatures, as summarized in Fig. 9 by observing high concentrations of Si, Al, and Ca at higher temperatures after basalt dissolutions. The study observed a significant increase in dissolution at temperatures exceeding 230 °C. Interestingly, magnesium (Mg) and iron (Fe) concentrations did not show this effect. Instead, Mg and Fe levels decreased as the temperature rose from 230 °C to 300 °C. This decrease might be linked to the formation of secondary minerals containing Mg and Fe, such as smectite, which are more prevalent at higher temperatures. For instance, 75 g/kg of  $\text{CO}_2$  was mineralized in basaltic rocks at 300 °C for 5 days, 12.1 times higher than that of 200 °C. The major dominant element released after dissolution was Ca, followed by Mg and Fe, which both precipitated to form carbonates. Na was also released in the system, which carbonated to Na silicates, especially analcime. In general, the main elements released from the dissolution process precipitated rapidly to form secondary carbonate rocks, which promoted more dissolution of metallic divalent cations, especially Ca. This proves the influence of  $\text{NaHCO}_3$ . Similar results on the effects of  $\text{NaHCO}_3$  on influencing  $\text{CO}_2$  sequestration in basaltic rocks were earlier

reported by Menefee et al. (2018), in which increasing  $\text{NaHCO}_3$  concentration from 6.3 mM to 640 mM enhanced mineral carbonation.

Moreover, Depp et al. (2022) did a pore scale investigation on monitoring and controlling mineral carbonation in Wallula injection wells to observe the secondary mineral formation and distributions after 977 tons of supercritical  $\text{CO}_2$  was injected. Optical petrography and electron scanning microscopy were used to characterize physical and chemical features of basalt core samples. Samples were collected through sidewall coring. Three zones were analyzed, including zone 1, which has a shallow depth range of 828–846 m characterized by high pre-injection porosity of 22% with a thickness of 18. Zone 2 has a pre-injection porosity of 13% with a thickness of 8 m at a depth range of 854–862 m which was less altered compared to zone 1. Zone 3 has a pre-injection porosity of 1% with a thickness of 9 m at a depth of 866–875 m, which was altered more than zone 2. It was found that Ca carbonates dominate the inner regions, with Fe carbonates dominating the outer region of the core. Fracture-filling carbonate cement and acicular aragonite were also found. Also, a novel fibro-palagonite-like, weakly crystalline silicate phase on carbonate nodules and pore-lining zeolites was observed. In addition, Fe-dominant carbonate precipitates surrounded by acicular aragonite and rhombohedral Ca-carbonate cores in zoned nodules were also observed to be different from earlier research findings. In general, in post-injection analysis, all zones were altered by precipitations of mineral carbonates, but zone 3 was most altered, followed by zone 2, then lastly, zone 1. Other recently conducted experiments on mineral carbonation investigations are shown in Table 5. Pressure versus temperature plot for the previously conducted experiments are shown in Fig. 10.

#### 4. Potential applications of nanoparticles on enhancing $\text{CO}_2$ sequestration in basaltic rocks

Nanoparticles have emerged as one of the promising technologies for enhancing  $\text{CO}_2$  sequestration in basalts because of inimitable features such as large surface area to volume ratio, ultrasmall size, low costs, and environmentally friendly (Ngata et al., 2022; Rathnaweera and Ranjith, 2020; Youns et al., 2023).  $\text{CO}_2$ -rock interactions such as wettability alteration and interfacial tension (IFT) are essential factors influencing  $\text{CO}_2$  trapping efficiency and mineral carbonation in basaltic rock. This section analyzes the roles of nanoparticles in enhancing  $\text{CO}_2$  sequestration in basaltic rocks.

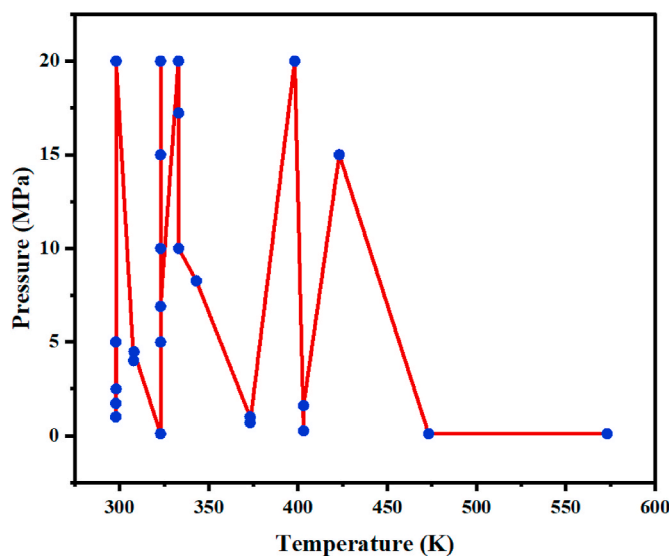
Ali et al. (2023b) tested the effects of nanofluid on enhancing the  $\text{CO}_2$

**Table 5**Few Recently published experimental papers on CO<sub>2</sub> sequestration potentiality in basaltic rocks.

References	Samples origin	Experimental conditions	Key findings
Raza et al. (2023)	Saudi Arabia	- Pressure 8.27 MPa - Temperature 343 K	- Porosity and permeability decreased. - Young's modulus and hardness increased. - Poison ratio remains constant. - Rapid mineral carbonation after interactions with CO <sub>2</sub> in two months.
Voigt et al. (2021)	Mid-ocean ridge basalt (MOR)	- Pressure 0.25–1.6 MPa - Temperature 403.15 K	- 20% of injected CO <sub>2</sub> was mineralized within 4 months. After 150 days, 30% of injected CO <sub>2</sub> was mineralized. - CO <sub>2</sub> -charged seawater mineralized more rapidly than compared to CO <sub>2</sub> -charged fresh water. - Increasing pressure from 0.25 to 1.6 MPa magnetite was dominant, while smectite was largely suppressed.
Moita et al. (2020)	Sines Massif, Portugal	- Pressure 0.7–12 MPa - Temperature 373.15 K	- No other carbonates precipitated, but increased textural roughness of basaltic rocks was observed within 64 days, and smectite formed. - Carbonates were precipitated after 64 days after simulating the experimental data.
Abdulah et al. (2021)	CarbFix injection site in Iceland	- Pressure 4–20 MPa - Temperature 308 and 333 K	- CO <sub>2</sub> -basalt interfacial tension (IFT) is low at shallow depth (low temperatures). - Lower IFT shows high affinity to CO <sub>2</sub> (more probability of CO <sub>2</sub> sequestration). - IFT decreased with an increase in pressure but decreased with an increase in temperature.
de Obeso et al. (2023)	Northern Mexico	- Pressure 20 MPa - Temperature 298.15–398.15 K	- Developed plagioclase dissolution rate equations that depend on temperature change at CO <sub>2</sub> -buffered pH.
Chen et al. (2023)	Henan province in China	- Pressure 10 MPa - Temperature 333.15 K	- CO <sub>2</sub> diffusion and reaction (mineral dissolution and carbonate precipitation) occur simultaneously and interact during carbonation. - Shallow depth is unsuitable for mineral carbonation when pressure is decreased, which is conducive to permanent CO <sub>2</sub> sequestration.
Hosseini et al. (2023)	New Zealand	- Pressure 1.72–6.9 MPa - Temperature 298 and 323 K	- Zeta potential can be used for determining the wetting state of basaltic rocks to assess their CO <sub>2</sub>

**Table 5 (continued)**

References	Samples origin	Experimental conditions	Key findings
Awolayo et al. (2022)	Western Idaho, USA	- Pressure 15–15.1108505 MPa - Temperature 423.15 K	- sequestration potentiality. - Zeta potential remained constant with increasing pressure - Zeta potential increased with temperature and pH, implying more CO <sub>2</sub> wettability state. - Estimated mineral reactive surface area through image analysis using scanning electron microscope and Raman spectroscopic, which is important for predicting CO <sub>2</sub> mineralization in basaltic rocks. - At the field scale, mineral carbonation occurs within 12 months but depends on the timescale and volume of injection. - Change in the accessible surface area affects mineral carbonation, permeability, and porosity evolution, which determine the destiny of injected CO <sub>2</sub> .

**Fig. 10.** Pressure versus temperature for the previous experiments.

trapping capacity of Saudi Arabian basalt for CO<sub>2</sub> sequestration purposes. Rock-CO<sub>2</sub>-brine wettability changes were observed through contact angle measurements, i.e., advancing ( $\theta_a$ ) and receding ( $\theta_r$ ) after nanofluid application under numerous pressures (0.1–20 MPa) and constant temperature (323 K) using the tilted plate goniometric method. Silica (SiO<sub>2</sub>), which had 0.05 to 0.75 wt% concentration, was used during the experiment and prepared under different laboratory conditions. Effects of nanofluid for advanced and receding contacts showed that contact angles increased as pressure increased under isothermal conditions. In addition, it was revealed that the organic acid-aged basalt was hydrophobic and CO<sub>2</sub> wet, unlike the pure basalt. SiO<sub>2</sub> nanofluids changed basalt wettability to weakly or intermediate water-wet conditions, depending on its concentration. 0.1 wt% of SiO<sub>2</sub> nanofluid

concentration was optimal for maximum water wettability alteration. Further, this wettability alteration by adding SiO<sub>2</sub> nanofluid in basaltic rocks influences the rapid mineral carbonation process and residual and structural trapping efficiencies because the negative charges of SiO<sub>2</sub> nanofluid adsorbed on the basaltic surfaces with positive charges due to electrostatic forces attractions which help on the wettability alteration towards water wet. In addition, SiO<sub>2</sub> nanofluid application reduced CO<sub>2</sub> seepage-associated risks for long-term storage.

Also, Al-Yaseri et al. (2021a) examined the effects of utilizing silica nanofluids (100, 1000, and 2000 mg L<sup>-1</sup>) on enhancing CO<sub>2</sub> trapping efficiencies during CO<sub>2</sub> sequestration in basaltic rocks collected from the injection site at Carb Fix Hellisheidi in Iceland at 500 m depth. After SiO<sub>2</sub> nanofluid addition under different operating conditions, i.e., pressure (5–20 MPa) and temperature (323 K), CO<sub>2</sub>-brine-basalt (three phase) wettability alteration was assessed through contact angle measurements using a tilted plate goniometric setup. After treating the basaltic rocks with silica nanofluids, the concentration was 1000 mg L<sup>-1</sup> enriched with brine, it was found that the basaltic rocks' wettability changed from CO<sub>2</sub>-wet to weakly water-wet, in which contact angles were reduced by approximately 40%. In addition, CO<sub>2</sub> column height was reduced after SiO<sub>2</sub> nanofluid treatments, which means that the leakage risk was reduced while residual and structural trapping efficiencies increased. Furthermore, the wettability alteration towards water-wet enhanced mineral carbonation due to the electrostatic attraction between divalent cations from the basalts rocks (Fe<sup>2+</sup>, Ca<sup>2+</sup>, and Mg<sup>2+</sup>) and anions from SiO<sub>2</sub> nanofluid. Apart from that, the basalt pore size distribution increased after SiO<sub>2</sub> applications, as shown in Fig. 11, from 0.000256 cc/g to 0.055 cc/g, which shows that the CO<sub>2</sub> sequestration will also increase due to the formation of new pore spaces.

Further, Al-Anssari et al. (2017) investigated the effects of nanofluid treatments on enhancing CO<sub>2</sub> sequestration in basaltic rocks at different pressures, temperatures, and salinity through contact angle measurements. The research suggests that higher nano-treatment temperatures lead to a reduced change in contact angle following the treatment, as shown in Fig. 12. This effect appears to be caused by a decrease in the adsorption rate of the nanoparticles on the calcite surface. Also, the study found that increasing CO<sub>2</sub> pressure lowered the contact angle for all tested temperatures, as shown in Fig. 12. This decrease is likely due to changes in the acidity of the calcite solution near the surface, which affects the interaction between the positively charged calcite and the negatively charged hydrophilic silica nanoparticles. The contact angle further decreased with higher nanoparticle concentration and longer exposure time, as shown in Fig. 13. The study also identified an optimal

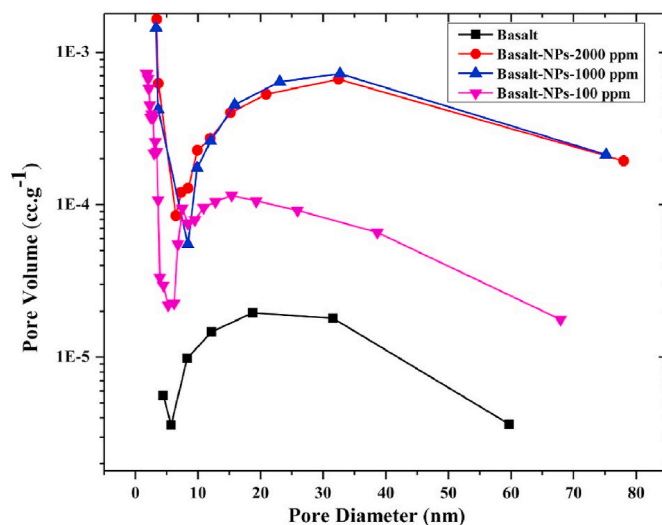


Fig. 11. Nanoparticles (NPs) effects in pore volume formation for basaltic rocks (Al-Yaseri et al., 2021a).

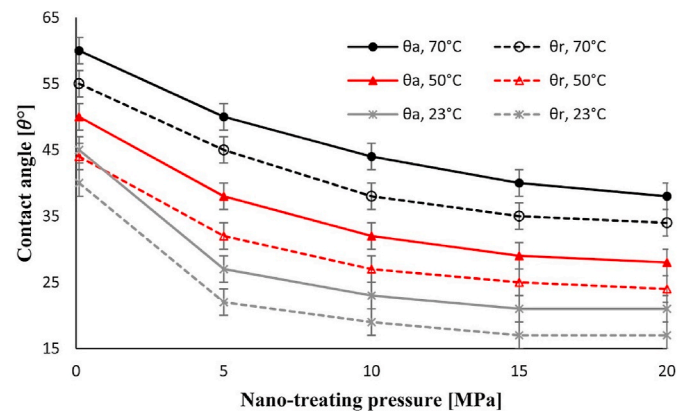


Fig. 12. Contact angle changes towards water wet due to nanofluids treatments at different pressures and temperatures (Al-Anssari et al., 2017).

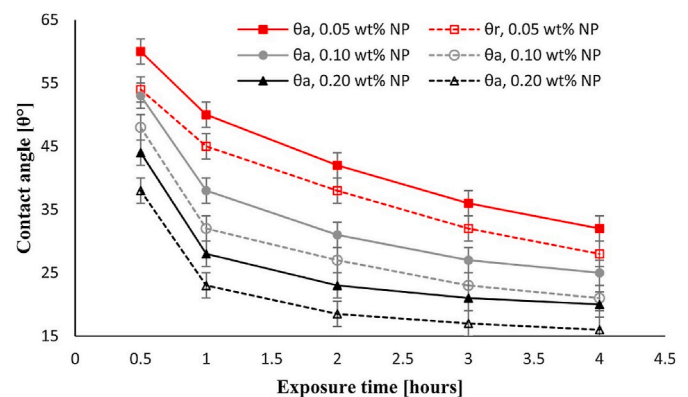


Fig. 13. Contact angle alteration due to nanofluids exposure time in basaltic rocks (Al-Anssari et al., 2017).

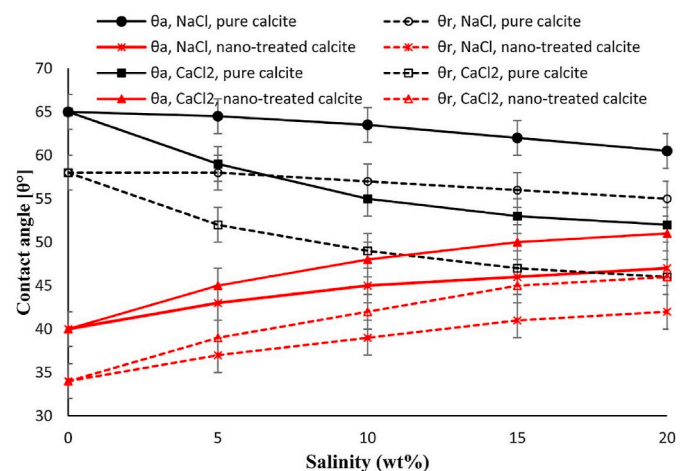


Fig. 14. Effects of salinity contact angle of pure basalts and nano-treated basalts (Al-Anssari et al., 2017).

pH range of 4–6 at ambient pressure for the nanoparticle modification to have the most significant impact. Further, it was found that salinity increase in pure basalt decreased the contact angle while, in nano-treated basalt, the contact angle increased and was more pronounced in CaCl<sub>2</sub> than NaCl, as shown in Fig. 14. It can be concluded that calcite in its natural state exhibits weak affinity for water under typical storage conditions. This can significantly reduce the capacity for CO<sub>2</sub> to be trapped within the rock formations, posing a potential



challenge for storing CO<sub>2</sub> in carbonate reservoirs. Fortunately, pre-treating the calcite surface with nanofluids significantly altered its wettability to water wet, which favors CO<sub>2</sub> sequestration.

Moreover, Al-Anssari et al. (2016) experimented to investigate the wettability change of basaltic rocks towards water wet after nanofluid application, which can enhance CO<sub>2</sub> sequestration in basaltic rocks. After scanning electron microscopy SEM images observation (Fig. 15), it was found that the surface of basaltic rocks changed after nanofluid treatments confirmed extensive adsorption of nanoparticles on the calcite surface. These adsorbed particles formed clusters of varying sizes (Fig. 15). The initial smooth calcite surface, except for a crystal layer edge, became significantly roughened after exposure to the nanofluid. This resulted in an uneven coating across the surface. Analogous observations were made for atomic force microscopy (AFM) images, as shown in Fig. 16. The root mean square (RMS) roughness increased substantially, ranging from 18 nm to 32 nm to 350–3000 nm. Similarly, the peak heights rose significantly from 30–300 nm to 550–5000 nm. Similar to other research findings, it was observed that the contact angle reduced (changed to water wet) as the nanofluid was introduced in basaltic rocks, which influenced CO<sub>2</sub> sequestration in basaltic rocks.

According to the published research, nanoparticles can enhance CO<sub>2</sub> sequestration through mineral carbonation and other trapping mechanisms for long-term storage plans in basaltic rocks. The wettability changes to water wet influence mineral carbonation and other trapping mechanisms; hence, high amounts of CO<sub>2</sub> can be sequestered. However, this technology application needs more experiments, simulations, and pilot tests for full-field operations.

## 5. Modeling and simulations

Modeling and simulation are crucial stages that need to be conducted towards field operations because they help to simulate the actual reservoir conditions of the basaltic formations and predict the project's performance. The amount of CO<sub>2</sub> stored in basaltic rocks can be estimated during this stage. The data used in this stage are collected from conducted experiments respective to their areas. Hence, different modeling and simulation studies are present in this section with different governing equations, especially for mineralization trapping.

### 5.1. Governing equations

The injection and mineral trapping of CO<sub>2</sub> in basalt formations is a reactive transport phenomenon encompassing three distinct phases: the

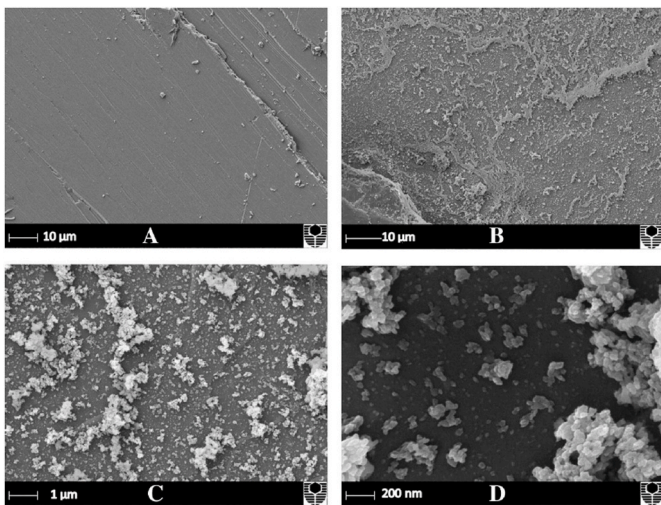


Fig. 15. SEM images on Nanofluids effects on basaltic rock surfaces a) Before nanofluid treatments b) After nanofluid treatments c) High resolution d) Maximum zoom resolution (Al-Anssari et al., 2016).

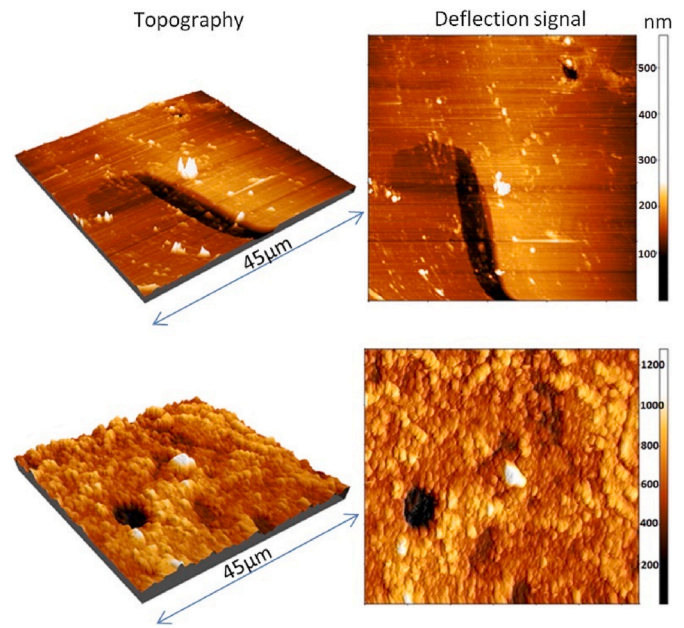


Fig. 16. AFM images before nanofluids treatments in upper images in which the RMS were 32 nm and lower images after nanofluid treatments, in which RMS increased to 1300 nm (Al-Anssari et al., 2016).

formation of water present in the reservoir, the CO<sub>2</sub> introduced into the system, and the rock matrix. The equations that govern mass transport in the system are discussed in sections 5.1.1 and 5.1.2, with geochemistry modeling in sections 5.1.3 and 5.1.4.

#### 5.1.1. Phases

Suppose the flow system has two fluid phases in a porous formation. If  $\alpha$  represents aqueous fluid phase or CO<sub>2</sub>-rich phase ( $\alpha \in \{a, c\}$ ), then the mass balance equation for each phase is as follows (Postma et al., 2021, 2022c; Postma, 2022):

$$\frac{\partial}{\partial t} (\rho_\alpha \phi S_\alpha) + \nabla \cdot (\rho_\alpha q_\alpha) = \psi^\alpha \quad (5)$$

where  $t$  represents time,  $\rho_\alpha$  stands for fluid density at  $\alpha$  phase,  $\phi$  represents porosity of porous formation (basalt),  $S_\alpha$  stands for saturations for phase  $\alpha$ ,  $\psi^\alpha$  represents source term for phase  $\alpha$ ,  $q_\alpha$  represents fluid flow rate for phase  $\alpha$ , which is given represented in Eq. (6), after applying Darcy's law (Postma et al., 2021, 2022c; Postma, 2022).

$$q_\alpha = -K \frac{k_{r,\alpha}}{\mu_\alpha} (\nabla p_\alpha - \rho_\alpha g) \quad (6)$$

where  $K$  stands for second order permeability tensor,  $g$  represents gravity,  $k_{r,\alpha}$  stands for relative permeability for  $\alpha$  phase,  $\mu_\alpha$  is dynamic viscosity for  $\alpha$  phase,  $p_\alpha$  is pressure for  $\alpha$  phase. Since the rock matrix, represented as "r" remains stationary, the associated mass balance equation, which excludes a transport term, is given as (Postma et al., 2021, 2022c; Postma, 2022):

$$\frac{\partial}{\partial t} (\rho_r (1 - \phi)) = \psi^r \quad (7)$$

#### 5.1.2. Components

Considering the principle mass of conservation for each chemical component that makes up each phase. Suppose  $\chi_i^\alpha$  is the mass fraction for each  $\alpha$  phase in component  $i$ , then the mass balance for each  $\alpha$  phase in component  $i$  is given as (Postma et al., 2021, 2022c; Postma, 2022);

$$\frac{\partial}{\partial t} (\rho_\alpha \chi_i^\alpha \phi S_\alpha) + \nabla \cdot f_i^\alpha = \psi_i^\alpha \quad (8)$$

where  $f_i^{\alpha}$  is the total mass flux for component  $i$  for the  $\alpha$  phase, including advective transport, dispersion, and diffusion. The mass balance for each component  $i$  in the rock matrix is given as (Postma et al., 2021, 2022c; Postma, 2022):

$$\frac{\partial}{\partial t} (\rho_r \chi_i (1 - \phi)) = \psi_i^{\alpha} \quad (9)$$

The  $\psi$  represent source term mass transfer of component  $i$  between phases occurs through non-kinetic processes like CO<sub>2</sub> partitioning equilibrium between the aqueous phase and CO<sub>2</sub> phase through kinetic processes like mineral reactions. In the current application, these mineral reactions link geochemistry and mass movement (Postma et al., 2021, 2022c; Postma, 2022).

### 5.1.3. Equilibrium: speciation in the aqueous phase

Using the procedures established by Bethke (2022), an equilibrium system can be developed by using the Tableau method, which states that only small aqueous phase species are linear independent within a system. Suppose the system is made up of water solvent species ( $A_w$ ) and other basis species ( $A_i$ ), then ( $A_j$ ) aqueous mixture species is formed through equilibrium reactions as shown in Eq. (10) (Postma et al., 2021, 2022c; Postma, 2022).

$$A_j \rightleftharpoons \sum_i^{K_j} v_{ij} A_i \quad (10)$$

where  $v_{wj}$  and  $v_{ij}$  are stoichiometric coefficients,  $K_j$  represent the equilibrium constant of a system. The equilibrium reactions demonstrate that the basis species function as the fundamental representatives for a collection of combined quantities known as components. These components pertain to the amount of basis species that would be present if all secondary species were to undergo decomposition into the basis species through the equilibrium reactions in Eq. (10). In equilibrium systems, a component's overall mass is conserved.

If the new phase formed is made up of 2 M components with different concentrations, i.e.,  $c_w$  and  $c_i$  (mol/L<sup>3</sup>), then a new geochemical system is formed by multiplying molar components with aqueous phase volume to get the total amount of new species,  $N_w$  and  $N_i$  (mol), respectively, as shown in Eqs. (11) and (12) (Postma et al., 2021, 2022c; Postma, 2022).

$$N_w = V \cdot c_w = n_w \left( b_w + \sum_j v_{wj} b_j \right) \quad (11)$$

$$N_i = V \cdot c_i = n_w \left( b_i + \sum_j v_{ij} b_j \right) \quad (12)$$

where  $b_i$  and  $b_j$  (mol/M) are the molarity of the primary and secondary species,  $V$  represents the volume of the aqueous phase,  $b_w$  is water molarity, which is the inverse of molar mass. For the case of reversible reaction under equilibrium conditions, equilibrium constant  $K$  becomes equal to product activity  $Q$ , as shown in Eq. (13) (Postma et al., 2021, 2022c; Postma, 2022).

$$K_j = Q_j = \frac{a_w^{v_{wj}} \prod_i a_i^{v_{ij}}}{a_j} = \frac{a_w^{v_{wj}} \prod_i (\gamma_i b_i)^{v_{ij}}}{\gamma_j b_j} \quad (13)$$

where  $\gamma$  and  $a$  represent activity coefficient and chemical activity, respectively. Rearranging Eq. (13), we obtain the mass molarity equation as shown in Eq. (14), which was obtained after finding molarities under equilibrium conditions (Postma et al., 2021, 2022c; Postma, 2022).

$$b_j = \frac{a_w^{v_{wj}}}{K_j \gamma_j} \prod_i (\gamma_i b_i)^{v_{ij}} \quad (14)$$

Then, substituting Eq. (14) into Eqs. (11) and (12), nonlinear

molarity system equations are obtained, i.e., Eqs. (15) and (16), in which the unknowns are the molarity of primary species and the mass of free water. This nonlinear system solution describes the state of equilibrium (Postma et al., 2021, 2022c; Postma, 2022).

$$N_w = V \cdot c_w = n_w \left( b_w + \sum_j v_{wj} \frac{a_w^{v_{wj}}}{K_j \gamma_j} \prod_i (\gamma_i b_i)^{v_{ij}} \right) \quad (15)$$

$$N_i = V \cdot c_i = n_w \left( b_i + \sum_j v_{ij} \frac{a_w^{v_{ij}}}{K_j \gamma_j} \prod_i (\gamma_i b_i)^{v_{ij}} \right) \quad (16)$$

### 5.1.4. Kinetic: dissolution and precipitation of minerals

Suppose mineral systems ( $A_{\rightarrow k}$ ) consist of primary and secondary minerals in which secondary minerals formed later also allowed to precipitate. Similar to the reactions that create the secondary species  $A_j$ , we may define reactions for each mineral ( $A_{\rightarrow k}$ ) in terms of the aqueous phase base species as follows (Postma et al., 2021, 2022c; Postma, 2022):



The use of semi-empirical kinetic rate equations determines the rates at which these mineral processes occur. The aforementioned equations establish a correlation between the pace of a reaction and many factors, such as temperature, the composition of the aqueous phase, and the available surface area of the mineral. This correlation is determined by a series of parameters that have been fitted to the data. Provided that each number of moles for every component in the aqueous phase is present at time  $t^0$ , then the number of moles after reaction in a time  $t$  is given as (Postma et al., 2021, 2022c; Postma, 2022);

$$N_w(t) = N_w(t_0) + \int_{t_0}^t \sum_k v_{wk} r_{\rightarrow k}(t') dt' \quad (18)$$

$$N_i(t) = N_i(t_0) + \int_{t_0}^t \sum_k v_{ik} r_{\rightarrow k}(t') dt' \quad (19)$$

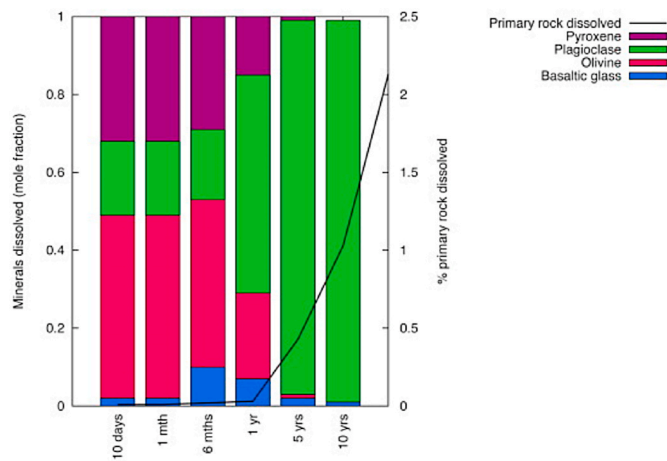
where  $r_{\rightarrow k}$  represent reaction rate in mol/T with all negative values implying mineral precipitations

Gysi and Stefánsson (2011) did a numerical simulation to investigate CO<sub>2</sub> sequestration in low-temperature basaltic rocks from 25 to 90 °C with an initial injection pressure of <1–30 bar. The datasets used were collected from Stapafell, Southwest Iceland. In their study, the numerical results were compared with experimental results. Reaction paths were modeled using PHREEQC geochemical reactions in which the basaltic dissolution rate was modeled using transition state theory (TST) and far from equilibrium rate expression. The results revealed that the basaltic dissolution after CO<sub>2</sub> injection matched the experimental findings for the mineral carbonation process and water compositions, but the reaction path depends on the pH of the water. For pH less than 6.5, SiO<sub>2</sub> and Al-Si minerals, Ca-Mg-Fe carbonates dominated the system, but Al, Fe, and Si were immobile, while Ca and Mg were mobile but depended on the number of carbonates formed and water pH. On the other hand, for a pH of >8, CO<sub>2</sub> mineralization resulted in calcite, Ca-Mg-Fe smectites, and zeolites, which limited the movement of elements within the system. For pH > 8, the Fe and Mg movement was limited due to the presence of clays within the system. It was concluded that the pH of the water is the dominant factor determining basaltic dissolution and mineral precipitations, which depends on concentrations and extent of reactions of CO<sub>2</sub> for low-temperature basaltic rocks.

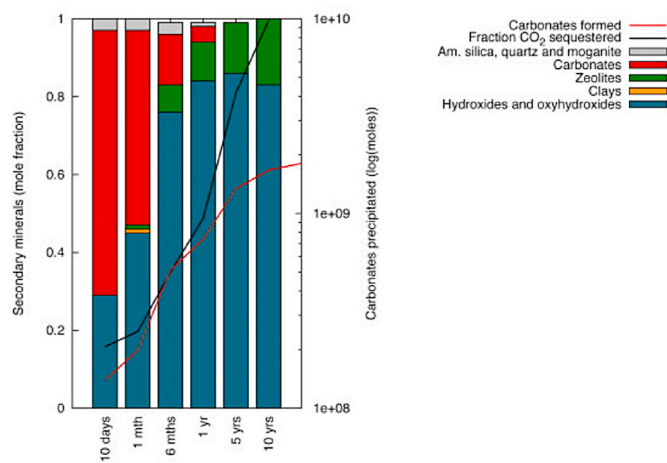
Also, Aradóttir et al. (2012) developed 2D and 3D reservoir models for CO<sub>2</sub> sequestration in basaltic rocks and adjusted against field data in

Hellisheidi, SW, Iceland. The developed models are also used to determine reservoir porosity and permeability. Precipitation rates for most minerals were estimated using neutral pH rate parameters due to lack of precipitation rate data for most of the minerals.  $\text{CO}_2\text{-H}_2\text{O}$ -basalt interaction models were built using TOUGHREACT, which involved pilot and full-scale  $\text{CO}_2$  injection. Reactive chemistry was integrated into standardized models and projected mass transport, and reactive transport simulations were performed for both 1,200 and 400,000 tons for pilot and full field  $\text{CO}_2$  injection, respectively. Reactive transport simulations predicted 100%  $\text{CO}_2$  mineralized in 10 years in a surface area of 5000 tons/ $\text{km}^2$  while a full field was 80% in 100 years in a surface area of 35,000 tons/ $\text{km}^2$ . The rates predicted for  $\text{CO}_2$  sequestration were 12,00 and 22,000 tons for pilot and full field, respectively. However, 3D simulations matched better with field data than 2D simulations. It was concluded that basaltic rocks are suitable for  $\text{CO}_2$  sequestration, with calcite being the most precipitated mineral at a depth greater than 500 m and feldspars (plagioclase) generally dissolved at faster rates than other common primary minerals for 2D and 3D simulations, as shown in Figs. 17 and 18, respectively. This is because feldspars have a crystal structure that is more susceptible to attack by water and dissolved ions in the environment. Furthermore, it was predicted that minerals like clay, oxides, and oxyhydroxides may compete with magnesite-siderite for magnesium and iron released from primary minerals. Similarly, zeolites may compete with calcite for dissolved calcium.

Further, Liu et al. (2022) simulated  $\text{CO}_2$  sequestration in 2D of

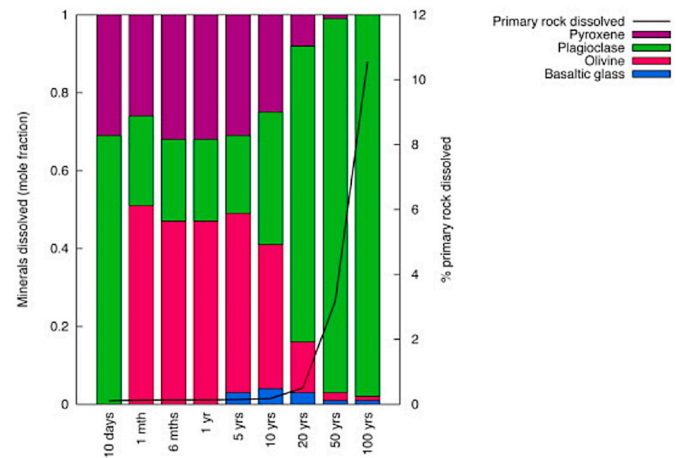


(a) Primary mineral abundance

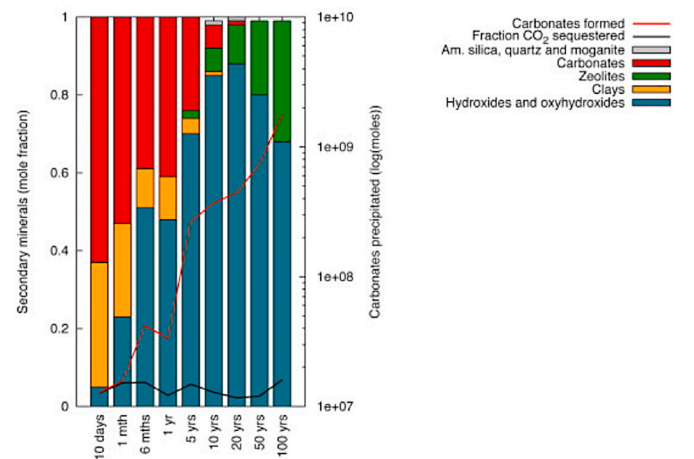


(b) Secondary mineral abundance

Fig. 17. 2D simulations a) Before the mineral carbonation process b) After the mineral carbonation process (Aradóttir et al., 2012).



(a) Primary mineral abundance



(b) Secondary mineral abundance

Fig. 18. DD simulations a) Before the mineral carbonation process b) After the mineral carbonation process (Aradóttir et al., 2012).

eastern Deccan basalt in India using TOUGHREACT, in which  $1.2096 \times 10^4$  tons were injected at an injection rate of 1 kg/s for 140 days. Three scenarios were considered to assess the mineralization process, such as different injection rates of 0.4 kg/s, 0.5 kg/s, 2 kg/s, and 3 kg/s. Another scenario examined the effects of clays on mineralization, and another analyzed the effects of aluminosilicate minerals on precipitation and rate of injection. It was found that around 50% of  $\text{CO}_2$  injected into Deccan basalt rock (Mandla lobe) can be mineralized within 140 days, as shown in Fig. 19 (a), similar to findings from the CarFix2 project. The captured  $\text{CO}_2$  primarily forms stable minerals like ankerite (65%), siderite (28%), and calcite (7%), as shown in Fig. 19 (b). Additionally, significant amounts of clay minerals, particularly chlorite (57%) and smectite (43%), were produced during the mineralization process, as depicted in Fig. 19 (c). This suggests that calcium released from dissolving rock minerals is incorporated into calcite and ankerite for  $\text{CO}_2$  storage, while magnesium, iron, and silicon contribute to the formation of new clay minerals. However, a 3D model was recommended for future studies to obtain accurate results. Also, it was revealed that the injection rate increases the mineralization process, but an optimal injection rate needs to be obtained to avoid risk leakages. Further, it was found that clays enhance the mineralization process by releasing  $\text{H}^+$  which helps basaltic rock dissolution. Also, aluminosilicate helps to dissolve basaltic rock, which is essential for mineral carbonation.

Moreover, Bacon et al. (2014) simulated the supercritical  $\text{CO}_2$  sequestration potentiality in basaltic rocks with impurities ( $\text{H}_2\text{S}$ ) in



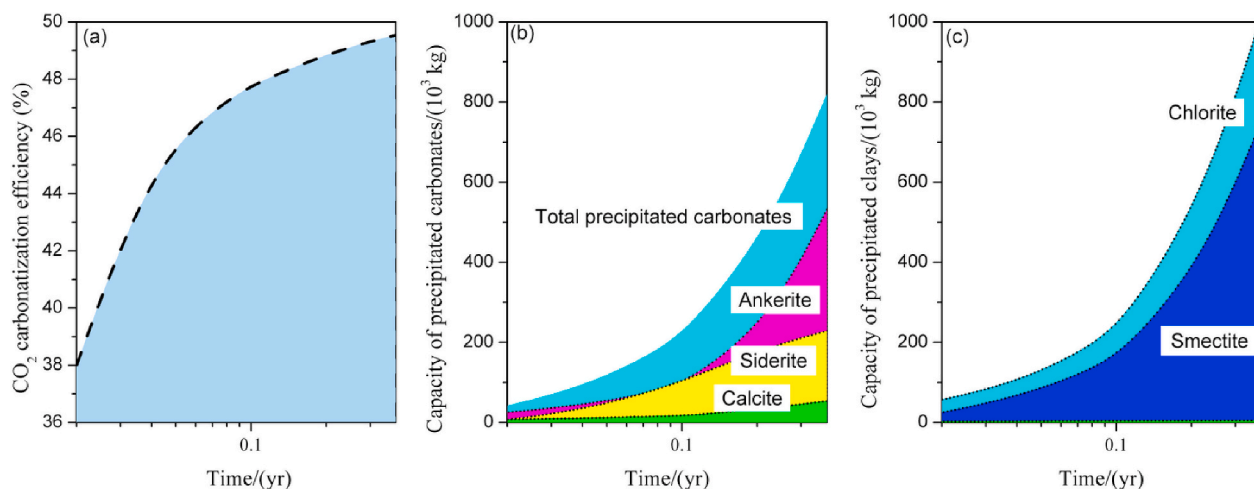


Fig. 19. a) CO<sub>2</sub> carbonization efficiency b) Capacity of precipitated carbonates c) Capacity of precipitated clays (Liu et al., 2022).

Columbia River Basalt located in the eastern part of the USA. The STOMP-COMP simulator was used to build the model in their study. It was assumed that the reservoir properties were homogeneous. From 1000 tons of injected gas, 99% was CO<sub>2</sub> with 1% H<sub>2</sub>S. It was revealed that from the injected 1000 tons of mixture, gases were sequestered rapidly in solubility and mineral trapping mechanisms. Most injected CO<sub>2</sub> was stored in the form of calcite, with other few in siderite, dolomite and dawsonite, and H<sub>2</sub>S precipitated into pyrite form after four years. Iron for pyrite formation likely comes mainly from dissolving the glass-like material between mineral grains (mesostasis) and to a minor degree, from the breakdown of a specific mineral called hedenbergite. In contrast, calcium for calcite formation originated from anorthite, diopside, and hedenbergite primary minerals. Among the primary minerals utilized, anorthite dissolves faster, followed by mesostasis.

Moreover, McGrail et al. (2011) simulated injecting CO<sub>2</sub> in the Wallula basalt pilot area by injecting 1000 tons of CO<sub>2</sub> for 14 or 30 days. The model was built using the STOMP-H<sub>2</sub>O-CO<sub>2</sub>-NaCl model simulator in which there were three injection horizons, which are the Ortlely flow top (OFT), the Slack Canyon #1 flow top (SCFT1) and the Slack Canyon #2 flow top (SCFT2). It was revealed that after one year of injection, 18% of injected CO<sub>2</sub> was dissolved in brine, which helps in basalts dissolutions, which release metallic cations that are important for the mineral carbonation process and thus help in tracking the mineralization process within the host rock. In addition, Al Maqbali et al. (2023b) did a 3D numerical simulation using CMG for mineral carbonation for basaltic rocks in Southwest Oklahoma. The model was designed to simulate chemical reactions between brine and injected supercritical CO<sub>2</sub>. The CO<sub>2</sub> was injected at a rate of 200 MCF/day for 4 years. It was revealed that 97% of injected CO<sub>2</sub> was mineralized with other stored as residual and solution form and mineralization resulted into 5% of porosity reduction. Magnesite account 89% with calcite account 11% of the CO<sub>2</sub> mineralized, as shown in Fig. 20, due to the fact forsterite (Mg<sup>2+</sup> source) underwent dissolution for several years while wollastonite (Ca<sup>2+</sup> source) dissolved faster within a few years. In general, basaltic rocks in Southwest Oklahoma have shown great potential for storing CO<sub>2</sub>.

In addition, Gierzynski and Pollyea (2017) modeled and simulated three-phase flows and CO<sub>2</sub> sequestration in fractured basalt formation from mapping conducted in outcrop mapping of LiDAR in Columbia River Basalt in the USA. TOUGH3 software was used to build the model, and ECOM2M was used to simulate mixtures of fluid flows. After 10 years of injection, it was revealed that most of the injected CO<sub>2</sub> accumulated at the intersections of fractures. It can be enhanced to mineral carbonates with the flow of CO<sub>2</sub> converging on a single dominant path flow. Also, it was found that permeability variation occurs after an interval of 1.6 m and supercritical CO<sub>2</sub> is changed to subcritical gas or

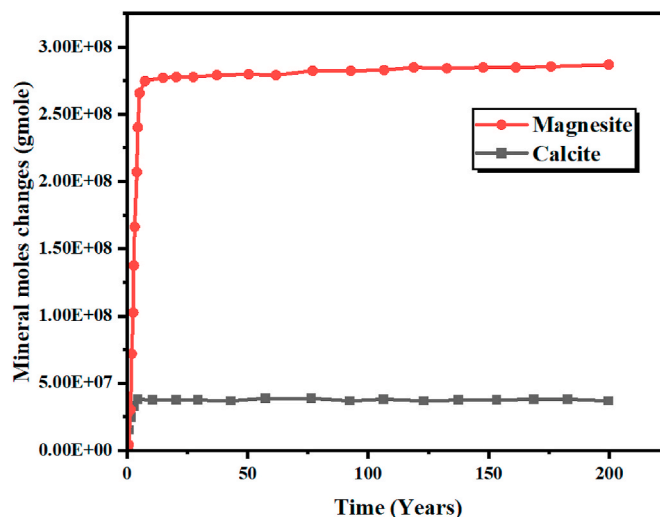


Fig. 20. Amount of CO<sub>2</sub> mineralized into different minerals (Al Maqbali et al., 2023b).

liquid. Similarly, Wu et al. (2021) simulated CO<sub>2</sub> sequestration potentiality in fractured basaltic rocks to understand its flows and mineralization process. TOUGHREACT v3.2-OMP software was used to build the model with ECOM2N used to simulate mixtures of fluid flows, porosity, and permeability changes. It was revealed that CO<sub>2</sub> mineralization occurs at the intersection of fractures with good porosity and permeability, enhancing the mineralization process but hinder the injection process after mineral carbonation. However, when the connection between porosity and permeability is stronger, less CO<sub>2</sub> mass enters the crack, which means less mineral precipitation. Fig. 21 proved that calcite was the most precipitated secondary mineral after 10 years of simulations with a small amount of magnesite and siderite, as shown in Fig. 22.

Furthermore, Postma et al. (2022b) developed a vertically integrated approach for modeling CO<sub>2</sub> sequestration on a field scale through mineral trapping in basaltic rocks using the CarbFix method. The model built was for two-phase flows with the ability to execute geochemical reactions at field scale level for a long-term storage plan. In addition, the developed model was flexible, efficient reactive transport, and could run many simulations compared to other models. The simulation was conducted for 50 years for both supercritical and CO<sub>2</sub> saturated with formation water at an injection rate of 0.1 megatons per year. It was revealed that most injected CO<sub>2</sub> were sequestered as minerals, as

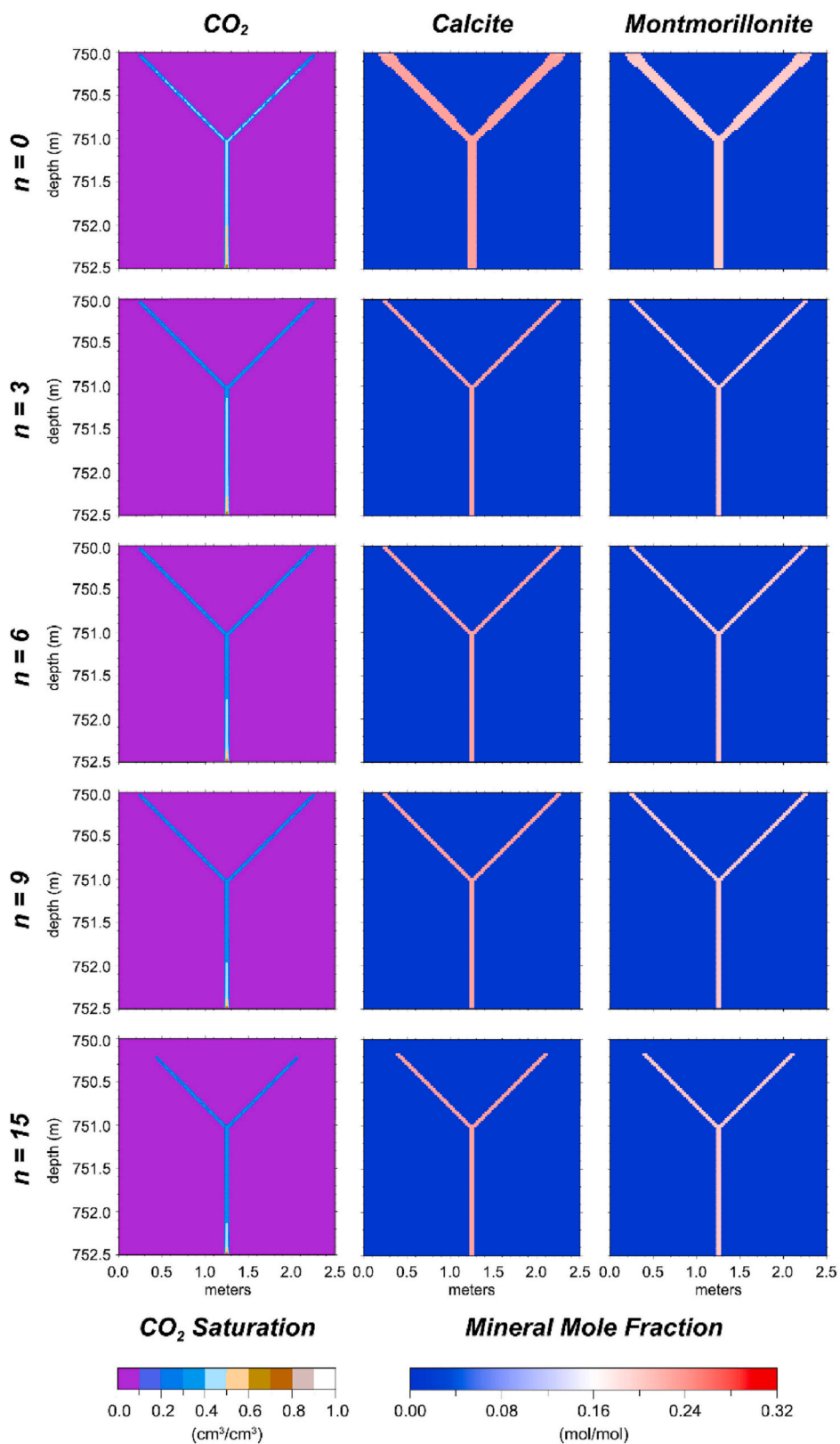


Fig. 21. Amount of secondary precipitated minerals (Wu et al., 2021).

reported in many literatures, where injecting supercritical CO<sub>2</sub> led to the hindrance of mineralization to occur faster, as shown in Fig. 23 (left side). Still, the CarbFix method (right side of Fig. 23) led to mineralization occurring faster, matching other researchers' findings. In addition, it was found that when supercritical CO<sub>2</sub> was injected, its

mineralization rate was much lower than that of injected CO<sub>2</sub> saturated with water due to limited chemical reactions between injected CO<sub>2</sub> and basaltic rocks. Also, Snæbjörnsdóttir et al. (2018) did a simulation using PHREEQC to investigate the reaction path of mineral carbonation of injected CO<sub>2</sub> at the CarbFix site in Hellisheidi, SW-Iceland. After the

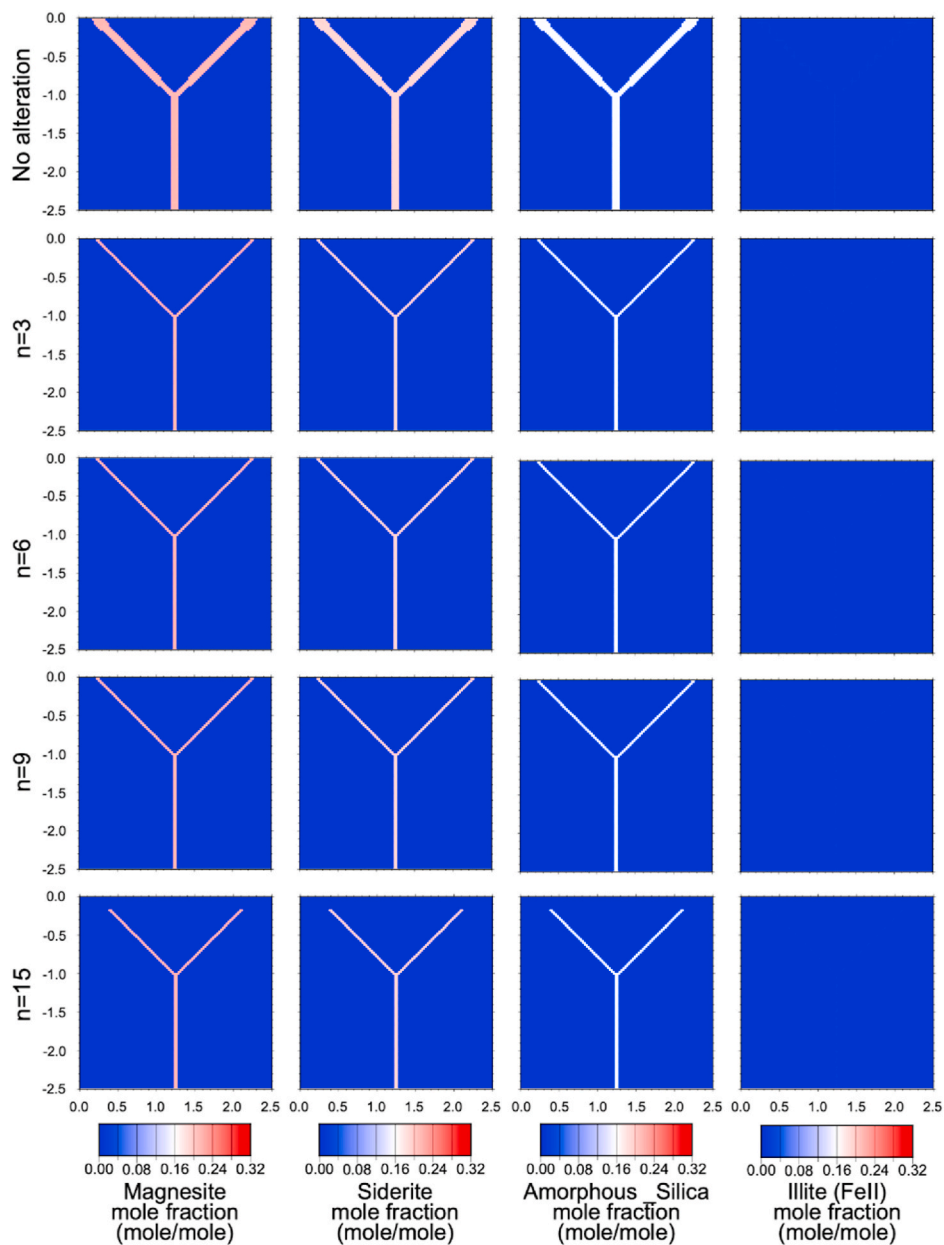


Fig. 22. Amount of secondary precipitated minerals (Wu et al., 2021).

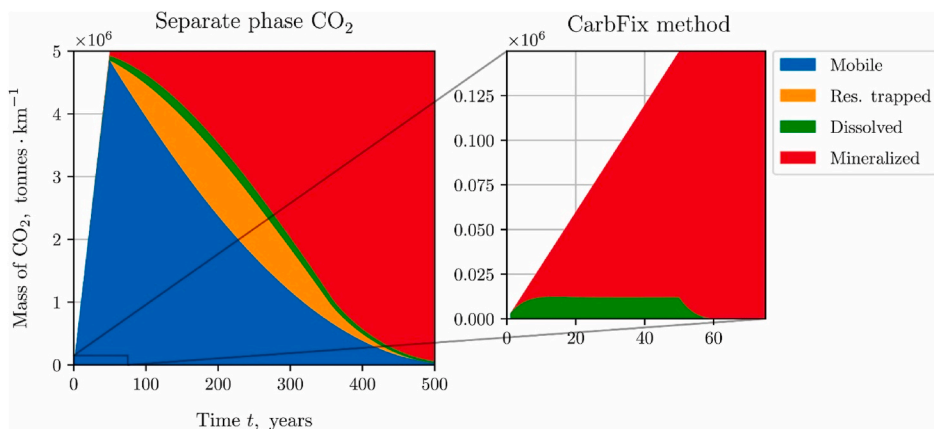


Fig. 23. Comparisons between the CarbFix method (right) for CO<sub>2</sub> mineralized and when separate phases of CO<sub>2</sub> injected to be mineralized (Postma et al., 2022b).



injection of 175 tons of CO<sub>2</sub>, it was revealed that basaltic rock dissolution was the major driving factor for the mineral carbonation process, which took place within 400 days. Also, reaction path modeling revealed that a pH range of 5.2–6.5 of basaltic rocks having a low temperature of 20–50 °C was suitable for mineralization process. Further, injecting CO<sub>2</sub> at high pressure was recommended to avoid permeability and porosity reduction due to zeolite and clay formation near the wellbore. Moreover, it was found that ~95% of injected CO<sub>2</sub> at CarbFix were mineralized but consumed 500 tons of basaltic rocks, resulting in 420 tons of carbonates, 450 tons of zeolites, and 100 tons of smectites.

Moreover, Cao et al. (2023) did a simulation to investigate CO<sub>2</sub> mineralization reactive transport in stacked Columbia River basalt reservoirs using the STOMP-CO<sub>2</sub> simulator with the ECKEChem. The simulation considered geochemical reactions of host rock, precipitation of brines, and CO<sub>2</sub> injected. In their simulation, 977 tons of CO<sub>2</sub> were injected at a depth range of 830–886 m. Two scenarios were considered in their simulations. In scenario A, the injected zone is enriched with initial basalt of plagioclase, clinopyroxene, and glass, with secondary lithology having phyllosilicate and carbonate minerals. In scenario B, the clinopyroxene dissolution rate was intermediate compared to faster glassy mesostasis and plagioclase feldspar. After 10 years, the results revealed that 20% of injected CO<sub>2</sub> was mineralized for scenario A and 39% was stored in aqueous form, while for scenario B, 90% was mineralized, 8% was stored in aqueous form, and 2% remained as free phase in basaltic rocks. With reference to the two scenarios' results, it implies that it is important to understand basalt mineral compositions and their dissolution rate to have accuracy in predicting CO<sub>2</sub> to be sequestered. It was concluded that the developed numerical simulations transport model can be adapted for field applications to reduce risk leakages and storage capacity optimizations. Other literature on CO<sub>2</sub> sequestration in basalts is summarized in Table 6.

## 6. Pilot test applications

The success of experiments and modeling and simulation from previous literature inspired two larger pilot tests in Iceland and the USA towards full field operations in the future. In these two pilot tests, it has been demonstrated that basaltic rocks can store CO<sub>2</sub> gas in the form of carbonate minerals, and the process occurs in less than two years and seems safe with less leakage risk for long-term planning. These two pilot tests are:

### 6.1. Hellisheidi, Iceland - the CarbFix project

CarbFix pilot test can be traced back to 2006, followed by securing funds in 2007, in which tracer slug tests were conducted. From 2008 to 2009, permits and licenses for injection and monitoring were obtained. After that, experiments, design, field studies, modeling and simulations were conducted, and in 2010, preparation of capturing design and facilities were installed in 2012, 175 tons of pure CO<sub>2</sub> and 73 tons of gas mixture (75% CO<sub>2</sub>, 24% H<sub>2</sub>S, and 1% H<sub>2</sub>) mixed with water were injected for the first time captured from Hellisheidi geothermal power plant which emits 60,000 tons per year in southwest of Iceland at a depth of 350 m at a temperature range of 20–50 °C in which 95% of injected CO<sub>2</sub> were mineralized within two years mostly calcite determined through mass balance and tracer tests (Ragnheidardottir et al., 2011). In 2014, on an industrial scale (CarbonFix2), mixtures of captured (CO<sub>2</sub>+H<sub>2</sub>S) were continuously injected below 700 m depth at a temperature of >250 °C. In 2017, the first scale industrial operations were conducted in which 15,000 tons of mixture (CO<sub>2</sub>+H<sub>2</sub>S) were injected. Also, in 2017, direct air capture (DAC) started, funded by the EU to develop technology to store CO<sub>2</sub> in deep ocean subsurface rocks (basaltic rocks). Due to the formation of the gas-charged condensate water injection from 2013 to 2017, 23,200 tons of CO<sub>2</sub> and 11,800 tons of H<sub>2</sub>S were injected at a depth of 750 m (Clark et al., 2020). The cost of

this pilot test was 12 million EUR from 2006 to 2016, excluding pilot test gas capture and well infrastructure, which Reykjavík Energy donated. USA funded two-thirds of the cost. Reykjavík Energy reported that the CarbFix project will save money because the cost used to mitigate emission of H<sub>2</sub>S was over 100 million Euro up to 2018. It is estimated that CarbFix can help to store 100,000–250,000 giga tons of CO<sub>2</sub> under the sea floor (mid oceanic ridges) globally (McGrail et al., 2006; Snæbjörnsdóttir et al., 2020). The major source of CO<sub>2</sub> in the CarbFix project is the geothermal power plant, which generates 83% of CO<sub>2</sub>, 16% of H<sub>2</sub>S, and the remaining from CH<sub>4</sub>, N<sub>2</sub>, and H<sub>2</sub> production (Matter et al., 2009).

Despite the success of storing CO<sub>2</sub> in basaltic rocks, there are several challenges that CarbFix faced, such as severe broken of condensers and other equipment caused by corrosion due to H<sub>2</sub>S and water vapor presence, which caused the delay of the project, permeability reduction, which cause difficulty in injection, damage of the pipeline used to transport gases to injection sites caused by road construction activities, pipe explosion which connects capture and injection plant due to high pressure (Gíslason et al., 2018). The CarbFix project has the purpose of storing more than 90% of emitted CO<sub>2</sub> from the Hellisheidi geothermal power plant in the future. In 2020, approximately 65% of injected CO<sub>2</sub> was mineralized within two months (Snæbjörnsdóttir et al., 2020).

### 6.2. Wallula, USA

CO<sub>2</sub> injection took place for 25 days from July 17, 2013, to August 11, 2013, which were supplied through truck tankers that were received from rail transport tankers collected from a refinery in Washington state or California to Wallula, USA. Before injection, CO<sub>2</sub> was heated to 44 °C and pressurized with continuous monitoring of flows, temperature, and pressures through the delivery system and sensors (McGrail et al., 2014a, 2017b). In these 25 days, approximately 1000 tons of liquid CO<sub>2</sub> were injected (McGrail et al., 2017b). The liquid CO<sub>2</sub> was injected at a continuous injection rate of roughly 40 tons per day at a depth of 800–900 m, with geochemical reactions between injected CO<sub>2</sub>, basaltic rocks, and formation water monitored throughout. Approximately 977 tons of CO<sub>2</sub> were injected into the Columbia River basalt reservoir with a limited injection pressure of 2.8 MPa to match the downhole test interval pressure. Perfluorodimethylcyclobutane and perfluorocarbon tracer (PFT) were infused within 48 h of injection in the CO<sub>2</sub> stream (McGrail et al., 2017a). After two years of post-injection, side well cores were conducted, which revealed that carbonate nodules rich in Ca and Fe were formed in basalt pores and fractures. These carbonates originated from injected CO<sub>2</sub> confirmed after isotopic analysis. However, after geophysical analysis, it was found that there so much free phase of injected CO<sub>2</sub> within the formation after two years of injection (Snæbjörnsdóttir et al., 2020; White et al., 2020a). The suggested monitoring techniques for CO<sub>2</sub> sequestration in basaltic rocks are summarized in Table 7.

### 6.3. Economic analysis on CO<sub>2</sub> sequestration in basaltic rocks

CO<sub>2</sub> capture currently dominates the cost of CO<sub>2</sub> sequestration, holding 70–80% of the overall costs due to several factors like the technical complexity of capture processes, the energy required to separate CO<sub>2</sub> and the relative immaturity of the technology (Dziejarski et al., 2023). Pre-combustion and post-combustion capture both have drawbacks, while direct air capture is promising but faces significant development hurdles (Kanniche et al., 2010). CO<sub>2</sub> sequestration in basalts holds promise for mitigating climate change, but successful implementation requires a comprehensive techno-socio-economic analysis. Addressing technological challenges, achieving social acceptance, and ensuring economic viability are crucial for realizing the full potential of this technology. Continuous research and development efforts are needed to improve capture, transportation, and storage technologies. At the same time, robust regulatory frameworks and economic

**Table 6**  
Other few simulations literature in CO<sub>2</sub> sequestration in basalt.

Reference(s)	Aims	Software(s) used	CO <sub>2</sub> phase	Carbonate precipitated	Key findings
Zhao et al. (2024)	To explore the CO <sub>2</sub> sequestration potentiality in basalt in the Xingouzui Formation in Jiangling Depression, Jiangnan Basin, through dissolution and precipitation	TOUGHREACT	ScCO <sub>2</sub>	Siderite and ankerite	<ul style="list-style-type: none"> <li>- Jiangling Depression basalt has the potential to store 2.804 Gt of CO<sub>2</sub>.</li> <li>- Co-injecting CO<sub>2</sub> and water in basalts offers a two-fold benefit: water enhances CO<sub>2</sub> dissolution, and the slightly acidic solution created by this process promotes the dissolution of minerals in the rock formation; hence, leakage risk is minimized.</li> <li>- Unaltered basalt formations exhibit high reactivity with CO<sub>2</sub>, potentially capturing between 22 and 49 kg/m<sup>3</sup> of rock within the first month of injection, and after one year, the CO<sub>2</sub> mineralized reached 52 kg/m<sup>3</sup>.</li> </ul>
Berndsen et al. (2024)	Compare experimental and simulation results on CO <sub>2</sub> sequestrations in basaltic rocks.	PHREEQC	ScCO <sub>2</sub>	Calcite	<ul style="list-style-type: none"> <li>- Experiments and modeling suggest that the mineral composition of glassy basaltic rocks provides a potential source of divalent cations (positively charged ions with two valence electrons) that could be favorable for CO<sub>2</sub> sequestration.</li> <li>- Simulations overestimate CO<sub>2</sub> stored in glassy basaltic rocks for higher temperatures.</li> <li>- To ensure the accuracy of numerical modeling, the study emphasizes the value of complementing it with experimental validation.</li> </ul>
Huerta et al. (2020)	To investigate the influence of hydraulic fracturing on injectivity and storage performance of CO <sub>2</sub> .	STOMP-CO <sub>2</sub>	ScCO <sub>2</sub>	Calcite, magnesite, magnetite	<ul style="list-style-type: none"> <li>- The simulation results revealed that the injectivity of the fractured well was improved from 13 to 71%, depending on the horizontal well lengths, number of fractures, fracture geometries, and fracture properties.</li> <li>- Vertical fractured wells achieved 60% of injected CO<sub>2</sub> (22 Mt) for 20 years, while horizontal fractured wells attained a maximum of 80% of injected CO<sub>2</sub> (22 Mt) for 20 years.</li> <li>- The most injected CO<sub>2</sub> was stored as the free phase, followed by the aqueous phase, with a small amount stored in the trapped phase.</li> </ul>
Lei et al. (2021)	To explore the use of hydraulic fracturing as a method to enhance CO <sub>2</sub> injectivity and storage performance.	TOUGH2-REACT	ScCO <sub>2</sub>	Calcite, kaolinite, smectite, and ankerite.	<ul style="list-style-type: none"> <li>- Simulation results indicated enhanced basalt reservoirs are promising for CO<sub>2</sub> sequestration in space-constrained environments through hydraulic fracturing.</li> <li>- In the fractured zone, there was a minimal decline in permeability by 4.5% and 22.2% for the non-fractured zone after CO<sub>2</sub> injection in 10 years. This shows that CO<sub>2</sub> sequestration in basalt reservoirs, zones with higher initial permeability, is preferable due to slower permeability decline.</li> </ul>
Van Pham et al. (2012)	To investigate the effects of temperature on carbonate formations	PHREEQC-2	ScCO <sub>2</sub>	Magnesite, siderite, ankerite, hematite	<ul style="list-style-type: none"> <li>- Lower temperatures (40 °C) favor iron-based carbonates (siderite and Fe-Mg carbonates) formations.</li> <li>- Calcium prioritizes forming zeolites and oxides over carbonates at 40 °C.</li> <li>- Higher temperatures (60–100 °C) allow for magnesite formation alongside siderite and ankerite.</li> <li>- The total amount of CO<sub>2</sub> stored as stable carbonate minerals depends on available pore space. As the simulations progressed, both hydration and carbonation reactions increased the solid volume within the basalt, potentially limiting further CO<sub>2</sub> storage due to pore blockage.</li> </ul>
Kumar et al. (2017)	Compare experimental and numerical simulation in carbon dioxide sequestration in Mandla basalt rocks.	EQ (3)/6	ScCO <sub>2</sub>	Calcite, aragonite, siderite, and secondary silicates.	<ul style="list-style-type: none"> <li>- There were discrepancies between the results obtained from numerical simulations and those observed in experiments for CO<sub>2</sub> mineralization.</li> <li>- Time is the primary driver of carbonate and secondary silicate formation, in which a short time influences carbonation while increasing pH increases the mineral carbonation process.</li> </ul>
Marieni et al. (2021)	To analyze the effects of injecting CO <sub>2</sub> with H <sub>2</sub> S impurities in basalt at different temperatures.	PHREEQC	ScCO <sub>2</sub> + H <sub>2</sub> S	Calcite, ankerite	<ul style="list-style-type: none"> <li>- 80 to 100% of injected H<sub>2</sub>S were mineralized to pyrite.</li> <li>- 260 °C or above is not a favorable temperature for mineral carbonations to occur.</li> <li>- The best mineralization temperature was 25–170 °C for mineralization to occur.</li> </ul>

**Table 7**  
Recommended CO<sub>2</sub> monitoring methods for CO<sub>2</sub> storage in basalts.

Techniques	Description	Advantages	Disadvantages
Geochemical monitoring	Analysis of produced fluids at the wellhead for dissolved CO <sub>2</sub> , major ions, and trace elements.	<ul style="list-style-type: none"> <li>- Provides direct information on the fate of injected CO<sub>2</sub> and potential leakage.</li> <li>- Geochemical reactions occurring within the basalt formation can be identified.</li> </ul>	<ul style="list-style-type: none"> <li>- Requires careful sampling and analysis procedures.</li> <li>- May not detect small-scale leakage events.</li> </ul>
Pressure monitoring	Measurement of pressure changes within the injection well and the storage formation.	<ul style="list-style-type: none"> <li>- Pressure buildup can be detected, indicative of potential leakage pathways.</li> <li>- Provides insights into reservoir performance and injectivity.</li> </ul>	<ul style="list-style-type: none"> <li>- Limited spatial coverage may not capture pressure changes in distant areas of the formation.</li> </ul>
Seismic monitoring	Deployment of seismic sensors on the surface or downhole to detect microseismic events.	<ul style="list-style-type: none"> <li>- Can identify potential fracturing or induced seismicity associated with CO<sub>2</sub> injection.</li> <li>- Provides broader spatial coverage than pressure monitoring.</li> </ul>	<ul style="list-style-type: none"> <li>- Requires interpretation of seismic data, differentiating between natural and CO<sub>2</sub>-induced events.</li> <li>- High upfront costs for deploying seismic sensor networks.</li> </ul>
Gravity monitoring	Repeated high-precision gravity measurements at the surface.	Can detect changes in subsurface mass distribution due to CO <sub>2</sub> injection or migration.	<ul style="list-style-type: none"> <li>- Requires sophisticated equipment and expertise for data interpretation.</li> <li>- Sensitive to other factors like water table fluctuations.</li> </ul>
Satellite-based InSAR (Interferometric Synthetic Aperture Radar)	Analysis of satellite radar data to detect subtle ground surface deformations.	It offers broad spatial coverage for monitoring potential surface uplift or subsidence.	<ul style="list-style-type: none"> <li>- Requires advanced data processing techniques.</li> <li>- Sensitive to atmospheric conditions and other factors.</li> </ul>
Soil gas monitoring	- Measurement of CO <sub>2</sub> concentrations in soil gas samples collected from the surface.	Can detect leaks of CO <sub>2</sub> migrating upwards through the soil.	<ul style="list-style-type: none"> <li>- Limited depth penetration may not capture deep leakage pathways.</li> <li>- A dense network of sampling points is required for adequate coverage.</li> </ul>
Tracer studies	Injection of inert tracers like SF <sub>6</sub> alongside CO <sub>2</sub> and monitoring their migration behavior.	Provides direct information on CO <sub>2</sub> plume movement and potential leakage pathways.	<ul style="list-style-type: none"> <li>- Additional costs are required for tracer injection and monitoring.</li> <li>- May require complex modeling to interpret tracer data.</li> </ul>

**Table 8**  
Overall cost of CCS in CarbFix project for (CO<sub>2</sub> +H<sub>2</sub>S) mixtures (Gunnarsson et al., 2018).

Stage	Case 1 <sup>a</sup> (US \$/ton)	Case 2 <sup>b</sup> (US \$/ton)	Case 3 <sup>c</sup> (US \$/ton)
Capture	21.3	21.3	42.1
Transport	1.3	1.3	1.3
Injection	1.3	4.1	4.1
Monitoring	0.9	0.9	0.9
Total CCS costs per tonne	24.8	27.6	48.4

<sup>a</sup> On-site scaled up cost at Hellisheidi power plant.

<sup>b</sup> On-site scaled-up cost at Hellisheidi power plant, including drilling a well for injection.

<sup>c</sup> On-site scaled-up cost at Hellisheidi power plant, including drilling a well for injection and using the average OECD electricity price for the industry in 2014 (US \$ 123.9/MWh).

incentives can pave the way for the widespread adoption of CO<sub>2</sub> sequestration in basalts. The summary of costs of one of the successful CCS pilot tests conducted in 2012 is shown in Table 8, in which the overall costs ranged from 24.8 to 48.4 US dollars per tonne from capture to monitoring (Gunnarsson et al., 2018; Kali et al., 2022). For other sedimentary basins' CO<sub>2</sub> geological options, the costs are summarized in Table 9. The cost of CO<sub>2</sub> storage in basalts can be higher initially due to detailed site characterization and slower injection rates. Still, it offers significant long-term stability and reduces monitoring costs due to permanent mineralization. Sedimentary basins, while cheaper and faster to deploy initially, incur higher long-term monitoring and potential remediation costs due to the risk of leakage. The choice between basalts and sedimentary basins depends on the specific project requirements, available infrastructure, and long-term storage goals.

In conclusion, while basalts hold a promising future for CO<sub>2</sub> storage, the need for new infrastructure development and potential challenges with geochemical compatibility currently make sedimentary basins more cost-effective option due to existing infrastructure and a better

**Table 9**  
CO<sub>2</sub> sequestration cost estimates in sedimentary basins (USD \$ per tonne CO<sub>2</sub>).

Stage	Cost range (US \$/ton)	Details	References
Capture	40–100	Highly variable depending on technology and emission source. Pre-combustion capture from power plants is generally cheaper than post-combustion capture.	(Dziejarski et al., 2023; Feron and Paterson, 2011; Hochman and Appasamy, 2024; Shen et al., 2022)
Transport	5–30	It depends on the distance and transport method (pipeline vs. ship). Pipelines are generally cheaper for large-scale projects with nearby storage sites.	(Hochman and Appasamy, 2024; Leeson et al., 2017; Shen et al., 2022)
Injection	5–20	Costs associated with drilling and maintaining injection wells.	(Hochman and Appasamy, 2024; Shen et al., 2022)
Monitoring	1–5	Includes costs of geophysical and geochemical techniques to track CO <sub>2</sub> plume movement.	(Hochman and Appasamy, 2024; Rodriguez Calzado, 2023; Shen et al., 2022)
Total CCS costs per tonne	51–155	The sum of all stages. The wide range reflects variations in capture technology, transport distance, and specific project characteristics.	



understanding of geological properties. As CO<sub>2</sub> sequestration technology advances, basalts may become a more viable choice in the future, especially if effective strategies for mitigating formation damage are developed and reducing costs on site characterizations, drilling, monitoring techniques, etc.

## 7. Impacts of surface facilities for CO<sub>2</sub> injection in basaltic rocks

During carbon dioxide sequestration in basaltic rocks, the role of surface facilities is crucial for the successful implementation of injection processes. These facilities are responsible for preparing the CO<sub>2</sub> for injection by ensuring it meets the necessary conditions, particularly in pressure and temperature. Key factors to be considered are:

### a) High-pressure requirements

One of the key requirements for CO<sub>2</sub> injection into reservoirs is maintaining high-pressure conditions. This is essential to ensure that the CO<sub>2</sub> remains in a supercritical state, which enhances its ability to penetrate the rock formations and increases the prospect of successful mineralization reactions with the basalt. Surface facilities typically include high-pressure compressors and pumps that compress the CO<sub>2</sub> to the required pressure levels before it is injected into the subsurface. The design and operation of these facilities must account for the geo-mechanical properties of the target reservoir and the desired injection rates (Hassing et al., 2024; McGrail et al., 2017a; Raza et al., 2016).

### b) Technical and safety considerations

Operating high-pressure systems involves significant technical and safety considerations. The materials used in constructing pipelines and injection equipment must withstand the high pressures and corrosive nature of CO<sub>2</sub>, mainly when impurities are present. Regular maintenance and monitoring are essential to prevent leaks and ensure the system's integrity. Safety measures include pressure relief valves, automatic shutdown systems, and rigorous inspection protocols to mitigate the risks associated with high-pressure CO<sub>2</sub> handling (Berndsen et al., 2024; McGrail et al., 2017a; Raza et al., 2022; White et al., 2020b).

### c) Energy requirements

The compression of CO<sub>2</sub> to the required pressure levels is energy-intensive and can constitute a significant portion of the overall cost of the sequestration process. The energy consumption of compressors and pumps needs to be optimized to reduce operational costs and the carbon footprint of the sequestration project. Utilizing renewable energy sources or waste heat recovery systems can help minimize these impacts and improve the sustainability of the sequestration operation (Jayne et al., 2019; McGrail et al., 2017a; Stanfield et al., 2024).

### d) Environmental impacts

The construction and operation of surface facilities for CO<sub>2</sub> injection can have environmental impacts that need to be carefully managed. This includes land use changes, potential disturbances to local ecosystems, and the risk of accidental CO<sub>2</sub> releases. Environmental impact assessments and mitigation strategies should be developed to address these concerns, ensuring that the benefits of CO<sub>2</sub> sequestration are not offset by negative environmental consequences (Adeoye et al., 2017; Lu et al., 2024c; McGrail et al., 2014b, 2017a).

### e) Technical challenges

High-pressure conditions in CO<sub>2</sub> injection facilities can accelerate equipment wear and tear, requiring frequent maintenance and replacements to ensure continued functionality. Using durable materials

and adhering to regular maintenance schedules are essential to sustain operations. Additionally, maintaining the integrity of all joints, valves, and connections under high pressure is critical to prevent leaks and ensure operational safety (McGrail et al., 2017a; Sandalow et al., 2021; White et al., 2020b).

Addressing these unique challenges and impacts of high-pressure injection facilities can help to enhance the safety, efficiency, and effectiveness of CO<sub>2</sub> sequestration in basaltic rock formations. Proper planning and management of these aspects are vital for maximizing the benefits of this technology while minimizing potential drawbacks.

## 8. Well integrity in CO<sub>2</sub> sequestration in basaltic rocks

Well integrity is a critical factor in the success of CO<sub>2</sub> sequestration projects, particularly in basaltic rocks, where the geological and geochemical interactions can be quite different from those in more conventional sedimentary storage sites. Ensuring well integrity involves maintaining the ability of the well to contain and control the CO<sub>2</sub> without leakage from the surface to the target storage formation throughout the lifecycle of the sequestration project (Kiran et al., 2017; Peng et al., 2024). This includes during drilling, completion, injection, and post-injection phases. Here, we will discuss the key considerations for well integrity in the context of CO<sub>2</sub> sequestration in basaltic rocks, drawing on current research and case studies.

### a) Material selection and compatibility

The choice of materials for well construction (including casing, cement, and seals) is crucial, especially in the reactive environment of basalt formations. Basalt rocks are rich in minerals like olivine and pyroxene, which can react with CO<sub>2</sub> to form stable carbonates. However, this mineralization process also involves the production of acidic fluids, which can potentially degrade well materials.

- ❖ Casing and tubing: 1) Corrosion resistance: Materials must resist corrosion induced by CO<sub>2</sub>, water, and any resulting acidic fluids. Stainless steel and corrosion-resistant alloys are commonly considered. 2) Mechanical strength: The casing and tubing must withstand high pressures associated with CO<sub>2</sub> injection and the geological stresses present in basalt formations (Rasool et al., 2023; Udebhulu et al., 2024).
- ❖ Cementing: 1) Chemical durability: Cement used in wellbore construction should be chemically durable to withstand potential CO<sub>2</sub>-induced degradation. Portland cement modified with additives to enhance resistance to acidic environments is often used. 2) Seal integrity: Ensuring the seal integrity between the casing and the wellbore is critical to prevent CO<sub>2</sub> migration along the wellbore annulus (Mokhtari Jadid, 2011; Okoli et al., 2024).

### b) Well design and construction

The design of the well must account for the unique properties of basalt formations and the behavior of CO<sub>2</sub> under injection conditions.

- ❖ Zonal isolation: Effective zonal isolation is necessary to prevent CO<sub>2</sub> from migrating to unintended formations or the surface. This involves using multiple barriers, including cement plugs and packers, to isolate different zones along the wellbore (D'Aniello et al., 2021; Neerup et al., 2022).
- ❖ Monitoring and logging: 1) Cement bond logs (CBL) and ultrasonic imaging: These techniques are used to evaluate the quality of the cement job and ensure there are no voids or channels that could compromise well integrity. 2) Temperature and pressure sensors: Real-time monitoring of temperature and pressure within the well can help detect anomalies that may indicate issues with well integrity (Jayne et al., 2019; Lu et al., 2024a).

### c) Injection strategy

The strategy for injecting CO<sub>2</sub> must be carefully planned to maintain well integrity.

- ❖ Injection rates: High injection rates can induce thermal and mechanical stresses on the wellbore and the surrounding rock, potentially leading to integrity issues. Controlled rates help manage these stresses (Jahanbakhsh et al., 2021; Verba et al., 2014).
  - ❖ Injection pressure: Injection pressures must be managed to avoid fracturing the formation or damaging the wellbore. This is particularly important in basalts, which can have variable permeability and fracture networks (D'Aniello et al., 2021; McGrail et al., 2011).
- d) Long-term monitoring and maintenance

Ensuring well integrity over the long term involves ongoing monitoring and maintenance activities.

- ❖ Post-injection monitoring: Regular inspections using downhole tools can detect early signs of casing corrosion, cement degradation, or other integrity issues (White et al., 2020a; Zapata et al., 2020).
- ❖ Leak detection systems: Systems for detecting CO<sub>2</sub> leaks, such as gas sampling and geochemical monitoring, are essential for early identification and remediation of potential leaks (Khan et al., 2024; McGrail et al., 2017a).

Maintaining well integrity in CO<sub>2</sub> sequestration projects in basaltic rocks is a multifaceted challenge that requires careful planning, material selection, and monitoring. The unique geochemical environment of basalt formations demands robust and corrosion-resistant materials, effective well design for zonal isolation, and comprehensive long-term monitoring to ensure the containment of CO<sub>2</sub>. Successful case studies like Carbfix and Wallula provide valuable insights and best practices that can be applied to future projects, underscoring the importance of well integrity in achieving safe and effective CO<sub>2</sub> sequestration.

## 9. Geomechanical effects for CO<sub>2</sub> sequestration on basalts

Understanding the geomechanical effects on CO<sub>2</sub> sequestration in basalts is crucial for ensuring storage capacity and stability, as it helps predict and manage the behavior of natural fractures and faults that could affect CO<sub>2</sub> storage. Although there is limited literature on geomechanical effects on basalts during CO<sub>2</sub> sequestration, some of them are discussed in this section as follows:

### 9.1. Potential induced shear failure

Potential induced shear failure during CO<sub>2</sub> sequestration in basalts is a significant concern due to the pressure changes associated with the injection process. When CO<sub>2</sub> is injected into basalt formations, it can increase the pore pressure within the rock, potentially reducing the effective normal stress on existing fractures and faults (Guha Roy et al., 2016). This reduction in effective stress can lead to shear failure if the stress state surpasses the shear strength of the rock, as shown in Fig. 24, after one year of CO<sub>2</sub> injection for the Columbian River Basalt Group (CRBG) (Jayne et al., 2019). Such failures can create new fractures or reactivate existing ones, providing pathways for CO<sub>2</sub> leakage, and compromising the integrity of the storage site. Successful CO<sub>2</sub> sequestration in basalt depends on the rapid conversion of CO<sub>2</sub> into stable mineral forms, gradually reducing permeability as fractures fill with new minerals. This potential self-sealing property could counteract the increased permeability caused by fracture widening (Wu, 2018). However, the complex interplay between fluid flow, chemical reactions, and rock deformation requires further investigation.

### 9.2. Joint initiation

Joint initiation during CO<sub>2</sub> sequestration in basalts involves the

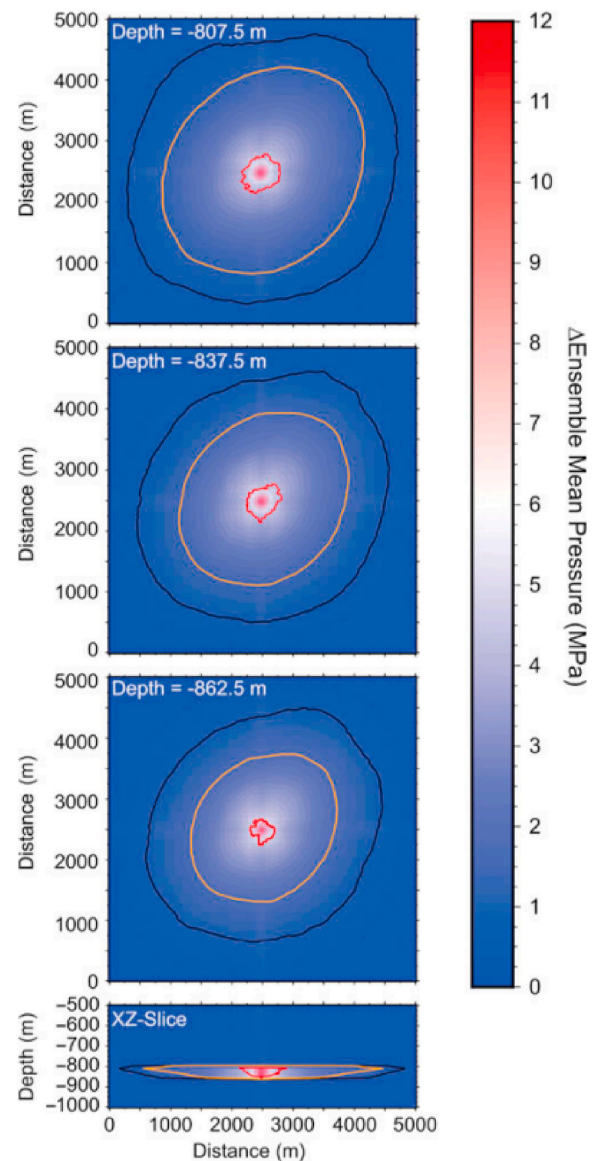
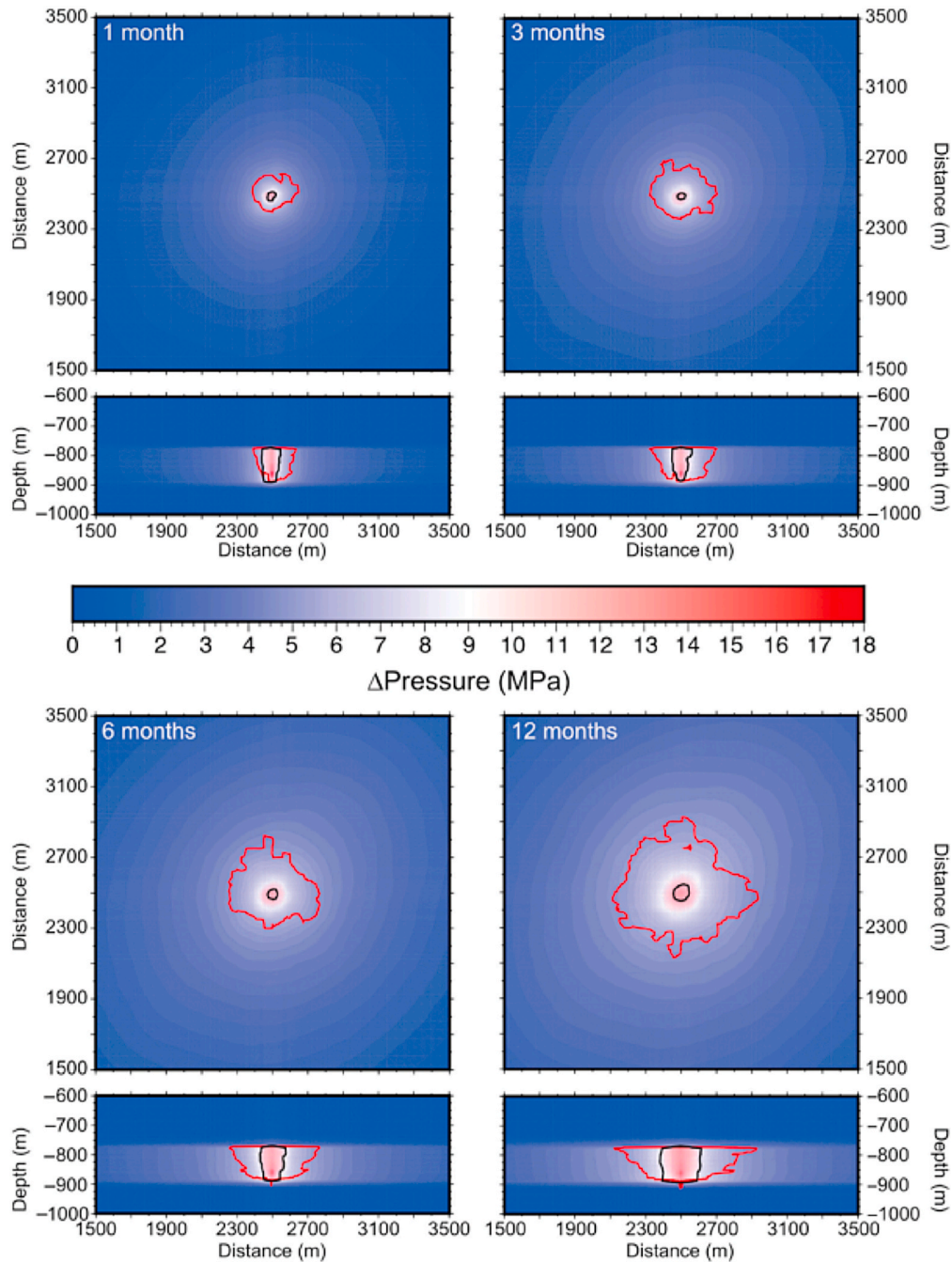


Fig. 24. Potential shear failure of basaltic rocks. The region enclosed by the black contour indicates areas exceeding the Mohr-Coulomb failure criterion. The orange contour encompasses zones with at least a 1% probability of shear failure. Area within the red contour outlines areas with a minimum of 1% free-phase CO<sub>2</sub> saturation (Jayne et al., 2019).

formation or activation of fractures due to increased pressure from CO<sub>2</sub> injection, stress redistribution, thermal effects, and chemical interactions. The injection process raises pressure within the basalt, potentially initiating new fractures or reactivating existing ones, as shown in Fig. 25, after CO<sub>2</sub> injection for 1, 3, 6, and 12 months for CRBG. Changes in stress distribution and temperature can also contribute to joint formation. Additionally, chemical reactions between CO<sub>2</sub> and basalt minerals can weaken the rock, facilitating fractures (Jayne et al., 2019). Effective reservoir management, including careful control of injection rates and pressures, minimises joint initiation and ensures safe, long-term CO<sub>2</sub> storage in basalt formations.

### 9.3. Borehole breakdown

Borehole breakdown during CO<sub>2</sub> sequestration in basalts is a significant concern, as it can undermine the storage process's integrity and effectiveness. This breakdown can result from high injection pressures exceeding the rock's tensile strength (Fig. 26), thermal stresses caused



**Fig. 25.** Joint initiation during CO<sub>2</sub> sequestration in basalts. The area within black contours indicates areas with at least a 1% probability of joint formation. Red contours mark zones with 1% CO<sub>2</sub> concentration (Jayne et al., 2019).

by temperature differentials between injected CO<sub>2</sub> and the surrounding rock, and chemical reactions that weaken the rock structure (Jayne et al., 2019). Additionally, pre-existing fractures in basalt can be reactivated or enlarged during injection, leading to instability. Effective risk mitigation involves monitoring and managing injection pressures and temperatures, understanding the formation's geomechanical properties, and reinforcing the borehole structure to prevent mechanical failure.

#### 9.4. Fracture dilation in overlying flow interior

Fracture dilation in the overlying flow interior during CO<sub>2</sub> sequestration in basalts is an important geomechanical phenomenon that can influence the storage capacity and security of the sequestration site. When CO<sub>2</sub> is injected into basalt formations, the increased pore pressure

can cause existing fractures to dilate or new fractures to form, as shown in Fig. 27. This process can enhance the permeability of the overlying flow interior, facilitating the movement and distribution of CO<sub>2</sub> within the rock. However, fracture dilation poses potential risks, as it may create pathways for CO<sub>2</sub> leakage to the surface or into adjacent formations (Jayne et al., 2019). To manage these risks, it is crucial to understand the fracture network's characteristics and how they respond to pressure changes. Monitoring fracture dilation and conducting detailed geological and geomechanical analyses help predict how the fractures will behave under different conditions. This knowledge allows for developing strategies to control CO<sub>2</sub> injection rates and pressures, ensuring the integrity and effectiveness of the sequestration process while minimizing the risk of leakage.

The geomechanical effects influence rock-fluid interactions,



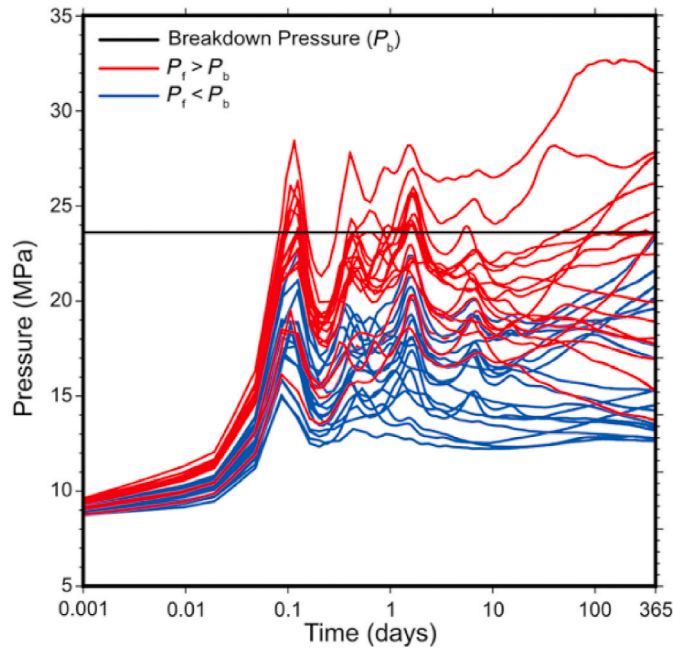


**Fig. 26.** A series of injection pressure simulations over time are presented. A black line marks the pressure threshold ( $P_b$ ) above which borehole failure is likely. Simulations where this threshold is exceeded within a one-year injection period are shown in red, while those remaining below the threshold are in blue. In half of the simulations, the pressure surpasses  $P_b$  (Jayne et al., 2019).

particularly mineralization, which is essential for permanent storage. Optimized injection strategies can be developed by studying geomechanical properties to prevent pressure build-up and ensure efficient  $\text{CO}_2$  distribution. Additionally, this knowledge enhances monitoring systems and risk assessment, ensuring early detection and management of reservoir changes, and aids in meeting regulatory requirements for safe and sustainable sequestration projects. However, to optimize  $\text{CO}_2$  sequestration in basalt formations, in-depth research is essential to elucidate the geomechanical effects and overall reservoir behavior under industrial-scale conditions.

## 10. Estimation of $\text{CO}_2$ storage capacity in basaltic rocks

Estimating the amount of  $\text{CO}_2$  to be sequestered in geological formation is very important to ensure effective and safe long-term storage. The quantity of  $\text{CO}_2$  that can be stored in geological formations is primarily correlated with the type of geological formation and trapping mechanisms associated with those formations. This storage capacity is important for selecting sites suitable for  $\text{CO}_2$  sequestration (Alalimi et al., 2022; Pingping et al., 2009). The mineral trapping mechanism is dominant in basaltic rocks, in which more than 95% of  $\text{CO}_2$  is sequestered in this form. Zhang et al. (2023) developed a method to estimate basalt storage capacity of China as follows:

$$m_{\text{CO}_2} = \sum \rho_r \cdot f_i / n_i \cdot n_{\text{CO}_2}, i = \text{CaO, MgO, FeO} \quad (20)$$

$$M_{\text{CO}_2} = m_{\text{CO}_2} \cdot A \cdot H (1 - \varphi) \quad (21)$$

$$M_{\text{CO}_2 \text{ eff}} = M_{\text{CO}_2} \cdot C_{\text{eff}} \quad (22)$$

where  $m_{\text{CO}_2}$  stands for theoretical  $\text{CO}_2$  storage capacity per unit volume in  $\text{t/m}^3$ ,  $\rho_r$  is the density of basaltic rocks in  $\text{t/m}^3$ ,  $f_i$  represent mass fraction in basaltic rocks of MgO, CaO, and FeO,  $n_i$  stands for the molecular weight of MgO, CaO, and FeO in g/mol,  $n_{\text{CO}_2}$  represent the molecular weight of  $\text{CO}_2$  in g/mol,  $M_{\text{CO}_2}$  represent theoretical mineral storage capacity of  $\text{CO}_2$  in basalt in  $10^6 \text{ t}$ ,  $A$  stands for basalt reservoir

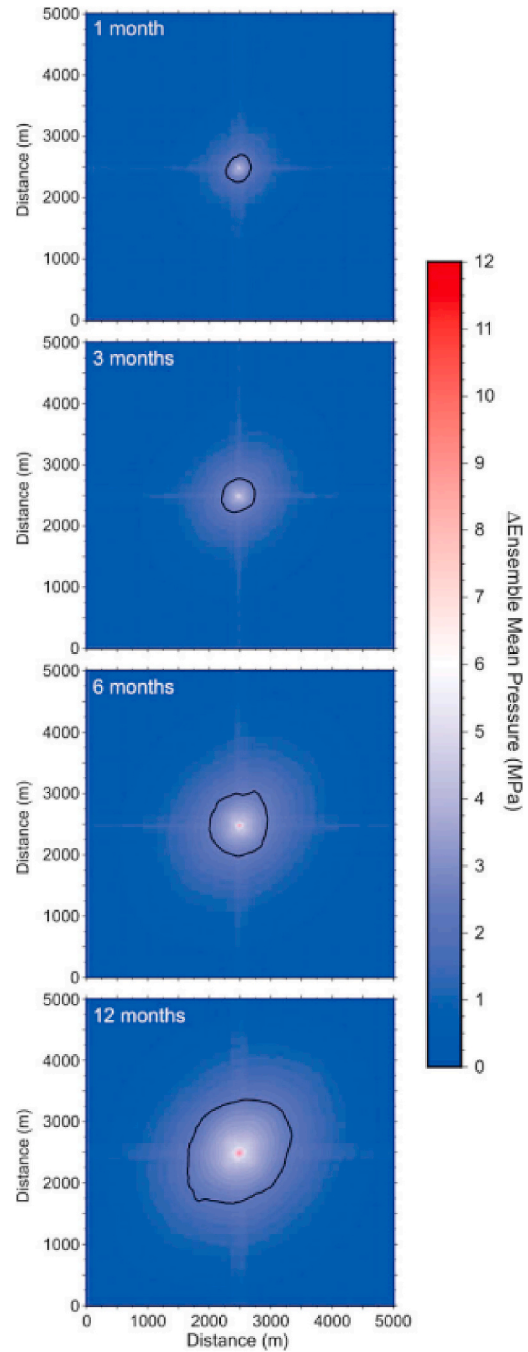


**Fig. 27.** Illustrates the possibility of fracture dilation occurring within the basalt flow interior above the composite injection zone (at depths of 770–775 m) over periods of 1, 3, 6, and 12 months. The areas inside the black contour lines represent a probability of 1% or greater that existing fractures may undergo dilation (Jayne et al., 2019).

surface area in  $\text{km}^2$ ,  $H$  stands for the thickness of basalt reservoir in m,  $\varphi$  represent porosity of reservoir in fraction,  $M_{\text{CO}_2 \text{ eff}}$  represent effective mineral storage capacity of  $\text{CO}_2$  in basalt in  $10^6 \text{ t}$ , and  $C_{\text{eff}}$  is effective storage coefficient of  $\text{CO}_2$  in basalts in fraction.

The most important parameter determining the effective storage capacity of  $\text{CO}_2$  in basalt is  $C_{\text{eff}}$  based on the sweeping efficiency of  $\text{CO}_2$  injected ( $C_{\text{swept}}$ ) and the utilization factor of carbon-fixing minerals when it reaches equilibrium ( $C_{\text{react}}$ ). Hence,  $C_{\text{eff}} = C_{\text{swept}} \cdot C_{\text{react}}$ . Upon computing  $M_{\text{CO}_2}$  and assuming that injected  $\text{CO}_2$  filled the whole basalt rocks in vertical and horizontal directions and carbon fixing minerals are fully reacted,  $C_{\text{eff}}$  is equal to one because  $C_{\text{swept}} = 1$  and  $C_{\text{react}} = 1$ . In

general,  $C_{\text{eff}}$  is determined in the laboratory or through numerical simulations and is discussed by Gislason and Oelkers (2014), considering two injection scenarios as discussed in section 2.5. In addition,  $C_{\text{react}}$  depends on the complexity of kinetics geochemical reactions between metallic cations and injected  $\text{CO}_2$ , as discussed by O'Connor et al. (2002) and Amy et al. (2012). It ranges from 0.06 to 0.265 (Vishal et al., 2021).

It was revealed that basaltic rocks on land in China have significant potential for  $\text{CO}_2$  storage, which could contribute to mitigating global climate change. The estimated theoretical capacity for mineral  $\text{CO}_2$  storage ranges from 39,792.5 to 54,325.44 gigatons (P10-P90), with an average capacity of 46,948.36 gigatons (P50). For injecting  $\text{CO}_2$  directly, the total theoretical mineral  $\text{CO}_2$  storage capacity was 607.79–1121.44 gigatons (P10-P90), with an average of 847.95 gigatons (P50). If  $\text{CO}_2$  was injected with water, the total theoretical mineral  $\text{CO}_2$  storage capacity was 201.13–303.85 gigatons (P10-P90), averaging 249.50 gigatons (P50). The  $C_{\text{eff}}$  used at P50 for both injection cases are 0.0181 and  $5.31 \times 10^{-3}$ , respectively. Moreover, the  $\text{CO}_2$  emission in China in different provinces is larger than the storage capacity of basaltic rocks in respective areas, so other storage options need to be analyzed (Zhang et al., 2023).

Several key factors need to be considered in estimating the  $\text{CO}_2$  storage capacity of basaltic rocks, such as: 1) Porosity and permeability: Porosity determines the volume of  $\text{CO}_2$  that can be stored. Basalts with higher porosity have more space to store  $\text{CO}_2$ . Permeability affects the ease with which  $\text{CO}_2$  can be injected and distributed within the basalt formation. High permeability facilitates efficient  $\text{CO}_2$  injection and distribution (Wu et al., 2021). 2) Mineral composition: basalts rich in calcium, magnesium, and iron are more reactive with  $\text{CO}_2$ , leading to the formation of stable carbonate minerals such as calcite, magnesite, and siderite. The presence of these minerals can significantly enhance  $\text{CO}_2$  sequestration through mineralization (Zhao et al., 2024). 3) Geochemical conditions: The injection site's temperature, pressure, and pH conditions influence  $\text{CO}_2$  solubility and reactivity. Higher temperatures and pressures can enhance the reaction rates between  $\text{CO}_2$  and basalt minerals (Izadpanahi et al., 2024). 4) Geomechanical properties: Understanding basalt's mechanical strength and fracture networks is crucial. Fractures can increase the surface area for reactions, improve permeability, and pose a risk of induced seismicity (Cao et al., 2024).

## 11. Challenges encountered during $\text{CO}_2$ sequestration in basaltic rocks

$\text{CO}_2$  sequestration in basaltic rocks is a viable technology for reducing greenhouse gas emissions and combatting global climatic change. While the process has considerable promise, several difficulties must be overcome during carbon dioxide sequestration in basaltic rocks. Among the major challenges are site selection; it is important to figure out suitable basaltic rock formations before  $\text{CO}_2$  injection. The availability and accessibility of suitable basalt reservoirs can be difficult to obtain. The basalt formation's depth, porosity, permeability, and geochemical properties must all be carefully studied (McGrail et al., 2011; Richardson and Tassinari, 2022). Further, geochemical reactions and mineralization rate; the efficient  $\text{CO}_2$  sequestration in basaltic rocks depends on mineral carbonation. The mineralization rate and the efficiency of the process can vary depending on the properties of the basalt and the amount of  $\text{CO}_2$  injected. Understanding the geochemical mechanisms and optimizing mineralization rates are continuing scientific endeavors (Harrison et al., 2019; Postma et al., 2022a). Also, storage capacity, understanding basalt's physical and chemical  $\text{CO}_2$  trapping mechanisms, and precisely determining the storage capability are significant issues. However, no accurate estimation method has been developed to estimate the storage capacity of basalt formation (Postma et al., 2022b; White et al., 2020a). Moreover, for long-term storage stability to mitigate  $\text{CO}_2$  leakage and storage site risks, it is important to assess structural deformation, seismic activity, and groundwater interactions. Furthermore, injection efficiency and optimizing injection

parameters such as rates, pressures, and volumes help  $\text{CO}_2$  injection into basaltic rocks efficiently. Maximizing storage capacity requires homogeneous  $\text{CO}_2$  distribution in the reservoir (Goldberg et al., 2018; Matter et al., 2009).

Another challenge is monitoring and leakage detection; establishing efficient surveillance methods to assure storage site integrity and detect  $\text{CO}_2$  leakage is difficult. Early leakage identification and mitigation need continuous monitoring of subsurface pressure, temperature, and geochemical indicators (Goldberg et al., 2018; Rabiou et al., 2020). Further, in-situ mineral carbonation, especially CarbFix, causes permeability reduction in host rock after  $\text{CO}_2$  injection due to secondary mineral precipitation. Reduction in permeability in the formation causes difficulty in the injection process. In addition, when these secondary mineral precipitates and solution become supersaturated with one of the phases within the basaltic rocks, it can reduce the dissolution of primary minerals (Adeoye et al., 2017; Stockmann et al., 2011, 2013). Moreover, the cost-effectiveness of basalt  $\text{CO}_2$  sequestration is difficult to assess. Site characterization, injection infrastructure, monitoring systems, and long-term site management must be weighed against climate benefits and revenue streams like carbon credits (Cao et al., 2020). Also, risk assessment and mitigation, as well as extensive risk assessments and effective mitigation techniques, are essential to identify potential hazards and develop appropriate mitigation strategies. Induced seismicity, groundwater contamination, and surface leaking must be addressed for safe and sustainable  $\text{CO}_2$  sequestration (Goldberg and Slagle, 2009; Liu et al., 2022). In addition to regulatory frameworks and public acceptance, it is critical to have strong regulatory frameworks and regulations for basalt sequestration to ensure environmental protection, stakeholder engagement, and societal acceptance. Addressing legal and governance issues and maintaining openness and public trust are critical components of successful implementation (Babarinde et al., 2023; Goldberg et al., 2018).

To improve  $\text{CO}_2$  sequestration in basaltic rocks as a climate change mitigation approach, scientists, engineers, policymakers, and stakeholders must work together to address these challenges.

## 12. Research gaps and future works

Basaltic rocks present significant potential for long-term  $\text{CO}_2$  storage, critical for mitigating global climate change. These rocks can mineralize over 95% of injected  $\text{CO}_2$  through mineral carbonation. Within 24 months, injected  $\text{CO}_2$  can transform into stable carbonate minerals. Despite their advantages, basaltic rocks have not received as much focus as other geological storage options. This section highlights areas requiring further research as identified in this review:

1. A study by Mohammed et al. (2024) analyzed the impact of  $\text{CO}_2$  on mineral surface charge, understanding the broader geomechanical implications of mineralization as crucial for long-term  $\text{CO}_2$  storage in basalts. However, future research should investigate how  $\text{CO}_2$  interaction with rock minerals alters the mechanical properties of the formation, such as porosity, permeability, and overall rock strength. Additionally, assessing the potential for induced seismicity associated with  $\text{CO}_2$  injection and developing mitigation strategies is essential. These investigations will contribute to a more comprehensive evaluation of candidate site selection for  $\text{CO}_2$  storage in basalts, considering the chemical suitability for mineralization and the geomechanical stability during  $\text{CO}_2$  injection. A holistic understanding of these factors will enhance the overall reliability of  $\text{CO}_2$  sequestration in basalts as a technology for mitigating climate change.
2. Future studies on  $\text{CO}_2$  mineralization in altered basalt should also focus on understanding long-term reaction kinetics and the temporal evolution of mineral phases to ensure the stability of carbonates over extended periods. Research should investigate the impact of the initial alteration state of basalt, varying brine compositions, and

geomechanical properties post-carbonation. Additionally, the specific reaction pathways and the potential role of microbial communities in enhancing or inhibiting carbonation need thorough exploration. Field-scale validation is essential to confirm laboratory findings and assess practical scalability and challenges. These efforts will provide a comprehensive understanding of the carbonation process in altered basalt, optimizing it for effective CO<sub>2</sub> sequestration.

3. Wettability alteration (CO<sub>2</sub>-water-basalt) is the key factor for mineral carbonation in basaltic rocks during CO<sub>2</sub> injection for CO<sub>2</sub> sequestration because it influences the spread and movement of the CO<sub>2</sub> inside the basalt's rock pore network, mass transfers, and mineralization rates. However, there is a lack of information on basalt-CO<sub>2</sub>-water wettability change and how it can be improved; hence, more research is needed in this area (Iglauer et al., 2020).
4. From an experimental perspective, it has been revealed that NaHCO<sub>3</sub> is one of the best enhancements for the mineral carbonation process in basaltic rocks during CO<sub>2</sub> sequestration for water-basalt-NaHCO<sub>3</sub> interactions under high temperatures (200–300 °C). The Na<sup>+</sup> presence in the solution helped rapidly to form Na<sup>+</sup> silicates like analcime and promoted further dissolution of metallic divalent cations from the basaltic rocks for mineral precipitations. However, the chemical mechanisms behind this process need investigation (Kikuchi et al., 2023).
5. Numerical modeling and simulation can improve our understanding of CO<sub>2</sub> behavior and storage in basaltic rocks. This is because most modeling and simulation results using different software do not match the experimental results. Hence, advanced geological, geochemical, and hydrological models are needed because they can forecast long-term storage capacity, analyze potential consequences, and optimize injection tactics.
6. Despite successful pilot tests in the USA and Iceland proving that basaltic rocks have great potential for sequestering CO<sub>2</sub>, full-field scale operations are hampered by a lack of understanding of multiphase flow properties in highly heterogeneous basalt fracture networks. So, this area needs more research. Further, scale-up and demonstration projects, moving from pilot-scale to commercial-scale basalt sequestration, are crucial. To speed up this technology's climate change mitigation deployment, studies should prove its feasibility, scalability, and economic viability.
7. Even though CO<sub>2</sub> diffusion and convection in porous media have been well studied, more work needs to be done to simulate reactive transport, analyze how reactions affect transport in heterogeneous porous media, and disclose the dynamic nature of CO<sub>2</sub> mineralization in basalts. Specifically, there is a need for advanced simulations that can accurately model the coupled processes of fluid flow, chemical reactions, and mineral transformations over varying spatial and temporal scales. Research should focus on understanding the impact of heterogeneous pore structures on CO<sub>2</sub> transport and reactivity, as these can significantly influence the efficiency and stability of the mineralization process. Furthermore, detailed experimental studies and in-situ observations are necessary to validate these models and provide insights into the kinetics and pathways of mineral formation. Investigating the role of different basalt compositions and environmental conditions on the mineralization process will also be crucial for optimizing CO<sub>2</sub> sequestration strategies. Additionally, exploring the long-term implications of CO<sub>2</sub> mineralization on the mechanical properties of basaltic formations will help to assess the sustainability and safety of using basalt for large-scale CO<sub>2</sub> storage.

### 13. Conclusions and recommendations

This review paper explored the latest developments in CO<sub>2</sub> sequestration within basaltic rocks. Experimental, modeling and simulations, and pilot tests findings have been analyzed. It has been found that

basaltic rocks can store more than 95% of injected CO<sub>2</sub> as carbonate minerals through the mineral carbonation process within 2 years, as reported from two pilot tests with a minimum leakage risk than other storage geological options. The following points have been noted from this review paper:

1. Forsterite is the most effective mineral for CO<sub>2</sub> sequestration in basaltic rocks; however, to store 4 million tons of carbon dioxide, 6.4 million tonnes of forsterite are required. This results in 2.6 million m<sup>3</sup> of magnesite being produced.
2. Today's scientific and technical knowledge of carbon mineralization to support pilot and demonstration projects is insufficient. Field pilots and research endeavors could enhance monitoring and verification techniques and increase understanding of carbon mineralization's possible effects and costs.
3. A high temperature, approximately 250 °C, is required for the mineral carbonation during CO<sub>2</sub> sequestration in basaltic rocks. However, 250 °C is the maximum temperature needed; beyond that, it results in decarbonization reactions within basaltic rocks.
4. The pilot tests and scale operations conducted in CarbFix projects found that injecting pure CO<sub>2</sub> into the basaltic rocks tends to lower permeability and bring difficulty during the injection process. However, injecting gas mixtures (CO<sub>2</sub> and H<sub>2</sub>S) into basaltic rocks did not reduce permeability. The injected fluids, concerning minerals in the targeted reservoirs, were undersaturated and acidic, which open fluid channels around injection wells.
5. Recent experiments have revealed that nanoparticles can enhance CO<sub>2</sub> sequestration through mineral carbonation and other trapping mechanisms for long-term storage plans in basaltic rocks. Nanoparticles help with wettability change to water wet, influencing mineral carbonation and other trapping mechanisms; hence, high amounts of CO<sub>2</sub> can be sequestered.
6. From the modeling and simulation perspective, it has been found that clays and alumino-silicate help to enhance mineral carbonation in basaltic rocks through the dissolution of basaltic rocks to form metallic divalent cations, which plays a significant role in the mineral carbonation process. Also, clays reduce reservoir conductivity to enhance geochemical reactions. Furthermore, in most cases, simulation results overestimate experimental findings on mineral carbonation; hence, simulations must be combined with experiments for validation.
7. Adding surfactants, especially sodium dodecyl benzene sulfonate (SDBS), to basaltic rocks changes the rocks' wettability to water wet even if used in small concentrations. However, other surfactants' effects on basaltic rocks' wettability are recommended before upgrading to pilot and field operation regarding economic costs. In contrast, NaHCO<sub>3</sub> enhances CO<sub>2</sub> sequestration in basaltic rocks by promoting the dissolution of host rocks

### CRedit authorship contribution statement

**Grant Charles Mwakipunda:** Writing – review & editing, Writing – original draft, Conceptualization. **Ping Yu:** Writing – review & editing, Visualization, Validation. **Norga Alloyce Komba:** Resources, Formal analysis, Conceptualization. **Edwin Twum Ayimadu:** Validation, Resources, Writing – review & editing. **Jennifer Sanford Moshi:** Validation, Resources, Investigation. **Fravian Mwizarubi:** Resources, Investigation, Formal analysis. **Irene Martin Ndunguru:** Resources, Investigation, Formal analysis. **Long Yu:** Writing – review & editing, Visualization, Conceptualization.

### Declaration of competing interest

The authors declare that there is no conflict of interest.



## Data availability

No data was used for the research described in the article.

## Acknowledgements

The authors acknowledge support from the Chinese Scholarship Council (2022GXZ005733).

## References

- Abdullah, H., Al-Yaseri, A., Ali, M., Giwelli, A., Negash, B.M., Sarmadivaleh, M., 2021. CO<sub>2</sub>/Basalt's interfacial tension and wettability directly from gas density: implications for Carbon Geo-sequestration. *J. Petrol. Sci. Eng.* 204, 108683.
- Adeoye, J.T., Menefee, A.H., Xiong, W., Wells, R.K., Skemer, P., Giammar, D.E., Ellis, B. R., 2017. Effect of transport limitations and fluid properties on reaction products in fractures of unaltered and serpentinized basalt exposed to high PCO<sub>2</sub> fluids. *Int. J. Greenh. Gas Control* 63, 310–320.
- Al-Anssari, S., Arif, M., Wang, S., Barifcani, A., Lebedev, M., Iglauer, S., 2017. Wettability of nano-treated calcite/CO<sub>2</sub>/brine systems: implication for enhanced CO<sub>2</sub> storage potential. *Int. J. Greenh. Gas Control* 66, 97–105.
- Al-Anssari, S., Barifcani, A., Wang, S., Maxim, L., Iglauer, S., 2016. Wettability alteration of oil-wet carbonate by silica nanofluid. *J. Colloid Interface Sci.* 461, 435–442.
- Al-Yaseri, A., Ali, M., Abbasi, G.R., Abid, H.R., Jha, N.K., 2021a. Enhancing CO<sub>2</sub> storage capacity and containment security of basaltic formation using silica nanofluids. *Int. J. Greenh. Gas Control* 112, 103516.
- Al-Yaseri, A., Ali, M., Ali, M., Taheri, R., Wolff-Boenisch, D., 2021b. Western Australia basalt-CO<sub>2</sub>-brine wettability at geo-storage conditions. *J. Colloid Interface Sci.* 603, 165–171.
- Al Maqbali, Q., Hussain, S., Mask, G., Xingru, W., 2023a. Numerical simulation of in-situ CO<sub>2</sub> mineralization in mafic basaltic formations in Southwest Oklahoma. In: SPE Oklahoma City Oil and Gas Symposium.
- Al Maqbali, Q., Hussain, S., Mask, G., Xingru, W., 2023b. Numerical simulation of in-situ CO<sub>2</sub> mineralization in mafic basaltic formations in Southwest Oklahoma. In: SPE Oklahoma City Oil and Gas Symposium/Production and Operations Symposium. SPE. D021S005R002.
- Alalimi, A., AlRassas, A.M., Vo Thanh, H., Al-qaness, M.A., Pan, L., Ashraf, U., Al-Alimi, D., Moharam, S., 2022. Developing the efficiency-modeling framework to explore the potential of CO<sub>2</sub> storage capacity of S3 reservoir, Tahe oilfield, China. *Geomechanics and Geophysics for Geo-Energy and Geo-Resources* 8 (4), 128.
- Ali, M., Yekeen, N., Alanazi, A., Keshavarz, A., Iglauer, S., Finkbeiner, T., Hoteit, H., 2023a. Saudi Arabian basalt/CO<sub>2</sub>/brine wettability: implications for CO<sub>2</sub> geo-storage. *J. Energy Storage* 62, 106921.
- Ali, M., Yekeen, N., Hosseini, M., Abbasi, G.R., Alanazi, A., Keshavarz, A., Finkbeiner, T., Hoteit, H., 2023b. Enhancing the CO<sub>2</sub> trapping capacity of Saudi Arabian basalt via nanofluid treatment: implications for CO<sub>2</sub> geo-storage. *Chemosphere*, 139135.
- Amy, U., Changzhi, W., Junfeng, J., Zhenyu, W., Lianxing, G., Ping, S., Rix, D., 2012. Potential capacity and feasibility of CO<sub>2</sub> sequestration in petroleum reservoirs of basaltic rocks: example from basaltic hydrocarbon reservoir in the Xujiaweizi fault depression the Songliao Basin, East China. *Geol. J. China Univ.* 18 (2), 239.
- Aradóttir, E.S.P., Sonnenthal, E.L., Björnsson, G., Jónsson, H., 2012. Multidimensional reactive transport modeling of CO<sub>2</sub> mineral sequestration in basalts at the Hellisheiði geothermal field, Iceland. *Int. J. Greenh. Gas Control* 9, 24–40.
- Awolayo, A.N., Laureijs, C.T., Byng, J., Luhmann, A.J., Lauer, R., Tutolo, B.M., 2022. Mineral surface area accessibility and sensitivity constraints on carbon mineralization in basaltic aquifers. *Geochem. Cosmochim. Acta* 334, 293–315.
- Babarinde, O., Schwartz, B., Meng, J., Kim, S., Segura, J.M., Schultz, R.A., Soroush, H., 2023. An overview of geological carbon sequestration and its geomechanical aspects. *Geological Society, London, Special Publications* 528 (1). SP528-2022-51.
- Bacon, D.H., Ramanathan, R., Schaeff, H.T., McGrail, B.P., 2014. Simulating geologic co-sequestration of carbon dioxide and hydrogen sulfide in a basalt formation. *Int. J. Greenh. Gas Control* 21, 165–176.
- Balani, K., 2023. In: Meeting Global Energy Demand in a Sustainable Future. Emerald Publishing Limited, pp. 90–91.
- Bergougui, B., 2024. Moving toward environmental mitigation in Algeria: asymmetric impact of fossil fuel energy, renewable energy and technological innovation on CO<sub>2</sub> emissions. *Energy Strategy Rev.* 51, 101281.
- Berndsen, M., Erol, S., Akın, T., Akın, S., Nardini, I., Immenhauser, A., Nehler, M., 2024. Experimental study and kinetic modeling of high temperature and pressure CO<sub>2</sub> mineralization. *Int. J. Greenh. Gas Control* 132, 104044.
- Berrezueta, E., Moita, P., Pedro, J., Abdouhghafour, H., Mirão, J., et al., 2023. Laboratory experiments and modelling of the geochemical interaction of a gabbro-anorthosite with seawater and supercritical CO<sub>2</sub>: a mineral carbonation study. *Geoenery Science and Engineering*, 212010.
- Bethke, C.M., 2022. *Geochemical and Biogeochemical Reaction Modeling*. Cambridge university press.
- Bigdeli, A., Delshad, M., 2024. The evolving landscape of oil and gas chemicals: convergence of artificial intelligence and chemical-enhanced oil recovery in the energy transition toward sustainable energy systems and net-zero emissions. *Journal of Data Science and Intelligent Systems* 2 (2), 65–78.
- Boot-Handford, M.E., Abanades, J.C., Anthony, E.J., Blunt, M.J., Brandani, S., et al., 2014. Carbon capture and storage update. *Energy Environ. Sci.* 7 (1), 130–189.
- Bowen, F., 2011. Carbon capture and storage as a corporate technology strategy challenge. *Energy Pol.* 39 (5), 2256–2264.
- Bruant, R., Guswa, A., Celia, M., Peters, C., 2002. Safe storage of CO<sub>2</sub> in deep saline aquifers. *Environmental Science and Technology-Washington DC-* 36 (11), 240A–245A.
- Bullock, L.A., Alcalde, J., Tornos, F., Fernandez-Turiel, J.-L., 2023. Geochemical carbon dioxide removal potential of Spain. *Sci. Total Environ.* 867, 161287.
- Cao, C., Liu, H., Hou, Z., Mehmood, F., Liao, J., Feng, W., 2020. A review of CO<sub>2</sub> storage in view of safety and cost-effectiveness. *Energies* 13 (3), 600.
- Cao, R., Muller, K.A., Miller, Q.R., White, M.D., Bacon, D.H., Schaeff, H.T., 2023. Reactive Transport Modeling of Anthropogenic Carbon Mineralization in Stacked Columbia River Basalt Reservoirs. SPE/AAPG/SEG Unconventional Resources Technology Conference. URTEC. D021S032R001.
- Cao, X., Li, Q., Xu, L., Tan, Y., 2024. Experiments of CO<sub>2</sub>-basalt-fluid interactions and micromechanical alterations: implications for carbon mineralization. *Energy Fuels* 38 (7), 6205–6214.
- Chen, M., Zhang, Y., Liu, S., Zhao, C., Dong, S., Song, Y., 2023. CO<sub>2</sub> transport and carbonate precipitation in the coupled diffusion-reaction process during CO<sub>2</sub> storage. *Fuel* 334, 126805.
- Clark, D.E., Oelkers, E.H., Gunnarsson, I., Sigfússon, B., Snæbjörnsdóttir, S.Ó., Aradóttir, E.S., Gíslason, S.R., 2020. CarbFix2: CO<sub>2</sub> and H<sub>2</sub>S mineralization during 3.5 years of continuous injection into basaltic rocks at more than 250 C. *Geochem. Cosmochim. Acta* 279, 45–66.
- D'Aniello, A., Tómasdóttir, S., Sigfússon, B., Fabbricino, M., 2021. Modeling gaseous CO<sub>2</sub> flow behavior in layered basalts: dimensional analysis and aquifer response. *Ground Water* 59 (5), 677–693.
- de Obeso, J.C., Awolayo, A.N., Nightingale, M.J., Tan, C., Tutolo, B.M., 2023. Experimental study on plagioclase dissolution rates at conditions relevant to mineral carbonation of seafloor basalts. *Chem. Geol.* 620, 121348.
- Depp, C.T., Miller, Q.R., Crum, J.V., Horner, J.A., Schaeff, H.T., 2022. Pore-scale microenvironments control anthropogenic carbon mineralization outcomes in basalt. *ACS Earth Space Chem.* 6 (12), 2836–2847.
- Dong, K., Jiang, Q., Liu, Y., Shen, Z., Vardanyan, M., 2024. Is energy aid allocated fairly? A global energy vulnerability perspective. *World Dev.* 173, 106409.
- Dziejarski, B., Krzyżyńska, R., Andersson, K., 2023. Current status of carbon capture, utilization, and storage technologies in the global economy: a survey of technical assessment. *Fuel* 342, 127776.
- Feron, P., Paterson, L., 2011. Reducing the Costs of CO<sub>2</sub> Capture and Storage (CCS). CSIRO, Canberra.
- Finstad, K.M., Smith, M.M., Beaudoin, G., Dipple, G.M., Aines, R.D., 2023. Radiocarbon analysis as a method for verifying atmospheric CO<sub>2</sub> uptake during carbon mineralization. *Nucl. Instrum. Methods Phys. Res. Sect. B Beam Interact. Mater. Atoms* 534, 35–38.
- Galeczka, I., Wolff-Boenisch, D., Gíslason, S., 2013. Experimental studies of basalt-H<sub>2</sub>O-CO<sub>2</sub> interaction with a high pressure column flow reactor: the mobility of metals. *Energy Proc.* 37, 5823–5833.
- Galeczka, I., Wolff-Boenisch, D., Oelkers, E.H., Gíslason, S.R., 2014. An experimental study of basaltic glass-H<sub>2</sub>O-CO<sub>2</sub> interaction at 22 and 50 C: Implications for subsurface storage of CO<sub>2</sub>. *Geochem. Cosmochim. Acta* 126, 123–145.
- Gierzynski, A.O., Pollyea, R.M., 2017. Three-phase CO<sub>2</sub> flow in a basalt fracture network. *Water Resour. Res.* 53 (11), 8980–8998.
- Gíslason, S.R., Oelkers, E.H., 2003. Mechanism, rates, and consequences of basaltic glass dissolution: II. An experimental study of the dissolution rates of basaltic glass as a function of pH and temperature. *Geochem. Cosmochim. Acta* 67 (20), 3817–3832.
- Gíslason, S.R., Oelkers, E.H., 2014. Carbon storage in basalt. *Science* 344 (6182), 373–374.
- Gíslason, S.R., Sigurdardóttir, H., Aradóttir, E.S., Oelkers, E.H., 2018. A brief history of CarbFix: challenges and victories of the project's pilot phase. *Energy Proc.* 146, 103–114.
- Gíslason, S.R., Wolff-Boenisch, D., Stefansson, A., Oelkers, E.H., Gunnlaugsson, E., et al., 2010. Mineral sequestration of carbon dioxide in basalt: a pre-injection overview of the CarbFix project. *Int. J. Greenh. Gas Control* 4 (3), 537–545.
- Goldberg, D., Aston, L., Bonneville, A., Demirkanli, I., Evans, C., et al., 2018. Geological storage of CO<sub>2</sub> in sub-seafloor basalt: the CarbonSAFE pre-feasibility study offshore Washington State and British Columbia. *Energy Proc.* 146, 158–165.
- Goldberg, D., Slagle, A.L., 2009. A global assessment of deep-sea basalt sites for carbon sequestration. *Energy Proc.* 1 (1), 3675–3682.
- Guha Roy, D., Vishal, V., Singh, T.N., 2016. Effect of carbon dioxide sequestration on the mechanical properties of Deccan basalt. *Environ. Earth Sci.* 75, 1–13.
- Gunnarsson, I., Aradóttir, E.S., Oelkers, E.H., Clark, D.E., Arnarson, M.þ., et al., 2018. The rapid and cost-effective capture and subsurface mineral storage of carbon and sulfur at the CarbFix2 site. *Int. J. Greenh. Gas Control* 79, 117–126.
- Gysi, A.P., Stefánsson, A., 2011. CO<sub>2</sub>-water-basalt interaction. Numerical simulation of low temperature CO<sub>2</sub> sequestration into basalts. *Geochem. Cosmochim. Acta* 75 (17), 4728–4751.
- Harrison, A.L., Tutolo, B.M., DePaolo, D.J., 2019. The role of reactive transport modeling in geologic carbon storage. *Elements: An International Magazine of Mineralogy, Geochemistry, and Petrology* 15 (2), 93–98.
- Hassing, S.H., Draganov, D., Janssen, M., Barnhoorn, A., Wolf, K.H., et al., 2024. Imaging CO<sub>2</sub> reinjection into basalts at the CarbFix2 reinjection reservoir (Hellisheiði, Iceland) with body-wave seismic interferometry. *Geophys. Prospect.* 72 (5), 1919–1933.
- Hochman, G., Appasamy, V., 2024. The case for carbon capture and storage technologies. *Environments* 11 (3), 52.

- Hohendorff Filho, J.C.V., Victorino, I.R.S., Bigdeli, A., Castro, M.S., Schiozer, D.J., 2024. Effect of production system uncertainties on production forecast, energy demand, and carbon emissions. *J. Braz. Soc. Mech. Sci. Eng.* 46 (3), 115.
- Hosseini, M., Awan, F.U.R., Jha, N.K., Keshavarz, A., Iglauer, S., 2023. Streaming and zeta potentials of basalt as a function of pressure, temperature, salinity, and pH. *Fuel* 351, 128996.
- Hosseinzadeh, S., Haghighi, M., Salmachi, A., Shokrollahi, A., 2024. Carbon dioxide storage within coal reservoirs: a comprehensive review. *Geoenery Science and Engineering* 241, 213198.
- Huerta, N.J., Cantrell, K.J., White, S.K., Brown, C.F., 2020. Hydraulic fracturing to enhance injectivity and storage capacity of CO<sub>2</sub> storage reservoirs: benefits and risks. *Int. J. Greenh. Gas Control* 100, 103105.
- Iglauer, S., Al-Yaseri, A., 2021. Improving basalt wettability to de-risk CO<sub>2</sub> geo-storage in basaltic formations 5, 347–350.
- Iglauer, S., Al-Yaseri, A.Z., Wolff-Boenisch, D., 2020. Basalt-CO<sub>2</sub>-brine wettability at storage conditions in basaltic formations. *Int. J. Greenh. Gas Control* 102, 103148.
- Izadpanahi, A., Blunt, M.J., Kumar, N., Ali, M., Tassinari, C.C.G., Sampaio, M.A., 2024. A review of carbon storage in saline aquifers: mechanisms, prerequisites, and key considerations. *Fuel* 369, 131744.
- Jahanbakhsh, A., Liu, Q., Hadi Mosleh, M., Agrawal, H., Farooqui, N.M., et al., 2021. An investigation into CO<sub>2</sub>-brine-cement-reservoir rock interactions for wellbore integrity in CO<sub>2</sub> geological storage. *Energies* 14 (16), 5033.
- Jayne, R.S., Wu, H., Pollyea, R.M., 2019. A probabilistic assessment of geomechanical reservoir integrity during CO<sub>2</sub> sequestration in flood basalt formations. *Greenhouse Gases: Sci. Technol.* 9 (5), 979–998.
- Kali, R.F.S., Fan, D., Hazel, N., Striolo, A., 2022. Techno-socio-economic analysis of geological carbon sequestration opportunities. *Environ. Sci. J. Integr. Environ. Res.: Advances* 1 (2), 138–155.
- Kanniche, M., Gros-Bonnivard, R., Jaud, P., Valle-Marcos, J., Amann, J.-M., Bouallou, C., 2010. Pre-combustion, post-combustion and oxy-combustion in thermal power plant for CO<sub>2</sub> capture. *Appl. Therm. Eng.* 30 (1), 53–62.
- Kebede, B., Mammo, T., Shawel, M., Alemu, T., 2023. Integrated seismic stratigraphic and structural analysis of Southern main Ethiopian rift basin: implications for hydrocarbon potentials. *Acta Geophys* 72, 597–617.
- Khan, S., Khulief, Y., Juanes, R., Bashmal, S., Usman, M., Al-Shuhail, A., 2024. Geomechanical modeling of CO<sub>2</sub> sequestration: a review focused on CO<sub>2</sub> injection and monitoring. *J. Environ. Chem. Eng.* 12 (3), 112847.
- Kikuchi, S., Wang, J., Dandar, O., Uno, M., Watanabe, N., Hirano, N., Tsuchiya, N., 2023. NaHCO<sub>3</sub> as a carrier of CO<sub>2</sub> and its enhancement effect on mineralization during hydrothermal alteration of basalt. *Front. Environ. Sci.* 11, 199.
- Kiran, R., Teodoru, C., Dadmohammadi, Y., Nygaard, R., Wood, D., Mokhtari, M., Salehi, S., 2017. Identification and evaluation of well integrity and causes of failure of well integrity barriers (A review). *J. Nat. Gas Sci. Eng.* 45, 511–526.
- Kumar, A., Shrivastava, J.P., Pathak, V., 2017. Mineral carbonation reactions under water-saturated, hydrothermal-like conditions and numerical simulations of CO<sub>2</sub> sequestration in tholeiitic basalt of the Eastern Deccan Volcanic Province, India. *Appl. Geochem.* 84, 87–104.
- Kumar, N., Verma, A., Ahmad, T., Sahu, R.K., Mandal, A., Mubashir, M., Ali, M., Pal, N., 2024. Carbon capture and sequestration technology for environmental remediation: a CO<sub>2</sub> utilization approach through EOR. *Geoenery Science and Engineering* 234, 212619.
- Leeson, D., Mac Dowell, N., Shah, N., Petit, C., Fennell, P.S., 2017. A Techno-economic analysis and systematic review of carbon capture and storage (CCS) applied to the iron and steel, cement, oil refining and pulp and paper industries, as well as other high purity sources. *Int. J. Greenh. Gas Control* 61, 71–84.
- Lei, Z., Zhang, Y., Zhou, L., Zhou, J., 2021. Numerical simulation of CO<sub>2</sub> mineral sequestration in basalt reservoir through an abandoned oil well: a case study in Xujiaweizi area, Northeast China. *Environ. Earth Sci.* 80 (16), 527.
- Li, N., Feng, W., Yu, J., Chen, F., Zhang, Q., Zhu, S., Hu, Y., Li, Y., 2023. Recent advances in geological storage: trapping mechanisms, storage sites, projects, and application of machine learning. *Energy Fuels* 37, 10087–10111.
- Li, Z., Dong, M., Li, S., Huang, S., 2006. CO<sub>2</sub> sequestration in depleted oil and gas reservoirs—caprock characterization and storage capacity. *Energy Convers. Manag.* 47 (11–12), 1372–1382.
- Liu, D., Agarwal, R., Liu, F., Yang, S., Li, Y., 2022. Modeling and assessment of CO<sub>2</sub> geological storage in the eastern Deccan basalt of India. *Environ. Sci. Pollut. Control Ser.* 29 (56), 85465–85481.
- Liu, H., Lu, H., Hu, H., 2024. CO<sub>2</sub> capture and mineral storage: state of the art and future challenges. *Renew. Sustain. Energy Rev.* 189, 113908.
- Liu, W., Teng, L., Rohani, S., Qin, Z., Zhao, B., Xu, C.C., Ren, S., Liu, Q., Liang, B., 2021. CO<sub>2</sub> mineral carbonation using industrial solid wastes: a review of recent developments. *Chem. Eng. J.* 416, 129093.
- Lu, J., Lv, Y., Fang, X., Zuo, J., Wang, S., Li, H., Yuan, C., Liu, W., 2024a. Fault leakage behaviors and CO<sub>2</sub> migration in different types of geological carbon storage. *Chem. Technol. Fuels Oils* 1–10.
- Lu, P., Apps, J., Zhang, G., Gysi, A., Zhu, C., 2024b. Knowledge gaps and research needs for modeling CO<sub>2</sub> mineralization in the basalt-CO<sub>2</sub>-water system: a review of laboratory experiments. *Earth Sci. Rev.*, 104813.
- Lu, S., Hu, C., Wang, X., Quaye, J.A., Lv, N., Deng, L., 2024c. Carbon dioxide storage in magmatic rocks: review and perspectives. *Renew. Sustain. Energy Rev.* 202, 114728.
- Mao, J., Jahanbani Ghahfarokhi, A., 2024. A review of intelligent decision-making strategy for geological CO<sub>2</sub> storage: insights from reservoir engineering. *Geoenery Science and Engineering* 240, 212951.
- Marieni, C., Voigt, M., Clark, D.E., Gislason, S.R., Oelkers, E.H., 2021. Mineralization potential of water-dissolved CO<sub>2</sub> and H<sub>2</sub>S injected into basalts as function of temperature: freshwater versus seawater. *Int. J. Greenh. Gas Control* 109, 103357.
- Matter, J.M., Broecker, W., Stute, M., Gislason, S., Oelkers, E., et al., 2009. Permanent carbon dioxide storage into basalt: the CarbFix pilot project, Iceland. *Energy Proc.* 1 (1), 3641–3646.
- Matter, J.M., Takahashi, T., Goldberg, D., 2007. Experimental evaluation of in situ CO<sub>2</sub>-water-rock reactions during CO<sub>2</sub> injection in basaltic rocks: implications for geological CO<sub>2</sub> sequestration. *G-cubed* 8 (2).
- McGrail, B., Spane, F., Sullivan, E., Bacon, D., Hund, G., 2011. The Wallula basalt sequestration pilot project. *Energy Proc.* 4, 5653–5660.
- McGrail, B.P., Schaefer, H.T., Ho, A.M., Chien, Y.J., Davidson, C.L., 2006. Potential for carbon dioxide sequestration in flood basalts. *J. Geophys. Res. Solid Earth* 111 (B12).
- McGrail, B.P., Schaefer, H.T., Spane, F.A., Cliff, J.B., Qafoku, O., Horner, J.A., Thompson, C.J., Owen, A.T., Sullivan, C.E., 2017a. Field validation of supercritical CO<sub>2</sub> reactivity with basalts. *Environ. Sci. Technol. Lett.* 4 (1), 6–10.
- McGrail, B.P., Schaefer, H.T., Spane, F.A., Horner, J.A., Owen, A.T., Cliff, J.B., Qafoku, O., Thompson, C.J., Sullivan, E.C., 2017b. Wallula basalt pilot demonstration project: post-injection results and conclusions. *Energy Proc.* 114, 5783–5790.
- McGrail, B.P., Spane, F.A., Amonette, J.E., Thompson, C., Brown, C.F., 2014a. Injection and monitoring at the Wallula basalt pilot project. *Energy Proc.* 63, 2939–2948.
- McGrail, B.P., Spane, F.A., Amonette, J.E., Thompson, C.R., Brown, C.F., 2014b. Injection and monitoring at the Wallula basalt pilot project. *Energy Proc.* 63, 2939–2948.
- Menefee, A.H., Giammar, D.E., Ellis, B.R., 2018. Permanent CO<sub>2</sub> trapping through localized and chemical gradient-driven basalt carbonation. *Environ. Sci. Technol.* 52 (15), 8954–8964.
- Mkono, C.N., Chuanbo, S., Mulashani, A.K., Mwakipunda, G.C., 2023. Deep learning integrated approach for hydrocarbon source rock evaluation and geochemical indicators prediction in the Jurassic-Paleogene of the Mandawa basin, SE Tanzania. *Energy* 284, 129232.
- Mohammed, I., Yaseri, A., Al Shehri, D., Mahmoud, M., 2024. Basalt mineral surface charge and the effect of mineralization on its colloidal stability: implications of subsurface CO<sub>2</sub> storage. *Fuel* 356, 129569.
- Moita, P., Berrezueta, E., Abdoulghafour, H., Beltrame, M., Pedro, J., et al., 2020. Mineral carbonation of CO<sub>2</sub> in Mafic Plutonic rocks, II—laboratory experiments on early-phase supercritical CO<sub>2</sub>-brine-rock interactions. *Appl. Sci.* 10 (15), 5083.
- Mokhtari, J., 2011. Chemical Alteration of Oil Well Cement with Basalt Additive during Carbon Storage Application. Middle East Technical University.
- Mouallem, J., Fathy, A., Arif, M., Mahmoud, M., 2023. CO<sub>2</sub> mineral trapping potential of carbonates: a numerical investigation. *Middle East Oil, Gas and Geosciences Show.*
- Mwakipunda, G.C., Abelly, E.N., Mgimba, M.M., Ngata, M.R., Nyakilla, E.E., Yu, L., 2023a. Critical review on carbon dioxide sequestration potentiality in methane hydrate reservoirs via CO<sub>2</sub>-CH<sub>4</sub> exchange: experiments, simulations, and pilot test applications. *Energy Fuels* 37 (15), 10843–10868.
- Mwakipunda, G.C., Mgimba, M.M., Ngata, M.R., Yu, L., 2024. Recent advances on carbon dioxide sequestration potentiality in salt caverns: a review. *Int. J. Greenh. Gas Control* 133, 104109.
- Mwakipunda, G.C., Ngata, M.R., Mgimba, M.M., Yu, L., 2023b. Carbon dioxide sequestration in low porosity and permeability deep saline aquifer: numerical simulation method. *J. Energy Resour. Technol.* 145 (7).
- Mwakipunda, G.C., Wang, Y., Mgimba, M.M., Ngata, M.R., Alhassan, J., Mkono, C.N., Yu, L., 2023c. Recent advances in carbon dioxide sequestration in deep unmineable coal seams using CO<sub>2</sub>-ECBM technology: experimental studies, simulation, and field applications. *Energy Fuels* 37 (22), 17161–17186.
- Myers, C., Nakagaki, T., 2020. Direct mineralization of atmospheric CO<sub>2</sub> using natural rocks in Japan. *Environ. Res. Lett.* 15 (12), 124018.
- Nadege, M.N., Jiang, S., Mwakipunda, G.C., Kouassi, A.K.F., Harold, P.K., Roland, K.Y. H., 2024. Brittleness index prediction using modified random forest based on particle swarm optimization of Upper Ordovician Wufeng to Lower Silurian Longmaxi shale gas reservoir in the Weiyuan Shale Gas Field, Sichuan Basin, China. *Geoenery Science and Engineering* 233, 212518.
- Neerup, R., Loge, I.A., Helgason, K., Snaebjörnisdóttir, S.O., Sigfússon, B., et al., 2022. A call for standards in the CO<sub>2</sub> value chain. *Environ. Sci. Technol.* 56 (24), 17502–17505.
- Ngata, M.R., Yang, B., Aminu, M.D., Emmanuelli, B.L., Said, A.A., Kalibwami, D.C., Mwakipunda, G.C., Ochilov, E., Nyakilla, E.E., 2022. Minireview of formation damage control through nanotechnology utilization at fieldwork conditions. *Energy Fuels* 36 (8), 4174–4185.
- Ngata, M.R., Yang, B., Khalid, W., Ochilov, E., Mwakipunda, G.C., Aminu, M.D., 2023. Review on experimental investigation into formation damage during geologic carbon sequestration: advances and outlook. *Energy Fuels* 37 (9), 6382–6400.
- O'Connor, W.K., Dahlin, D.C., Rush, G., Dahlin, C.L., Collins, W.K., 2002. Carbon dioxide sequestration by direct mineral carbonation: process mineralogy of feed and products. *Mining, Metallurgy & Exploration* 19, 95–101.
- Oelkers, E.H., Arkadaskiy, S., Affi, A.M., Hoteit, H., Richards, M., et al., 2022. The subsurface carbonation potential of basaltic rocks from the Jizan region of Southwest Saudi Arabia. *Int. J. Greenh. Gas Control* 120, 103772.
- Oelkers, E.H., Gislason, S.R., Matter, J., 2008. Mineral carbonation of CO<sub>2</sub>. *Elements* 4 (5), 333–337.
- Okoli, A.E., Kolawole, O., Akaolisa, C.Z., Ikoro, D.O., Ozotta, O., 2024. Alterations in petrophysical and mechanical properties due to basaltic rock-CO<sub>2</sub> interactions: comprehensive review. *Arabian J. Geosci.* 17 (1), 10.
- Omari, A., Wang, C., Li, Y., Xu, X., 2022. The progress of enhanced gas recovery (EGR) in shale gas reservoirs: a review of theory, experiments, and simulations. *J. Petrol. Sci. Eng.* 213, 110461.
- Paulo, C., Power, I.M., Zeyen, N., Wang, B., Wilson, S.A., 2023. Geochemical modeling of CO<sub>2</sub> sequestration in ultramafic mine wastes from Australia, Canada, and South

- Africa: implications for carbon accounting and monitoring. *Appl. Geochem.* 152, 105630.
- Peng, H., Xu, Z.-D., Xia, Z., Zang, X., Xi, D., Jiang, X., Zhao, W., Lu, H., 2024. Closed wellbore integrity failure induced by casing corrosion based on solid-chemical coupling model in CO<sub>2</sub> sequestration. *Geoenery Science and Engineering* 241, 213140.
- Pingping, S., Xinwei, L., Qiujie, L., 2009. Methodology for estimation of CO<sub>2</sub> storage capacity in reservoirs. *Petrol. Explor. Dev.* 36 (2), 216–220.
- Postma, T., Bandilla, K., Peters, C., Celia, M., 2022a. Field-scale modeling of CO<sub>2</sub> mineral trapping in reactive rocks: a vertically integrated approach. *Water Resour. Res.* 58 (1), e2021WR030626.
- Postma, T., Bandilla, K.W., Celia, M., 2021. A computationally efficient method for field-scale reservoir simulation of CCS in basalt formations. In: *Proceedings of the 15th Greenhouse Gas Control Technologies Conference*, pp. 15–18.
- Postma, T.J., Bandilla, K.W., Celia, M.A., 2022b. Implications of CO<sub>2</sub> mass transport dynamics for large-scale CCS in basalt formations. *Int. J. Greenh. Gas Control* 121, 103779.
- Postma, T.J.W., 2022. Prospects for large-scale implementation of carbon sequestration in basalt: capacity. In: *Storage Security, and the Rate of Mineral Trapping*. Princeton University.
- Postma, T.J.W., Bandilla, K.W., Peters, C.A., Celia, M.A., 2022c. Field-scale modeling of CO<sub>2</sub> mineral trapping in reactive rocks: a vertically integrated approach. *Water Resour. Res.* 58 (1), e2021WR030626.
- Punnam, P.R., Krishnamurthy, B., Surasani, V.K., 2021. Investigations of structural and residual trapping phenomena during CO<sub>2</sub> sequestration in Deccan volcanic Province of the Saurashtra region, Gujarat. *Int. J. Chem. Eng.* 2021, 1–16.
- Punnam, P.R., Krishnamurthy, B., Surasani, V.K., 2022. Investigation of solubility trapping mechanism during geologic CO<sub>2</sub> sequestration in Deccan Volcanic Provinces, Saurashtra, Gujarat, India. *Int. J. Greenh. Gas Control* 120, 103769.
- Rabiu, K., Abidoye, L., Das, D., 2020. Physico-chemical and dielectric parameters for the monitoring of carbon sequestration in basalt and silica media. *Environ. Technol. Innovat.* 20, 101052.
- Ragnheiddottir, E., Sigurdardottir, H., Kristjansdottir, H., Harvey, W., 2011. Opportunities and challenges for CarbFix: an evaluation of capacities and costs for the pilot scale mineralization sequestration project at Hellisheidi, Iceland and beyond. *Int. J. Greenh. Gas Control* 5 (4), 1065–1072.
- Rasool, M.H., Ahmad, M., 2023. Reactivity of basaltic minerals for CO<sub>2</sub> sequestration via in situ mineralization: a review. *Minerals* 13 (9), 1154.
- Rasool, M.H., Ahmad, M., Ayoub, M., 2023. Selecting geological formations for CO<sub>2</sub> storage: a comparative rating system. *Sustainability* 15 (8), 6599.
- Rathnaweera, T., Ranjith, P., 2020. Nano-modified CO<sub>2</sub> for enhanced deep saline CO<sub>2</sub> sequestration: a review and perspective study. *Earth Sci. Rev.* 200, 103035.
- Raza, A., Glatz, G., Gholami, R., Mahmoud, M., Alafnan, S., 2022. Carbon mineralization and geological storage of CO<sub>2</sub> in basalt: mechanisms and technical challenges. *Earth Sci. Rev.* 229, 104036.
- Raza, A., Mahmoud, M., Murtaza, M., Arif, M., Hassan, A., Glatz, G., Alafnan, S., Kamal, M.S., Al-Karnos, A., 2023. Experimental investigation of mafic rocks for carbon mineralization prospect. *Energy Fuels* 37 (8), 5976–5985.
- Raza, A., Rezaee, R., Gholami, R., Bing, C.H., Nagarajan, R., Hamid, M.A., 2016. A screening criterion for selection of suitable CO<sub>2</sub> storage sites. *J. Nat. Gas Sci. Eng.* 28, 317–327.
- Richardson, A.-A.M., Tassinari, C.C., 2022. CO<sub>2</sub> storage efficiency involving basalt-sedimentary interaction within the Parana basin, Brazil. *AAPG (Am. Assoc. Pet. Geol.) Bull.* 107, 357–386, 20,221,001.
- Ritchie, H., Roser, M., Rosado, P., 2020. CO<sub>2</sub> and greenhouse gas emissions. *Our world in data*. <https://ourworldindata.org/co2-and-greenhouse-gas-emissions>.
- Rodríguez Calzado, E., 2023. Estimating CO<sub>2</sub> storage capacity, injectivity, and storage costs for large-scale CCS deployment & carbon dioxide removal goals. <https://doi.org/10.26153/tsw/50054>.
- Roy, D.G., Vishal, V., Singh, T.N., 2016. Effect of carbon dioxide sequestration on the mechanical properties of Deccan basalt. *Environ. Earth Sci.* 75 (9), 1.
- Sambo, C., Dudun, A., Samuel, S.A., Esenenjor, P., Muhammed, N.S., Haq, B., 2022. A review on worldwide underground hydrogen storage operating and potential fields. *Int. J. Hydrogen Energy* 47 (54), 22840–22880.
- Sandalow, D., Aines, R., Friedmann, J., Kelemen, P., McCormick, C., Power, I., Schmidt, B., Wilson, S., 2021. *Carbon Mineralization Roadmap Draft October 2021*. Lawrence Livermore National Lab.(LLNL), Livermore, CA (United States).
- Sanna, A., Uibu, M., Caramanna, G., Kuusik, R., Maroto-Valer, M., 2014. A review of mineral carbonation technologies to sequester CO<sub>2</sub>. *Chem. Soc. Rev.* 43 (23), 8049–8080.
- Shen, M., Kong, F., Tong, L., Luo, Y., Yin, S., et al., 2022. Carbon capture and storage (CCS): development path based on carbon neutrality and economic policy. *Carbon Neutrality* 1 (1), 37.
- Singh, R.K., Nayak, N.P., 2023. Complications in drilling operations in basalt for CO<sub>2</sub> sequestration: an overview. *Mater. Today: Proc.* <https://doi.org/10.1016/j.matpr.2023.04.441>.
- Singh, R.K., Nayak, N.P., Kumar, S., Vishal, V., 2024. A critical meta-analysis of CO<sub>2</sub>-water-rock interaction in basalt for CO<sub>2</sub> storage: a review based on global and Indian perspective. *Mar. Petrol. Geol.* 168, 107002.
- Snæbjörnsdóttir, S.Ó., Gislason, S.R., Galeczka, I.M., Oelkers, E.H., 2018. Reaction path modelling of in-situ mineralisation of CO<sub>2</sub> at the CarbFix site at Hellisheidi, SW-Iceland. *Geochem. Cosmochim. Acta* 220, 348–366.
- Snæbjörnsdóttir, S.Ó., Oelkers, E.H., Mesfin, K., Aradóttir, E.S., Dideriksen, K., et al., 2017. The chemistry and saturation states of subsurface fluids during the in situ mineralisation of CO<sub>2</sub> and H<sub>2</sub>S at the CarbFix site in SW-Iceland. *Int. J. Greenh. Gas Control* 58, 87–102.
- Snæbjörnsdóttir, S.Ó., Sigfússon, B., Marieni, C., Goldberg, D., Gislason, S.R., Oelkers, E.H., 2020. Carbon dioxide storage through mineral carbonation. *Nat. Rev. Earth Environ.* 1 (2), 90–102.
- Snæbjörnsdóttir, S.Ó., Wiese, F., Fridriksson, T., Ármannsson, H., Einarsson, G.M., Gislason, S.R., 2014. CO<sub>2</sub> storage potential of basaltic rocks in Iceland and the oceanic ridges. *Energy Proc.* 63, 4585–4600.
- Stanfield, C.H., Miller, Q.R., Battu, A.K., Lahiri, N., Nagurney, A.B., et al., 2024. Carbon mineralization and critical mineral resource evaluation pathways for mafic-ultramafic assets. *ACS Earth Space Chem.* 8, 1204–1213.
- Statista, 2024. Average monthly carbon dioxide (CO<sub>2</sub>) levels in the atmosphere worldwide from 1990 to 2024. <https://www.statista.com/statistics/1091999/atmospheric-concentration-of-co2-historic/>.
- Stockmann, G.J., Wolff-Boenisch, D., Gislason, S.R., Oelkers, E.H., 2011. Do carbonate precipitates affect dissolution kinetics? 1: basaltic glass. *Chem. Geol.* 284 (3–4), 306–316.
- Stockmann, G.J., Wolff-Boenisch, D., Gislason, S.R., Oelkers, E.H., 2013. Do carbonate precipitates affect dissolution kinetics? 2: diopside. *Chem. Geol.* 337, 56–66.
- Tutolo, C.M., Awolayo, A., Brown, C., 2021. Alkalinity generation constraints on basalt carbonation for carbon dioxide removal at the Gigaton-per-year scale. *Environ. Sci. Technol.* 55 (17), 11906–11915.
- Udebhulu, O.D., Aladeitan, Y., Azevedo, R.C., De Tomi, G., 2024. A review of cement sheath integrity evaluation techniques for carbon dioxide storage. *J. Pet. Explor. Prod. Technol.* 14 (1), 1–23.
- Van Pham, T.H., Aagaard, P., Hellevang, H., 2012. On the potential for CO<sub>2</sub> mineral storage in continental flood basalts – PHREEQC batch- and 1D diffusion-reaction simulations. *Geochem. Trans.* 13 (1), 5.
- Verba, C., O'Connor, W., Rush, G., Palandri, J., Reed, M., Ideker, J., 2014. Geochemical alteration of simulated wellbores of CO<sub>2</sub> injection sites within the Illinois and Pasco Basins. *Int. J. Greenh. Gas Control* 23, 119–134.
- Vishal, V., Verma, J., Chandra, D., Ashok, D., 2021. A systematic capacity assessment and classification of geologic CO<sub>2</sub> storage systems in India. *Int. J. Greenh. Gas Control* 111, 103458.
- Voigt, M., Marieni, C., Baldermann, A., Galeczka, I.M., Wolff-Boenisch, D., Oelkers, E.H., Gislason, S.R., 2021. An experimental study of basalt-seawater-CO<sub>2</sub> interaction at 130 °C. *Geochem. Cosmochim. Acta* 308, 21–41.
- Wells, R.K., Xiong, W., Giammar, D., Skemer, P., 2017. Dissolution and surface roughening of Columbia River flood basalt at geologic carbon sequestration conditions. *Chem. Geol.* 467, 100–109.
- White, S.K., Spane, F.A., Schaeff, H.T., Miller, Q.R., White, M.D., Horner, J.A., McGrail, B.P., 2020a. Quantification of CO<sub>2</sub> mineralization at the Wallula basalt pilot project. *Environ. Sci. Technol.* 54 (22), 14609–14616.
- White, S.K., Spane, F.A., Schaeff, H.T., Miller, Q.R.S., White, M.D., Horner, J.A., McGrail, B.P., 2020b. Quantification of CO<sub>2</sub> mineralization at the Wallula basalt pilot project. *Environ. Sci. Technol.* 54 (22), 14609–14616.
- Wilberforce, T., Baroutaji, A., Soudan, B., Al-Alami, A.H., Olabi, A.G., 2019. Outlook of carbon capture technology and challenges. *Sci. Total Environ.* 657, 56–72.
- Wolff-Boenisch, D., Wenau, S., Gislason, S.R., Oelkers, E.H., 2011. Dissolution of basalts and peridotite in seawater, in the presence of ligands, and CO<sub>2</sub>: implications for mineral sequestration of carbon dioxide. *Geochem. Cosmochim. Acta* 75 (19), 5510–5525.
- Wu, H., 2018. Quantifying permeability alteration effects to CO<sub>2</sub> storage potential in a basalt fracture network. *AGU Fall Meeting Abstracts* S51F-S401.
- Wu, H., Jayne, R.S., Bodnar, R.J., Pollyea, R.M., 2021. Simulation of CO<sub>2</sub> mineral trapping and permeability alteration in fractured basalt: implications for geologic carbon sequestration in mafic reservoirs. *Int. J. Greenh. Gas Control* 109, 103383.
- Xiong, W., Wells, R.K., Horner, J.A., Schaeff, H.T., Skemer, P.A., Giammar, D.E., 2018. CO<sub>2</sub> mineral sequestration in naturally porous basalt. *Environ. Sci. Technol. Lett.* 5 (3), 142–147.
- Youns, Y.T., Manshad, A.K., Ali, J.A., 2023. Sustainable aspects behind the application of nanotechnology in CO<sub>2</sub> sequestration. *Fuel* 349, 128680.
- Zapata, Y., Kristensen, M., Huerta, N., Brown, C., Kabir, C., Reza, Z., 2020. CO<sub>2</sub> geological storage: critical insights on plume dynamics and storage efficiency during long-term injection and post-injection periods. *J. Nat. Gas Sci. Eng.* 83, 103542.
- Zhang, L., Wen, R., Li, F., Li, C., Sun, Y., Yang, H., 2023. Assessment of CO<sub>2</sub> mineral storage potential in the terrestrial basalts of China. *Fuel* 348, 128602.
- Zhao, R., Zhong, Z., Yu, Y., Lü, R., Shi, T., Wang, N., Cheng, J., 2024. Numerical simulation of CO<sub>2</sub> storage by basalts in Xingouzui formation, Jiangnan Basin, China. *Int. J. Greenh. Gas Control* 134, 104133.
- Zheng, J., Chong, Z.R., Qureshi, M.F., Linga, P., 2020. Carbon dioxide sequestration via gas hydrates: a potential pathway toward decarbonization. *Energy Fuels* 34 (9), 10529–10546.
- Zheng, L., Nico, P., Spycher, N., Domen, J., Credoz, A., 2021. Potential impacts of CO<sub>2</sub> leakage on groundwater quality of overlying aquifer at geological carbon sequestration sites: a review and a proposed assessment procedure. *Greenhouse Gases: Sci. Technol.* 11 (5), 1134–1166.